Event-Triggered Dynamic State Estimation Based on Set Membership Filtering for Power Systems

B. N. Weerasinghe Mudiyanselage Rashmi
Amadini Boragolla

A Thesis submitted to the Faculty of Graduate Studies of The University of Manitoba in partial fulfilment of the requirements of the degree of

MASTER OF SCIENCE

Department of Electrical and Computer Engineering
University of Manitoba
Winnipeg

Abstract

In the future, dynamic state estimation (DSE) will be an important function in monitoring and control of smart power grids. In this context, data communication networks and phasor measurement units (PMU) that are currently being deployed in smart power grids, will play a major role. However, very high data rates of PMUs will necessitate event-triggered multi-area state estimation (MASE) to ease the burden on the communication networks. In MASE, a large power grid is divided into sectors and local state estimates of each sector are communicated to a monitoring center for fusion and decision making. Traditional DSE algorithms such as Kalman filter (KF) are not well suited for event-triggered state estimation and new approaches will be required.

The goal of this thesis is to investigate the applicability of a lesser-known class of algorithms known as set membership (SM) filtering to MASE. These algorithms have the important property known as data selective update. In the context of MASE, this property will allow the communication of sector-based estimates to the fusion center, only when the measurements observed by sensors within a sector are informative, that is, indicative of the existence of an abnormality such as a fault condition.

The contribution of this thesis consists of two parts. In the first part, a simple to implement SM algorithm incorporating data-selective updates is presented in detailed, and it's properties are investigated through a numerical study. It is shown that, despite sparse updates, the estimation accuracy of the SM algorithm is comparable to the traditional extended KF (EKF) algorithm. In the second part, a comprehensive case study involving

event-triggered state estimation in a single machine infinite bus system with a synchronous machine is presented. The simulation results show that, except during transient and fault conditions, the SM algorithm presented in this thesis rarely performs complete state updates, thus saving communication burden in a MASE context. The estimation accuracy, however, remains comparable with the EKF. As an important avenue for future research, methods of robust initialization of the SM algorithm is identified. It is shown that improper initialization can affect the ability of the SM algorithm to respond to fault conditions.

Acknowledgements

First and foremost, I wholeheartedly thank my adviser Prof. Pradeepa Yahampath for allowing me to work with him, and for the continuous encouragement and support throughout my M. Sc program. A special thanks must be conveyed to the examining committee Prof. Udaya Annakkage and Prof. Amine Mezghani for accepting this thesis for review.

Financial support form Mitacs and RTDS Technologies Inc. is gratefully acknowledged. A special thanks go again to Prof. Udaya Annakkage for showing an interest in my research and his valuable suggestions when understanding the power systems area. Also Dr. Harshani Konara, Thilini, and Dilini for answering my question and helping me to understand the power system example.

I would also like to acknowledge the support and inspiration given by the academic and non-academic staff of the Department of Electrical and Computer Engineering, Faculty of Graduate Studies and the University of Manitoba.

Last but not least, I would like to pay gratitude to the three greatest inspirations and pillars of my life, my father Nayanananda Boragolla, my mother Rupa Boragolla and my husband Jagannath Wijekoon. Without my parents support and encouragement, I would never be the person I am today. Many thanks to my friends, who have been immensely supportive through my ups and downs.

Contents

List of Tables

List of Figures

Abbreviations

CKF	**C**ubature **K**alman **F**ilter
EMS	**E**nergy **M**anagement **S**ystem
DSE	**D**ynamic **S**tate **E**stimation
EKF	**E**xtended **K**alman **F**ilter
GPS	**G**lobal **P**ositioning **S**ystem
KF	**K**alman **F**ilter
LHS	**L**eft **H**and **S**ide
MASE	**M**ulti-**A**rea **S**tate **E**stimation
MC	**M**onte-**C**arlo
MIMO	**M**ultiple-**I**nput and **M**ultiple-**O**utput
MSE	**M**ean **S**quare **E**rror
PMU	**P**hasor **M**easurement **U**nit
PS-DSE	**P**ower **S**ystem **D**ynamic **S**tate **E**stimation
RHS	**R**ight **H**and **S**ide
RTDS	**R**eal **T**ime **D**igital **S**imulator
RTU	**R**emote **T**erminal **U**nit
SCADA	**S**upervisory **C**ontrol **A**nd **D**ata **A**cquisition
SE	**S**tate **E**stimation
SM	**S**et **M**embership

SMIB	**S**inglr **M**achine **I**nfinite **B**us
SMU	**S**et **M**embership Algorithm with selective correction step **U**pdate Strategy
UD	**U**pper diagonal and **D**iagonal
UKF	**U**nscented **K**alman **F**ilter

To my family and friends.

Chapter 1

Introduction

1.1 Overview

The modern power systems are more complex than the conventional power systems due to ever-increasing demand, integration of renewable energy sources, smart grids, etc. Therefore, having a near real-time network model of the power system through dynamic state estimation (DSE) will permit energy management systems (EMS) to perform various important control and planning tasks more efficiently [1].

Advanced measurement technologies, such as phasor measurement units (PMUs) can report data at rates as high as 120 frames per second [2] and consequently providing an opportunity to monitor power system dynamics in near real-time. This is opposed to conventional measurements such as supervisory control and data acquisition (SCADA) data measurement which has data rates of 1 frame for $2 - 4$ seconds. Particularly during severe system disturbances to observe transients of the system, PMU measurements will be highly

useful as the measurements are synchronized, i.e. time-stamped by the global positioning system's (GPS's) universal clock. Typically state of a power system changes on a much larger time-scale compared to the measurement rate. Therefore, higher measurement rates from PMUs create a huge burden on the communication infrastructure and data processing facilities of the grid and a growing concern in the field of power system state estimation (SE). In particular, the conventional approach of a centralized monitoring center with a state estimator can become infeasible and multi-area state estimation (MASE) can be used as an alternative. In MASE, many distributed local state estimators are employed which communicate their estimates to a centralized monitoring center for fusion and decision making. If the MASE is equipped with real-time resource-efficient, data selective and event-triggered SE, this will play a vital role in reducing the communication overhead created by large data flow in the communication network. [1, 3].

Power system dynamic state estimation (PS-DSE) using Kalman filtering based methods has been investigated extensively in the literature [4–8]. Kalman filter is a statistical method that is based on the familiar prediction-correction recursive structure which estimates the state when the observations are available without considering the information content of the observations. This thesis investigates an alternative method known as set membership (SM) filtering which can achieve the same performance as the Kalman filter and is capable of data selective estimation based on the innovative nature of the observations.

1.2 State-space description of systems

In engineering, it is necessary to model physical systems using mathematical equations as it is crucial in understanding, analyzing, and controlling the physical system. A mathematical

model that is used to describe the relationship between the input and output of a physical system is simply referred to as a system. In general, systems can be categorized in many ways, for the purpose of this thesis we can classify the systems into the following categories,

1. continuous-time or discrete-time systems,
2. linear or non-linear systems, and
3. memoryless systems or systems with memory (dynamical systems).

Most of the physical systems are represented by linear models due to their simplicity and the availability of a rich body of analytical tools. A linear dynamical system can be represented by several equivalent means, differential equations or difference equations, Laplace or z-transform, and state-space representation. State-space representation alone possesses many advantages, for example, it gives an internal description of the system, intuition to the performance of the system, and in general, allows a better way for designing controllers for multiple-input and multiple-output (MIMO) systems. [9]. Thus state-space methods play a vital role in system analysis and control problems.

In the state-space approach, the *state* of a system at a given time is defined as the minimal information that is sufficient to describe the system response to an applied input. The state of a system is described by one or more variables referred to as the *state variables*. The set of equations that relate the current state variables to the previous state variables and the most recent input is called the *state equations (system dynamic model)*. The equations which relate the output variables to the state variables and the inputs are called the *output equations (system measurement model)*. The state-space representation of a linear dynamical system is the collection of state equations and output equations. [9, 10].

An important problem in analyzing and controlling a system based on a state-space model is the estimation of the state at a given time from observations. Typically, SE is a two-step procedure that is repeatedly carried out at each time step. In the prediction step, the current inputs along with previously estimated state are used to obtain a predicted value for the current state variables. Subsequently, in the correction-step, the available output measurements are used to correct the predicted. Figure 1.1 illustrate this idea in pictorial format.

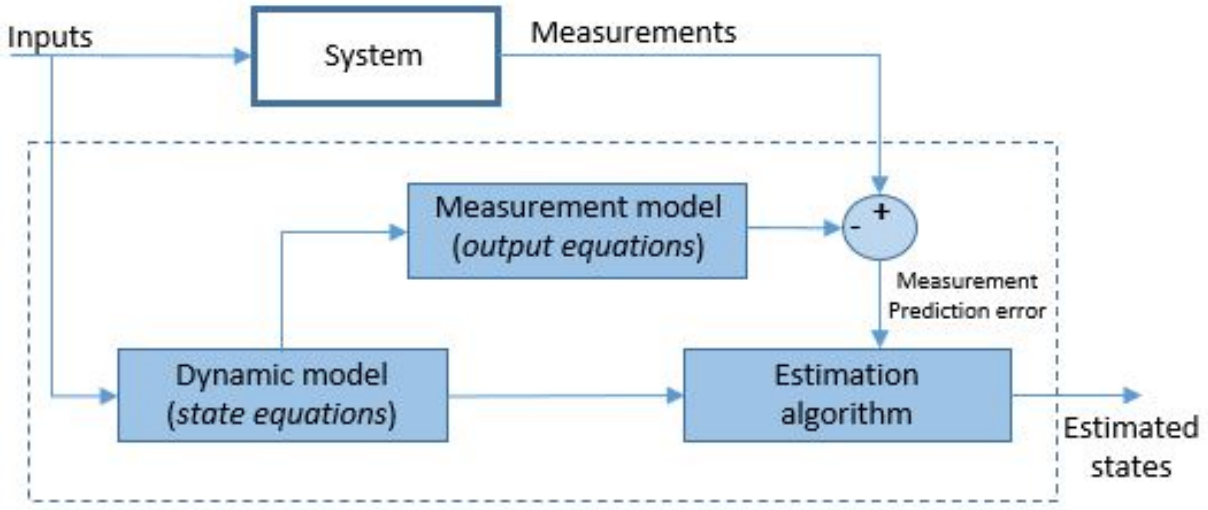

FIGURE 1.1: The state estimation process.

The inputs to a physical system as well as the measurements from the system normally inherit some degree of uncertainty due to noise. Therefore, the true state of any system is a problem of finding the best value by minimizing or maximizing a cost function based on some criteria.

The Kalman filter (KF) is the most widely used method for solving state estimation from the noisy measurements. This algorithm was originally introduced in [11] and further

investigated in [12]. The KF is a minimum mean square estimator for the unobserved state variables when all random variables (noise) in the state equations are jointly Gaussian. This is a two-step procedure which sequentially performs at each time instant, a prediction of the unknown current state based on the previous state (time update), and followed by a correction of the predicted state based on the current measurement (measurement update). The output of the KF is an estimate of the most probable state and the covariance of the estimation error. While the basic KF algorithm assumes a linear system, the extended KF (EKF) and the unscented KF (UKF) [13] are generalizations of the KF for non-linear dynamical systems. [14]. Other methods based on the KF can be found in [10, 15].

1.3 Motivation

A shortcoming of recursive estimation algorithms, such as the KF is that they require the aforementioned prediction and correction steps at every time step regardless of the value of the information contained in measurements. Every measurement may or may not contain any new information about the state being estimated. Therefore correction step may be an unnecessary computation if the correction of the state is negligible at a higher rate of measurements. Set membership algorithms are a class of algorithms in parameter estimation known to possess the capability of data selective updates. [16–18].

The main objective of the thesis is to investigate the SM algorithm to state estimation in dynamical systems and consider the feasibility of an event-triggered DSE in a power system with high measurement rates provided by PMUs. The key feature in the SM algorithm considered in this thesis is the ability to skip the correction step whenever possible. Another important feature in the SM algorithm is that the unknown variables are assumed

to belong to bounded sets, rather than modeling them as random variables with probability distributions. As a consequence, the state estimate would also be a set that is consistent with the system model, and the measurements rather than a single point estimate. The most common approach is to use ellipsoidal bounds. This is also the approach taken in this thesis.

The logical reasoning for using set-theoretic techniques in estimation is, it will give more definitive solutions when utilizing known information rather than imposing a subjective notion of optimality [19]. Given the measurements, the set found by the SM algorithm will include all attainable states. In the KF based state estimation algorithms, the uncertainties of the systems are modeled by random variables. But in practical situations, most often assumptions have to be made regarding the probability distributions of these random variables, and unless a model such as a Gaussian model is used the optimal solution is difficult to obtain. Often this can not be rationalized if not for the ease in mathematical tractability of the underlying optimization problem. Unlike statistical assumptions, bounds for unknown variables can be easily acquired. Furthermore, in applications where the reliability and safety are the concerns, an acceptable bound on the state, rather than a point estimate, maybe adequate [20].

1.4 Literature review

1.4.1 Set-membership approach to state estimation

Background material on the fundamentals of set-theoretic estimation can be found in [19, 21]. The idea of an ellipsoidal set approach to recursive state estimation was originally introduced by F. C. Schweppe in [22], where a method has been explored for estimating

the states of a linear dynamical system using noisy observations and unknown but bounded inputs and observation errors. Furthermore, an algorithm has been developed to calculate a time-varying ellipsoid in state-space that always contained the system's true state. A conceptually similar idea has been presented in [23] as well. SM algorithms for filtering, prediction, and smoothing in the continuous and discrete-time linear dynamical systems with uncertain quantities bounded by both energy and instantaneous constraints have been derived in [20, 24]. While [20, 22–24] use ellipsoids which contain the true state (membership set), they do not present ways to select an ellipsoid in an optimum manner.

Comprehensive studies on this subject have been carried out by Russian researchers in the context of parameter estimation. The methods of state estimation using membership sets for both linear and non-linear dynamical systems were explored in [21] by F. L. Chernousko, and a concise description of the properties of reachable sets and their approximation using ellipsoids optimal in the sense of minimal volume have been presented. Application of ellipsoidal SM algorithms in problems of controls and estimation have been discussed in detail and an algorithm for optimal state estimation together with numerical examples has been presented in [21]. Furthermore, the comparison of the SM estimation approach and a probabilistic estimation approach has been given. A summary of [21] can be found in Chapter 3 of [25].

Traditionally, the geometric size of an ellipsoid is measured by its volume. The volume of the ellipsoid is proportional to the square of the product of the lengths of its axes, which is referred to as the determinant criterion. An alternative measure of size is the sum of the squares of the semi-axis lengths, which is called the trace criterion. Using these optimal ellipsoid bounds are searched. [26]. SM algorithms that find the optimal ellipsoids by either minimal determinant or minimal trace criterion have been introduced in

[27]. Several algorithms for computing ellipsoidal outer bounds for the true state have been presented in [28]. SM state estimation via hypercubes, polytopes, parallelotopes, intervals, and zonotopes have been investigated in [29–34].

Whilst most of the aforementioned work is concerned with linear systems, the implementation of the SM algorithms for parameter estimation in non-linear models has been considered in [33, 35, 36]. The feasibility of applying set membership algorithms in non-linear models has been discussed in [21]. In [33] non-linear parameter estimation model has been formulated as a problem of set inversion and solved using interval analysis techniques discussed in [37]. The utilization of the SM algorithm for estimating the states of a non-linear dynamical system has been investigated in [38]. In this case similar to EKF, non-linear dynamics were linearized about the current estimate, but the linearization errors were used to bound the membership sets. In [39], the linearization error was bounded using interval analysis techniques, and incorporated into process and measurement noise bounds. The real-time version of the same algorithm was established and investigated for a general class of non-linear systems in [40]. A new method for SE was investigated in [41], which combines a set-inversion algorithm with forward-backward propagation of intervals.

The SM algorithms which could disregard uninformative measurements were introduced in the context of system identification and adaptive signal processing [16–18]. The basic idea was to consider the measurement informative only if they reduce the size of the membership set. A systematic procedure to select the optimal ellipsoid has been presented and the convergence of the algorithm was discussed in [16]. An optimal observation dependent membership set has been found in [18] by solving a quadratic equation at each time instant. Unlike reducing the trace or determinate of the ellipsoid which defines the membership set, an upper bound to the size of the ellipsoid has been minimized using an

information-dependent forgetting factor in [17]. This algorithm has shown to have lower computational complexity. References [16–18] consider scaler observation, where each observation yields two parallel hyperplane bounds instead of ellipsoids, a simpler case than finding the intersection of two ellipsoids. A method to find outer and inner bounding ellipsoids of the intersection of two ellipsoids has been presented in [42].

The parameter estimation method described in [17] has been used to estimate states of linear dynamical system in [43]. In [44], the same concept as in [17] has been used to track time-varying parameters of a system with incrementally bounded time variations with more than one observation. The algorithm in [44] shows the potential of using it in SE as well. In [45] this technique is explained in the context of SE in linear systems and is extended to non-linear systems in [46] with the linearization error bounded using interval analysis techniques as in [39]. The shape defining matrix of an ellipsoid should be a symmetric positive definite matrix. Considering this fact an upper diagonal and diagonal (UD) triangular factorization based SM algorithm has been developed in [47]. This algorithm can jointly estimate both time-varying parameters and states in linear and non-linear systems. Further, a relaxed selective update strategy which sequentially considers measurements is proposed.

1.4.2 Dynamic state estimation in power systems

A power system is a network of electric components deployed to generate, transmit and consume electric power. A complete understanding of the operating conditions of a power system at a given instant of time can be established if the network model and complex phasor voltages at every system bus are known [48]. Voltage magnitudes and phase angles at every bus are defined as the states of a power system. A power system is operated by system operators from area control centers. The main objective of a system operator is to maintain

the power system at a normal secure state which includes identifying the operating state of the power system by continuous monitoring and take precautionary actions in case the system state is found to be *insecure*. [48]. EMS or the SCADA systems are installed at the area control centers for this task [1]. The first step towards security analysis is monitoring the current state of the power system. This analysis requires measurements from the power system and processing of them to determine the system state [48].

F. C. Schweppe .et al [49–51] were the first to propose and develop the idea of SE in power systems. They showed the necessity of this toward the real-time security assessment and control of the power system. Debs and Larson in [4] have taken the first step towards DSE and developed an algorithm using Kalman-Bucy filtering theory for real-time SE of a power system. DSE allows the power system to know the predicted next state progressively in a short period. Further, PS-DSE has been investigated in [52–56] as well. The techniques used in PS-DSE have been reviewed in [1, 3, 48, 57].

The application of EKF in PS-DSE can be found in [5, 6, 8]. An iterated EKF based on the generalized maximum likelihood approach is proposed in [58]. In [59], two iterative methods have been suggested to include the dynamic system non-linearities in PS-DSE oppose to linearization in EKF. Application of UKF in PS-DSE has been discussed in [7]. Other methods used in PS-DSE can be found in [52–55, 55, 56, 56, 60–63]. PS-DSE problem has been investigated in [64] by using EKF, UKF, and cubature Kalman filter (CKF) in a real-time test system environment developed in Real Time Digital Simulator (RTDS) software, RSCAD. Further, DSE for a existing power system has been developed and tested in [54].

In [65], set membership method to power system SE has been proposed based on interval constraint propagation. A DSE method based on an SM algorithm has been

proposed in [66] for SE in synchronous machines. This method combines an estimation algorithm discussed in [28] with the linearization error bounding method discussed in [39]. Due to the linearization error bounding methods and the sequential correction step the method discussed in [39] is more complex.

1.5 Outline of the thesis

This thesis investigates the feasibility of applying an SM algorithm for event-triggered DSE in power systems. The SM algorithms have been extensively studied in controls and adaptive signal processing fields but not very widely known in the power system community.

The standard structure of the linear SM algorithm based on ellipsoidal sets and the important mathematical results are presented in Chapter 2. Furthermore, a selective correction step update strategy which enables the event-triggered SE is presented. Finally, an extension of the algorithm to deal with nonlinear dynamical systems has been discussed.

A comparison of the SM algorithms with and without selective updates is presented in Chapter 3. This also includes a comparison with the conventional KF and EKF. Three different systems have been considered to investigate the performance and properties of the algorithm.

The utilization of the SM algorithm with a selective correction step update strategy in a power system example has been demonstrated in Chapter 4. In this case, the states of a synchronous machine in a single machine infinite bus system have been estimated and the feasibility of an event-triggered SE has been investigated.

Finally, the conclusions and contributions of this study are presented, and future avenues for further research are suggested in Chapter 5.

Chapter 2

Bounded Ellipsoid Method for State Estimation

2.1 Introduction

This chapter presents an SM algorithm for state estimation in linear dynamical systems, based on the ellipsoid bounding of unknown variables. A data selective update strategy that will be useful for event-triggered state estimation is also described. Finally, an extension to nonlinear dynamical systems is presented.

2.1.1 Preliminaries

Definition 2.1. An ellipsoidal set $E(\mathbf{a}, \tilde{\mathbf{P}}) \subset \mathbb{R}^n$ with a vector representing the center $\mathbf{a} \in \mathbb{R}^n$ is defined by,

$$E(\mathbf{a}, \tilde{\mathbf{P}}) = \{\mathbf{x} \in \mathbb{R}^n : (\mathbf{x} - \mathbf{a})^T \tilde{\mathbf{P}}^{-1} (\mathbf{x} - \mathbf{a}) \leq 1\}, \tag{2.1}$$

where $\tilde{\mathbf{P}} \in \mathbb{R}^{n \times n}$ is a symmetric positive definite matrix that defines the shape of the ellipsoid (shape-matrix).

2.2 Set membership algorithm

2.2.1 Linear system model

Consider the discrete-time linear dynamical system given by the state-space model,

$$\mathbf{x}_k = \mathbf{F}_{k-1} \mathbf{x}_{k-1} + \mathbf{w}_k, \tag{2.2}$$

$$\mathbf{z}_k = \mathbf{H}_k \mathbf{x}_k + \mathbf{v}_k, \tag{2.3}$$

where k is time, $\mathbf{x}_k \in \mathbb{R}^n$ is the state vector, $\mathbf{z}_k \in \mathbb{R}^m$ is the measurement vector (n is the number of states, and m is the number of measurements), $\mathbf{F}_{k-1} \in \mathbb{R}^{n \times n}$ is the system matrix or state transition matrix and $\mathbf{H}_k \in \mathbb{R}^{m \times n}$ is the output matrix. It is assumed that both $\mathbf{F}_{k-1}$ and $\mathbf{H}_k$ are known matrices.

The random disturbances $\mathbf{w}_k \in \mathbb{R}^n$ and $\mathbf{v}_k \in \mathbb{R}^m$ in (2.2) and (2.3) are assumed to be bounded respectively by the ellipsoids,

$$E(0, \mathbf{W}_k) = \{\mathbf{w} \in \mathbb{R}^n : (\mathbf{w}^T \mathbf{W}_k^{-1} \mathbf{w}) \leq 1\},$$
$$E(0, \mathbf{V}_k) = \{\mathbf{v} \in \mathbb{R}^m : (\mathbf{v}^T \mathbf{V}_k^{-1} \mathbf{v}) \leq 1\},$$

where $\mathbf{W}_k$ and $\mathbf{V}_k$ are known positive definite matrices with appropriate dimensions which define the shape of the ellipsoids $E(0, \mathbf{W}_k)$ and $E(0, \mathbf{V}_k)$. It is assumed that the initial state of the system is known and given by,

$$(\hat{\mathbf{x}}_0, \tilde{\mathbf{P}}_0) = \{\mathbf{x} \in \mathbb{R}^n : (\mathbf{x} - \hat{\mathbf{x}}_0)^T \tilde{\mathbf{P}}_0^{-1} (\mathbf{x} - \hat{\mathbf{x}}_0) \leq 1\},$$

where $\hat{\mathbf{x}}_0$ is the center of the set and $\tilde{\mathbf{P}}_0$ is a known symmetric positive definite matrix defining the shape of the set.

The main problem here is to estimate a bounding ellipsoid containing all the possible values of the state at time k which is compatible with the state bounding ellipsoid found at time $k-1$, the observations $\mathbf{z}_k$, the system model, and the assumptions made above regarding the sets. The following section describes the basics of the SM algorithm. For more details, refer to [20, 39, 44–46]

2.2.2 Set membership state estimation

Given the ellipsoid $E(\hat{\mathbf{x}}_{k-1}, \tilde{\mathbf{P}}_{k-1})$ that contains the previous state $\mathbf{x}_{k-1}$ and the process disturbance bound, the state transition equation (2.2) dictates that the predicted state at time k, $\hat{\mathbf{x}}_{k|k-1}$ should lie in the vector sum of transformed ellipsoid $\mathbf{F}_{k-1} E(\hat{\mathbf{x}}_{k-1}, \tilde{\mathbf{P}}_{k-1})$ which

contains the set of all states reachable at time k from the set $E(\hat{\mathbf{x}}_{k-1}, \tilde{\mathbf{P}}_{k-1})$ and disturbance bound $E(0, \mathbf{W}_k)$. Therefore, we have,

$$\hat{\mathbf{x}}_{k|k-1} \in \mathbf{F}_{k-1} E(\hat{\mathbf{x}}_{k-1}, \tilde{\mathbf{P}}_{k-1}) \oplus E(0, \mathbf{W}_{k-1}),$$

where $\oplus$ denotes the vector sum.

In general, the vector sum of two ellipsoids is not an ellipsoid. But an ellipsoid can be used to outer bound the vector sum of ellipsoids. Here, this ellipsoid is called the predicted state ellipsoid, which is given by,

$$E(\hat{\mathbf{x}}_{k|k-1}, \tilde{\mathbf{P}}_{k|k-1}) \supset \mathbf{F}_{k-1} E(\hat{\mathbf{x}}_{k-1}, \tilde{\mathbf{P}}_{k-1}) \oplus E(0, \mathbf{W}_{k-1}). \tag{2.4}$$

Therefore, the predicted state $\hat{\mathbf{x}}_{k|k-1} \in E(\hat{\mathbf{x}}_{k|k-1}, \tilde{\mathbf{P}}_{k|k-1})$. Using the measurement $\mathbf{z}_k$ at the time step k and the measurement equation (2.3), we can obtain the observation set,

$$S_k = \{\mathbf{x}_k \in \mathbb{R}^n : (\mathbf{z}_k - \mathbf{H}_k \mathbf{x}_k)^T \mathbf{V}_k^{-1} (\mathbf{z}_k - \mathbf{H}_k \mathbf{x}_k) \leq 1\}. \tag{2.5}$$

The true state $\mathbf{x}_k$ should lie in the intersection of the observation set S_k and the predicted state ellipsoid $E(\hat{\mathbf{x}}_{k|k-1}, \tilde{\mathbf{P}}_{k|k-1})$ and therefore,

$$\mathbf{x}_k \in E(\hat{\mathbf{x}}_{k|k-1}, \tilde{\mathbf{P}}_{k|k-1}) \cap S_k.$$

However, the intersection of two sets is not necessarily an ellipsoid. But for computational efficiency and ease, we can find an outer bounding ellipsoid which contains this intersection

as

$$E(\hat{\mathbf{x}}_k, \tilde{\mathbf{P}}_k) \supset E(\hat{\mathbf{x}}_{k|k-1}, \tilde{\mathbf{P}}_{k|k-1}) \cap S_k, \tag{2.6}$$

where $\hat{\mathbf{x}}_k$ is the center of the estimated set which can be used as a single point estimate. We will refer to this ellipsoid as the updated state ellipsoid.

Figure 2.1 illustrates the logic behind the SM algorithm. For simplicity of explanation, this diagram considers a two-state system with a single measurement, where one of the states is taken as the measurement. Figure 2.1 (A) shows $E(\hat{\mathbf{x}}_{k-1}, \tilde{\mathbf{P}}_{k-1})$ the estimated state set in the previous time step. Figure 2.1 (B) shows the predicted state set $E(\hat{\mathbf{x}}_{k|k-1}, \tilde{\mathbf{P}}_{k|k-1})$, where the state set estimated in the previous time step is transformed and bounded by noise. In the figure 2.1 (C) the measurement and the uncertainty are represented by two vertical lines. Finally, figure 2.1 (D) shows the estimated state set $E(\hat{\mathbf{x}}_k, \tilde{\mathbf{P}}_k)$ which will contain the true state $\mathbf{x}_k$.

2.2.2.1 Prediction step

The predicted state set is a vector sum of two ellipsoids. It can be shown that a class of ellipsoids which outer-bounds the sum of the two ellipsoids $\mathbf{F}_{k-1}E(\hat{\mathbf{x}}_{k-1}, \tilde{\mathbf{P}}_{k-1})$ and $E(0, \mathbf{W}_k)$ can be given by,

$$E(\hat{\mathbf{x}}_{k|k-1}, \tilde{\mathbf{P}}_{k|k-1}) = \{\mathbf{x}_k \in \mathbb{R}^n : (\mathbf{x}_k - \hat{\mathbf{x}}_{k|k-1})^T \tilde{\mathbf{P}}_{k|k-1}^{-1} (\mathbf{x}_k - \hat{\mathbf{x}}_{k|k-1}) \leq 1\},$$

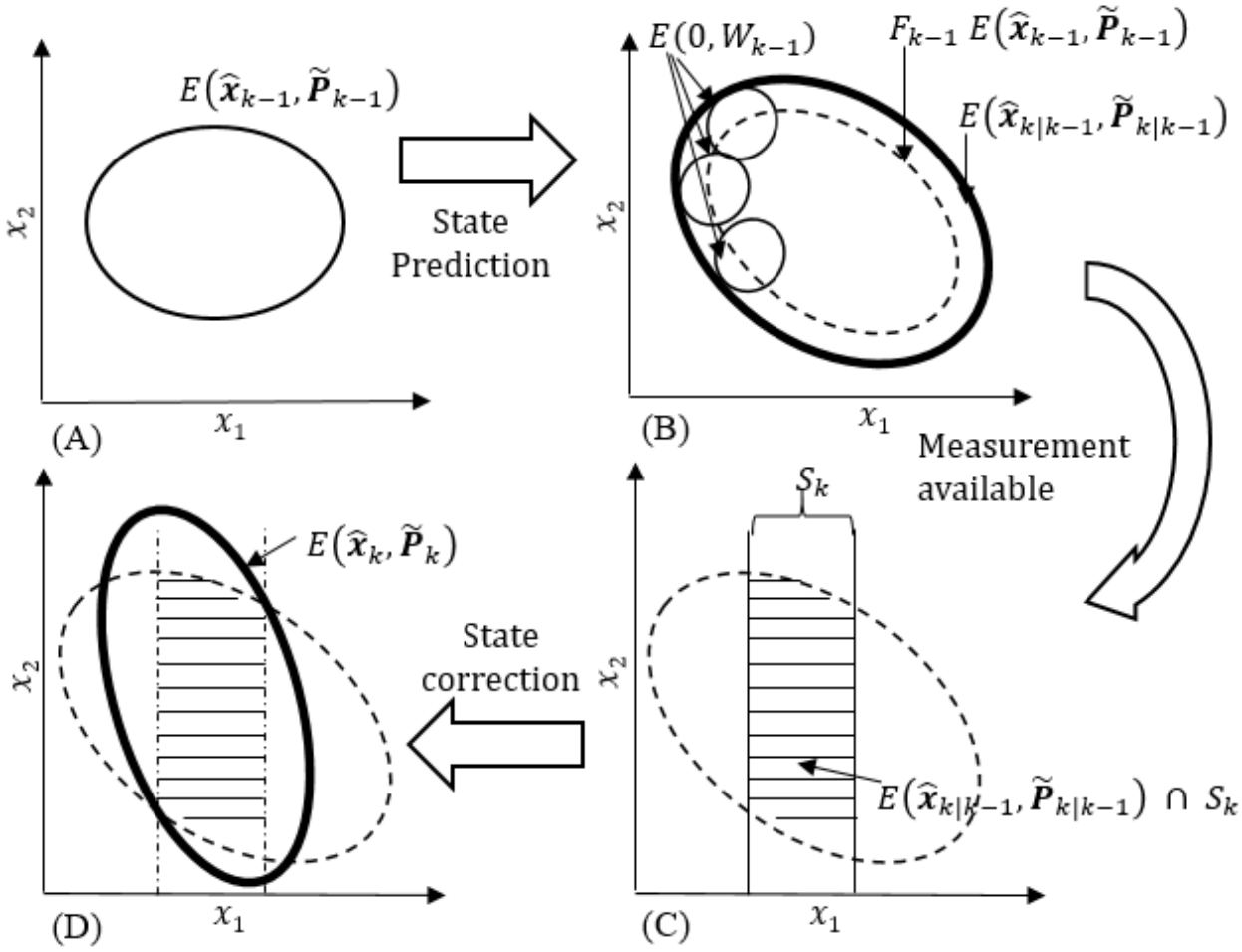

FIGURE 2.1: The logic behind the SM algorithm with ellipsoidal sets.

where

$$\hat{\mathbf{x}}_{k|k-1} = \mathbf{F}_{k-1}\hat{\mathbf{x}}_{k-1}, \tag{2.7}$$

$$\tilde{\mathbf{P}}_{k|k-1} = \frac{\mathbf{F}_{k-1}\tilde{\mathbf{P}}_{k-1}\mathbf{F}_{k-1}^T}{1-p_k} + \frac{\mathbf{W}_k}{p_k}, \tag{2.8}$$

and $0 \leqslant p_k \leqslant 1$ is a scalar parameter that defines the class. It is necessary to find an ellipsoid that contains the vector sum of the two ellipsoids which is optimal in some sense. In other

words, we have to find an optimal value for p_k. The geometric size of the ellipsoid can be used as a measure of optimality and can be measured using the volume of the ellipsoid. The volume of an ellipsoid is proportional to the square of the product of the lengths of its axes, which is referred to as the determinant criterion. An alternative measure of size is the sum of the squares of the semi-axis lengths, which is called the trace criterion. [26]. The trace criterion has certain advantages over the determinant criterion [26] and therefore will be used here. Various cost functions and criteria that can be used to minimize the size of an ellipsoid are summarized in Appendix C. An explicit solution to the problem of determining the optimal ellipsoid which contains the vector sum of ellipsoids can be found as described in [21, 26]. The optimal p_k based on the trace criterion for the predicted state set is given by,

$$p_k = \frac{\sqrt{trace(\mathbf{W}_k)}}{\sqrt{trace(\mathbf{F}_{k-1}\tilde{\mathbf{P}}_k\mathbf{F}_{k-1}^T)} + \sqrt{trace(\mathbf{W}_k)}}. \tag{2.9}$$

A complete set of calculations required to obtain the vector sum of two ellipsoids can be found in Appendix A.

2.2.2.2 Correction step

As mentioned earlier, the estimated state set is the intersection of two ellipsoids $E(\hat{\mathbf{x}}_{k|k-1}, \tilde{\mathbf{P}}_{k|k-1})$ and S_k, which will not be an ellipsoid. But an approximate ellipsoid set for the intersection

is derived in [20, 22]. The estimated state set can be given by [20] (see Appendix B),

$$\begin{aligned} E(\hat{\mathbf{x}}_k, \tilde{\mathbf{P}}_k) = \{\mathbf{x}_k \in \mathbb{R}^n : (1-\lambda_k)(\mathbf{x}_k - \hat{\mathbf{x}}_{k|k-1})^T \tilde{\mathbf{P}}_{k|k-1}^{-1}(\mathbf{x}_k - \hat{\mathbf{x}}_{k|k-1}) \\ + \lambda_k(\mathbf{z}_k - \mathbf{H}_k\mathbf{x}_k)^T \mathbf{V}_k^{-1}(\mathbf{z}_k - \mathbf{H}_k\mathbf{x}_k) \leq 1\}, \\ = \{\mathbf{x}_k \in \mathbb{R}^n : (\mathbf{x}_k - \hat{\mathbf{x}}_k)^T \tilde{\mathbf{P}}_k^{-1}(\mathbf{x}_k - \hat{\mathbf{x}}_k) \leq 1\}, \end{aligned}$$

where

$$\hat{\mathbf{x}}_k = \hat{\mathbf{x}}_{k|k-1} + \frac{\tilde{\mathbf{P}}_{k|k-1}}{1-\lambda_k}\mathbf{H}_k^T \left(\frac{\mathbf{H}_k \tilde{\mathbf{P}}_{k|k-1}\mathbf{H}_k^T}{1-\lambda_k} + \frac{\mathbf{V}_k}{\lambda_k}\right)^{-1} \boldsymbol{\delta}_k, \tag{2.10}$$

$$\tilde{\mathbf{P}}_k = \gamma_k^2 \left[\mathbf{I} - \frac{\tilde{\mathbf{P}}_{k|k-1}}{1-\lambda_k}\mathbf{H}_k^T \left(\frac{\mathbf{H}_k \tilde{\mathbf{P}}_{k|k-1}\mathbf{H}_k^T}{1-\lambda_k} + \frac{\mathbf{V}_k}{\lambda_k}\right)^{-1} \mathbf{H}_k\right] \frac{\tilde{\mathbf{P}}_{k|k-1}}{1-\lambda_k}, \tag{2.11}$$

$$\gamma_k^2 = 1 - \boldsymbol{\delta}_k^T \left(\frac{\mathbf{H}_k \tilde{\mathbf{P}}_{k|k-1}\mathbf{H}_k^T}{1-\lambda_k} + \frac{\mathbf{V}_k}{\lambda_k}\right)^{-1} \boldsymbol{\delta}_k, \tag{2.12}$$

$$\boldsymbol{\delta}_k = \mathbf{z}_k - \mathbf{H}_k \hat{\mathbf{x}}_{k|k-1}, \tag{2.13}$$

and $0 \leqslant \lambda_k \leqslant 1$ defines the set of ellipsoids which contains the intersection of ellipsoids found in the correction step. Finding an optimal ellipsoid for the updated state set is a problem of finding a proper value for λ_k. However, there is no known explicit solution to the problem of determining the optimal ellipsoid which bounds the intersection of two ellipsoids. But the optimum λ_k can be found by either minimizing the trace or the determinant of $\tilde{\mathbf{P}}_k$. An expression for the minimum trace of $\tilde{\mathbf{P}}_k$ can be found in [21]. Techniques that can be used to minimize the determinant or the trace of an ellipsoid that contains the intersection of two ellipsoids are described in [22, 28]. Further, due to computational complexity involved in the trace and the determinant criteria, a suboptimal but efficient criterion to minimize the size

of $\tilde{\mathbf{P}}_k$ would be to minimize a bound on γ_k^2 in (2.12). This leads to [47],

$$\lambda_k = \frac{\sqrt{maxeig(\mathbf{V}_k)}}{\sqrt{maxeig(\mathbf{H}_k \tilde{\mathbf{P}}_{k|k-1}^{-1} \mathbf{H}_k^T)} + \sqrt{maxeig(\mathbf{V}_k)}}, \tag{2.14}$$

where $maxeig(\mathbf{A})$ denotes the maximum eigenvalue of the matrix $\mathbf{A}$.

2.2.3 A strategy for data selective updates

Even though the standard structure of the SM algorithm already allows us to incorporate selective measurement updates in the correction step, it accompanies a significant computational complexity that can be undesirable in real-time state estimation [28]. However, by modifying the way ellipsoids are defined in (2.1), it is possible to obtain a low complexity selective update strategy. This approach, only gives a suboptimal ellipsoid bound for the intersection of two ellipsoids as required in (2.6). This method was first introduced in [17] and further studied in [43–45]. Furthermore, the application of the same method for state estimation in nonlinear dynamical systems has been studied in [46]. In the following, we describe the method discussed in [44, 45].

The method is based on expressing the shape matrix of the ellipsoid in (2.1) in the form $\tilde{\mathbf{P}} = \sigma^2 \mathbf{P}$, so that ellipsoid is defined as,

$$\begin{aligned} E(\mathbf{a}, \sigma^2 \mathbf{P}) &= \{\mathbf{x} \in \mathbb{R}^n : (\mathbf{x} - \mathbf{a})^T (\sigma^2 \mathbf{P})^{-1} (\mathbf{x} - \mathbf{a}) \leq 1\}, \\ &= \{\mathbf{x} \in \mathbb{R}^n : (\mathbf{x} - \mathbf{a})^T \mathbf{P}^{-1} (\mathbf{x} - \mathbf{a}) \leq \sigma^2\}, \end{aligned} \tag{2.15}$$

where σ^2 is a positive scalar which defines a bound on the size of $E(\mathbf{a}, \sigma^2\mathbf{P})$ based on the trace such that,

$$trace(E(\mathbf{a}, \sigma^2\mathbf{P})) = \sigma^2 \ \ trace(\mathbf{P}).$$

Also, σ^2 will have an effect on the volume of $E(\mathbf{a}, \sigma^2\mathbf{P})$ as,

$$Vol(E(\mathbf{a}, \sigma^2\mathbf{P})) = \sigma^{2n} \ \frac{\pi^{n/2}(det\ \mathbf{P})^{1/2}}{\Gamma(\frac{n}{2}+1)},$$

where Γ is the Eular gamma function [44]. The significance of this modification is that it allows us to use an alternative simple to use criterion to minimize the size of an ellipsoid.

Based on (2.15) we can express the shape matrix of the ellipsoid which contains the previous state estimates as $\tilde{\mathbf{P}}_{k-1} = \sigma^2_{k-1}\mathbf{P}_{k-1}$. The shape matrix of the predicted state ellipsoid is therefore $\tilde{\mathbf{P}}_{k|k-1} = \sigma^2_{k|k-1}\mathbf{P}_{k|k-1}$ where $\sigma^2_{k|k-1} = \sigma^2_{k-1}$. The prediction step equation (2.8) will be modified by substituting to $\tilde{\mathbf{P}}_{k-1} = \sigma^2_{k-1}\mathbf{P}_{k-1}$.

In the correction step, the intersection of the predicted state set and observation set will be contained in the ellipsoid

$$E(\hat{\mathbf{x}}_k, \sigma^2_k\mathbf{P}_k) \supset E(\hat{\mathbf{x}}_{k|k-1}, \sigma^2_{k|k-1}\mathbf{P}_{k|k-1}) \cap S_k,$$

which will be given by,

$$\begin{aligned} E(\hat{\mathbf{x}}_k, \sigma^2_k\mathbf{P}_k) = \{&\mathbf{x}_k \in \mathbb{R}^n : (1-\lambda_k)(\mathbf{x}_k - \hat{\mathbf{x}}_{k|k-1})^T\mathbf{P}^{-1}_{k|k-1}(\mathbf{x}_k - \hat{\mathbf{x}}_{k|k-1}) \\ &+ \lambda_k(\mathbf{z}_k - \mathbf{H}_k\mathbf{x}_k)^T\mathbf{V}^{-1}_k(\mathbf{z}_k - \mathbf{H}_k\mathbf{x}_k) \leq (1-\lambda_k)\sigma^2_{k|k-1} + \lambda_k\}, \\ = \{&\mathbf{x}_k \in \mathbb{R}^n : (\mathbf{x}_k - \hat{\mathbf{x}}_k)^T\mathbf{P}^{-1}_k(\mathbf{x}_k - \hat{\mathbf{x}}_k) \leq \sigma^2_k\}, \end{aligned}$$

where

$$\hat{\mathbf{x}}_k = \hat{\mathbf{x}}_{k|k-1} + \frac{\mathbf{P}_{k|k-1}}{1-\lambda_k}\mathbf{H}_k^T\left(\frac{\mathbf{H}_k\mathbf{P}_{k|k-1}\mathbf{H}_k^T}{1-\lambda_k} + \frac{\mathbf{V}_k}{\lambda_k}\right)^{-1}\boldsymbol{\delta}_k, \tag{2.16}$$

$$\mathbf{P}_k = \left[I - \frac{\mathbf{P}_{k|k-1}}{1-\lambda_k}\mathbf{H}_k^T\left(\frac{\mathbf{H}_k\mathbf{P}_{k|k-1}\mathbf{H}_k^T}{1-\lambda_k} + \frac{\mathbf{V}_k}{\lambda_k}\right)^{-1}\mathbf{H}_k\right]\frac{\mathbf{P}_{k|k-1}}{1-\lambda_k}, \tag{2.17}$$

$$\sigma_k^2 = (1-\lambda_k)\sigma_{k|k-1}^2 + \lambda_k - \boldsymbol{\delta}_k^T\left(\frac{\mathbf{H}_k\mathbf{P}_{k|k-1}\mathbf{H}_k^T}{1-\lambda_k} + \frac{\mathbf{V}_k}{\lambda_k}\right)^{-1}\boldsymbol{\delta}_k, \tag{2.18}$$

$$\boldsymbol{\delta}_k = \mathbf{z}_k - \mathbf{H}_k\hat{\mathbf{x}}_{k|k-1}. \tag{2.19}$$

After some straightforward manipulations we can rewrite (2.16 -2.18) as [45]

$$\begin{aligned}
\hat{\mathbf{x}}_k &= \hat{\mathbf{x}}_{k|k-1} + \mathbf{K}_k\boldsymbol{\delta}_k,\\
\mathbf{P}_k &= \frac{1}{1-\lambda_k}(\mathbf{I} - \mathbf{K}_k\mathbf{H}_k)\mathbf{P}_{k|k-1},\\
\sigma_k^2 &= (1-\lambda_k)\sigma_{k|k-1}^2 + \lambda_k - \boldsymbol{\delta}_k^T\mathbf{Q}_k^{-1}\boldsymbol{\delta}_k,\\
\mathbf{K}_k &= \frac{1}{1-\lambda_k}\mathbf{P}_{k|k-1}\mathbf{H}_k^T\mathbf{Q}_k^{-1},\\
\mathbf{Q}_k &= \frac{1}{1-\lambda_k}\mathbf{H}_k\mathbf{P}_{k|k-1}\mathbf{H}_k^T + \frac{1}{\lambda_k}\mathbf{V}_k.
\end{aligned}$$

A complete set of calculations required to obtain the intersection of two ellipsoids can be found in Appendix B. The optimum $\mathbf{P}_k$ is found by minimizing σ_k^2 with respect to λ_k which is a bound on the size of $\mathbf{P}_k$. Since minimizing σ_k^2 requires finding derivative of the matrix $\mathbf{Q}_k$ which is difficult, we minimize an approximate bound on σ_k^2 as proposed in [44, 45]. Taking the Cholesky factorization of $\mathbf{V}_k^{-1}$, an upper triangular matrix $\bar{\mathbf{V}}_k^T$ can be obtained,

i.e. $\mathbf{V}_k^{-1} = \bar{\mathbf{V}}_k^T \bar{\mathbf{V}}_k$ and (2.18) can be rewritten as,

$$\begin{aligned}\sigma_k^2 &= (1-\lambda_k)\sigma_{k|k-1}^2 + \lambda_k - \boldsymbol{\delta}_k^T \left(\frac{1}{1-\lambda_k} \mathbf{H}_k \mathbf{P}_{k|k-1} \mathbf{H}_k^T + \frac{1}{\lambda_k} (\bar{\mathbf{V}}_k^T \bar{\mathbf{V}}_k)^{-1} \right)^{-1} \boldsymbol{\delta}_k, \\ &= (1-\lambda_k)\sigma_{k|k-1}^2 + \lambda_k - \lambda_k(1-\lambda_k) \bar{\boldsymbol{\delta}}_k^T (\lambda_k \mathbf{G}_k + (1-\lambda_k)\mathbf{I})^{-1} \bar{\boldsymbol{\delta}}_k,\end{aligned}$$

where

$$\begin{aligned}\mathbf{G}_k &= \bar{\mathbf{V}}_k \mathbf{H}_k \mathbf{P}_{k|k-1} \mathbf{H}_k^T \bar{\mathbf{V}}_k^T, \\ \bar{\boldsymbol{\delta}}_k &= \bar{\mathbf{V}}_k \boldsymbol{\delta}_k.\end{aligned}$$

Then, a simplified but approximate bound on σ_k^2 can be obtained by assigning a scalar value to the matrix $(\lambda_k \mathbf{G}_k + (1-\lambda_k)\mathbf{I})$. Specifically, by taking $\bar{g}_k$ as the norm or the maximum eigenvalue of $\mathbf{G}_k$ we can write

$$\|\lambda_k \mathbf{G}_k + (1-\lambda_k)\mathbf{I}\|_2 \leqslant \lambda_k \bar{g}_k + 1 - \lambda_k.$$

The bound $\bar{\sigma_k^2}(\lambda_k)$ is given by,

$$\bar{\sigma_k^2}(\lambda_k) = (1-\lambda_k)\sigma_{k|k-1}^2 + \lambda_k - \lambda_k(1-\lambda_k) \frac{\bar{\boldsymbol{\delta}}_k^T \bar{\boldsymbol{\delta}}_k}{(1-\lambda_k) + \lambda_k \bar{g}_k}, \tag{2.20}$$

where $\bar{\sigma_k^2}(\lambda_k)$ is a convex function and if it has a local minimum for $\lambda_k \in (0,1)$. This local minimum can be found by solving

$$\frac{d\bar{\sigma_k^2}(\lambda_k)}{d\lambda_k} = 1 - \sigma_{k|k-1}^2 - \bar{\boldsymbol{\delta}}_k^T \bar{\boldsymbol{\delta}} \left(\frac{(1-\lambda_k)^2 - \lambda_k^2 \bar{g}_k}{(1-\lambda_k + \lambda_k \bar{g}_k)^2} \right) = 0.$$

This will yield

$$\lambda_k = \frac{1}{(1-\bar{g}_k)}\left(1 \pm \sqrt{\frac{\bar{g}_k}{(1+\beta_k(\bar{g}_k-1))}}\right),$$

where $\beta_k = \dfrac{1-\sigma^2_{k|k-1}}{\bar{\boldsymbol{\delta}}_k^T\bar{\boldsymbol{\delta}}_k}$. Since $\lambda_k \in (0,1)$, the optimum value of λ_k is

$$\lambda_k^* = \frac{1}{(1-\bar{g}_k)}\left(1 - \sqrt{\frac{\bar{g}_k}{(1+\beta_k(\bar{g}_k-1))}}\right).$$

But if the function $\bar{\sigma_k^2}(\lambda_k)$ is monotonically increasing function in (0,1) or if it has a critical point at $\lambda_k = 0$, then finding the minimum is not necessary. These conditions can be straightforwardly detected by considering the sign of the second derivative

$$\left.\frac{d\bar{\sigma_k^2}(\lambda_k)}{d\lambda_k}\right|_{\lambda_k=0} = 1 - \sigma^2_{k|k-1} - \bar{\boldsymbol{\delta}}_k^T\bar{\boldsymbol{\delta}},$$

The condition occurs if the second derivative is non-negative or equivalently

$$1 - \sigma^2_{k|k-1} - \bar{\boldsymbol{\delta}}_k^T\bar{\boldsymbol{\delta}} \geqslant 0,$$
$$\sigma^2_{k|k-1} + \bar{\boldsymbol{\delta}}_k^T\bar{\boldsymbol{\delta}} \leqslant 1.$$

If this is the case σ_k^2 will not have a minimum for $0 \leqslant \lambda_k \leqslant 1$. This yields following values for optimal λ_k,

$$\lambda_k^* = \begin{cases} 0 & \sigma_{k|k-1}^2 + \bar{\boldsymbol{\delta}}_k^T \bar{\boldsymbol{\delta}}_k \leq 1, \\ \dfrac{1-\beta_k}{2} & \bar{g}_k = 1, \\ \dfrac{1}{1-\bar{g}_k}\left[1 - \sqrt{\dfrac{\bar{g}_k}{1+\beta_k(\bar{g}_k - 1)}}\right] & \bar{g}_k \neq 1. \end{cases} \tag{2.21}$$

Detailed calculations are presented in Appendix D.

If $\lambda_k^* = 0$, we will have $\sigma_k^2 = \sigma_{k|k-1}^2$ and the estimated state ellipsoid will be the same as the predicted state ellipsoid. Since σ_k^2 depends on $\boldsymbol{\delta}_k$ which is the difference between actual measurement and the predicted measurement, the value of λ_k for which the minimum of σ_k^2 occur is an indication of the degree of innovation in the measurement observed at time k.

2.2.4 Extension to nonlinear dynamical systems

Application of the SM algorithms in nonlinear dynamical systems has been discussed in [21, 33, 35, 38, 39, 46]. In most of the work, non-linear dynamics were linearized about the current estimate, and the linearization errors were used to bound the membership sets. This is similar to the approach used in deriving the EKF. Consider the nonlinear dynamical

system given by the general state-space model

$$\mathbf{x}_k = f(\mathbf{x}_{k-1}) + \mathbf{w}_k, \tag{2.22}$$

$$\mathbf{z}_k = h(\mathbf{x}_k) + \mathbf{v}_k, \tag{2.23}$$

where $\mathbf{x}_k \in \mathbb{R}^n$ is the state vector and $\mathbf{z}_k \in \mathbb{R}^m$ is the measurement vector at time k. Additionally, it is assumed that both f and h are differentiable nonlinear functions having continuous first derivatives. To tackle the non-linearity, the same linearization approach used in EKF is used.

2.2.4.1 Prediction step

As before, the estimated state ellipsoid $E(\hat{\mathbf{x}}_{k-1}, \sigma^2_{k-1}\mathbf{P}_{k-1})$ contains the previous state $\mathbf{x}_{k-1}$. Assuming that the first order nonlinearities in the dynamical model are smooth, expanding $f(\mathbf{x}_{k-1})$ using Taylor series expansion about the center $\hat{\mathbf{x}}_{k-1}$ will yield

$$f(\mathbf{x}_{k-1}) = f(\hat{\mathbf{x}}_{k-1}) + \mathbf{F}_{k-1}\mathbf{e}_{k-1} + \epsilon_f(\mathbf{e}_{k-1}), \tag{2.24}$$

where $\mathbf{F}_{k-1} = \left.\dfrac{\partial f(\mathbf{x})}{\partial \mathbf{x}}\right|_{\mathbf{x}=\hat{\mathbf{x}}_{k-1}}$, $\mathbf{e}_{k-1} = \mathbf{x}_{k-1} - \hat{\mathbf{x}}_{k-1}$, and $\epsilon_f(\mathbf{e}_{k-1})$ indicates the terms involving the higher order derivatives which is considered as noise. Substituting (2.24) in (2.22) we can obtain a state equation linearized about $\hat{\mathbf{x}}_{k-1}$ and given by,

$$\mathbf{x}_k = f(\hat{\mathbf{x}}_{k-1}) + \mathbf{F}_{k-1}\mathbf{e}_{k-1} + \hat{\mathbf{w}}_k, \tag{2.25}$$

where $\hat{\mathbf{w}}_k = \epsilon_f(\mathbf{e}_{k-1}) + \mathbf{w}_k$. An ellipsoidal bound for $\hat{\mathbf{w}}_k$ must be determined by using suitable bounds for $\mathbf{w}_k$ in (2.22) as well as $\epsilon_f(\mathbf{e}_{k-1})$. Let this ellipsoid be defined by,

$$E(0, \hat{\mathbf{W}}_k) = \{\hat{\mathbf{w}} \in \mathbb{R}^n : (\hat{\mathbf{w}}^T \hat{\mathbf{W}}_k^{-1} \hat{\mathbf{w}}) \leq 1\}.$$

Given the estimated ellipsoid for $\mathbf{x}_{k-1}$ whose center is $\hat{\mathbf{x}}_{k-1}$, (2.25) can be used to find a prediction for a membership set for $\mathbf{x}_k$. Note that $\mathbf{e}_{k-1} = (\mathbf{x}_{k-1} - \hat{\mathbf{x}}_{k-1})$ is the error between predicted and true state at $(k-1)^{th}$ time step and represented by the ellipsoid $E(0, \sigma_{k-1}^2 \mathbf{P}_{k-1})$. In other words the $\mathbf{e}_{k-1}$ can be represented by an ellipsoid with shape matrix $\sigma_{k|k-1}^2 \mathbf{P}_{k|k-1}$ and origin as the center. This error ellipsoid can be transformed using $\mathbf{F}_{k-1}$ to obtain the predicted error ellipsoid at k^{th} time step. Substituting $\mathbf{x}_{k-1} = \hat{\mathbf{x}}_{k-1}$ in (2.25) we obtain the center of the transformed ellipsoid as $\hat{\mathbf{x}}_{k|k-1} = f(\mathbf{x}_{k-1})$, which is also the center of predicted state ellipsoid (2.4). This is illustrated in figure 2.2 for a two-state case. Taking the vector sum of the transformed ellipsoid and the noise ellipsoid $E(0, \hat{\mathbf{W}}_k)$ and using (2.7)-(2.8), we can obtain the predicted state ellipsoid (2.4) with center $\hat{\mathbf{x}}_{k|k-1} = f(\mathbf{x}_{k-1})$.

2.2.4.2 Correction step

Using arguments similar to those in previous section, linearizing (2.23) using Taylor series about $\hat{\mathbf{x}}_{k|k-1}$ will yield

$$\begin{aligned} \mathbf{z}_k &= h(\hat{\mathbf{x}}_{k|k-1}) + \mathbf{H}_k(\mathbf{x}_{k|k-1} - \hat{\mathbf{x}}_{k|k-1}) + \epsilon_h(\hat{\mathbf{x}}_{k|k-1}) + \mathbf{v}_k, \\ &= h(\hat{\mathbf{x}}_{k|k-1}) + \mathbf{H}_k(\mathbf{x}_{k|k-1} - \hat{\mathbf{x}}_{k|k-1}) + \hat{\mathbf{v}}_k, \end{aligned} \tag{2.26}$$

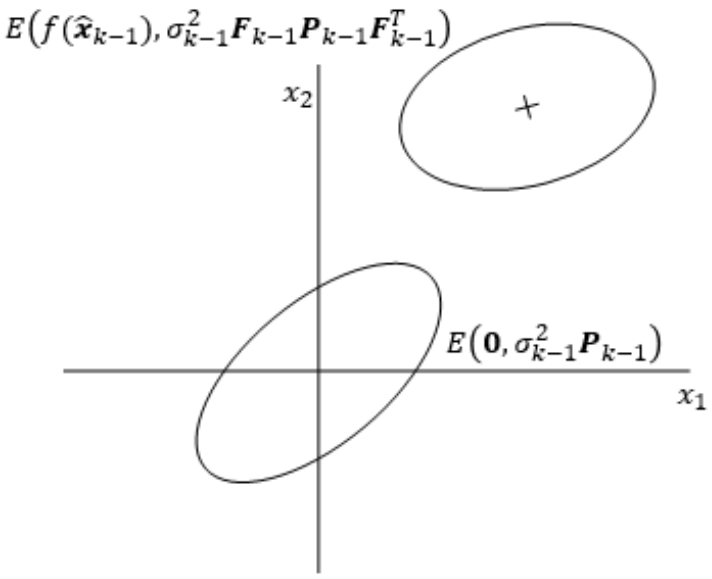

FIGURE 2.2: The linearization technique used in the prediction step of the SM algorithm.

where $\mathbf{H}_k = \left.\dfrac{\partial h(\mathbf{x})}{\partial \mathbf{x}}\right|_{\mathbf{x}=\hat{\mathbf{x}}_{k|k-1}}$, $\epsilon_h(\hat{\mathbf{x}}_{k|k-1})$ is the error due to higher order terms, and $\hat{\mathbf{v}}_k = \epsilon_h(\hat{\mathbf{x}}_{k|k-1}) + \mathbf{v}_k$. An ellipsoidal bound for $\hat{\mathbf{v}}_k$ can now be defined as,

$$E(0, \hat{\mathbf{V}}_k) = \{\hat{\mathbf{v}} \in \mathbb{R}^m : (\hat{\mathbf{v}}^T \hat{\mathbf{V}}_k^{-1} \hat{\mathbf{v}}) \leq 1\}.$$

Substituting $\hat{\mathbf{x}}_{k|k-1}$ in (2.26), we can find a prediction for the measurement $\mathbf{z}_k$ as, $\hat{\mathbf{z}}_k = h(\hat{\mathbf{x}}_{k|k-1})$. Then, the measurement prediction error is given by,

$$\boldsymbol{\delta}_k = \mathbf{z}_k - h(\hat{\mathbf{x}}_{k|k-1}). \tag{2.27}$$

The same equations as in the case of linear SM algorithm can be used in the correction step with $\boldsymbol{\delta}_k$ defined as in (2.27), and using the noise ellipsoid $E(0, \hat{\mathbf{V}}_k)$, to obtain updated state

ellipsoid.

Bounding of linearization noise using interval analysis techniques has been discussed in [39, 46] where $\epsilon_f(\hat{\mathbf{x}}_{k-1})$ is taken as the Lagrange remainder and an interval to bound the noise due to higher order terms has been found. This technique requires the calculation of the Hessians of the nonlinear functions $f(.)$ and $h(.)$. Therefore, the functions $f(.)$ and $h(.)$ should be twice differenciable with continuous first and second derivatives. This can add a significant complexity to the algorithm.

In this thesis, we have used estimates for linearization noise $\epsilon_f(\hat{\mathbf{x}}_{k-1})$ and $\epsilon_h(\hat{\mathbf{x}}_{k|k-1})$ obtianed by by trial and error. The interval bounding technique discussed in [21] has been used to obtain the initial noise ellipsoid $E(0, \hat{\mathbf{W}}_k)$ and $E(0, \hat{\mathbf{V}}_k)$. It has been assumed that noise ellipsoid do not vary with time.

Chapter 3

Properties of SM Algorithm: A Numerical Study

3.1 Introduction

The standard SM algorithm requires repeated application of a prediction step based on the state equations, and a corrections step when the current observations are available at each time step. A computationally efficient way to update the predicted state based on whether or not the current observations decrease the size of the state bounding set is discussed in the previous chapter. This modification can result in significant computational complexity savings when compared with standard SM algorithms. In this chapter, we will refer to the SM algorithm with a data-selective correction step update strategy as the SMU algorithm.

The main aim of this chapter is to use numerical examples to investigate the important properties of the SMU algorithm and evaluate the performance. To this end, we

compare the performance of the SMU algorithm with the standard SM algorithm. We use the classical KF algorithm as the baseline for evaluating the performance of the SM algorithms. Additionally, we will investigate the SMU algorithm's performance loss due to the use of the simplifying approximation given by (2.20) to decide on the data-selective update. For simplicity, we will refer to various SM algorithms considered in this chapter as follows

- SM 1 - standard SM algorithm where updated state set in correction step is derived by minimizing the determinant of $\tilde{\mathbf{P}}_k$,
- SM 2 - standard SM algorithm where updated state set in correction step is derived by minimizing the trace of $\tilde{\mathbf{P}}_k$,
- SM 3 - SMU algorithm where updated state set in correction step is derived by minimizing the approximated scaling factor σ_k^2 as given by (2.20) which minimizes the trace of $\mathbf{P}_k$, and
- SM 4 - SMU algorithm where updated state set in correction step is derived by minimizing the exact scaling factor σ_k^2 as given by (2.18) which minimizes the trace of $\mathbf{P}_k$.

3.2 Preliminaries

3.2.1 Performance criterion

The system performance has been evaluated using Monte-Carlo simulations. The estimation accuracy of each of the algorithm is measured by the time-averaged mean square error (MSE).

The instantaneous MSE is defined as,

$$e_{x_i}(k) = \frac{1}{S}\sum_{s=1}^{S}(x_{ik}^s - \hat{x}_{ik}^s)^2, \tag{3.1}$$

and then the time-averaged MSE is defined as,

$$\begin{aligned} e_{x_i} &= \frac{1}{S}\sum_{s=1}^{S}\frac{1}{K}\sum_{k=1}^{K}(x_{ik}^s - \hat{x}_{ik}^s)^2, \\ &= \frac{1}{K}\sum_{k=1}^{K} e_{x_i}(k), \end{aligned} \tag{3.2}$$

where S is the number of trials, K is the number of time steps per trial, x_{ik}^s is the i^{th} state variable at time step k in trial s, $\hat{x}_{ik}^s$ is the i^{th} state estimate at time step k in trial s and $i = 1, 2, 3, ..., n$ with n being the number of states.

Note that the size of the estimated state set or the updated state ellipsoid (2.6) in SM 1 and SM 2 will defer from those in SM 3 and SM 4 due to the selective correction step update strategy. To capture this difference, the volume of the updated state ellipsoid ($E(\hat{\mathbf{x}}_k, \tilde{\mathbf{P}}_k)$) is calculated at each time step (see (C.1) for volume calculation method). The number of times the SMU algorithms' perform the complete correction step has been observed as well.

3.2.2 System models

Two linear discrete-time system models and one non-linear discrete-time system model are considered to evaluate the performance of the SE algorithms. The two linear system models have been chosen so that one system is exactly-determined and the other is under-determined.

The under-determined system has been selected to evaluate the tracking capability of the algorithms under a lesser number of observations than the states.

Typically, a system will remain in steady state when there are no external disturbances or sudden changes in inputs. If that is the case, an algorithm can smoothly track the states. But in real world applications systems will be subjected to external disturbances which can cause sudden changes in the state. In the experiments to be presented below, we compare the robustness of SMU, SM, and KF algorithms against abrupt state changes caused by external disturbances. To this end, we investigate the behavior of all algorithms under steady state conditions (referred to as the steady state case) and in the presence of sudden disturbances (referred to as external disturbance case).

In most work related to SE, the system model uncertainties and measurement uncertainties are modeled as random variables with probability distributions. However, often the noise distributions can only be derived after observing the system for a considerable period of time. Furthermore, process noise can be represented by intervals easily, and the measurements obtained through sensors usually have limits. Therefore, in our numerical experiments, we assume that the uncertainties are uniformly distributed in pre-defined intervals. The noise ellipsoids for SM algorithms have been derived using the bounded interval methods discussed in [21]. Consider a noise interval vector $\mathbf{b} = [b_1^-, b_1^+; b_2^-, b_2^+]^T$. An ellipsoid which bounds the intervals can be obtained by defining a diagonal shape matrix $\mathbf{B}$ with diagonal elements

$$\mathbf{B}_{i,i} = 2(b_i^- - b_i^+)^2,$$

and center is the origin, where the subscript i represent a row, and the superscript $+$ and $-$

denote maximum and minimum values of the interval respectively. The noise covariance matrices for the KF algorithm have been derived by assuming that a noise interval corresponds to four standard deviations.

All numerical results presented in this section have been obtained by averaging over 100 Monte-Carlo simulations in MATLAB. In each Monte-Carlo trial, 10^5 time-steps have been used.

3.3 Numerical results

3.3.1 Linear system I

The linear system used in [43] with an additional measurement equation is considered as the completely determined linear system. This system has three states and three measurements, and is given by,

$$\mathbf{x}_k = \begin{pmatrix} 0 & 1 & 1 \\ 0 & 0 & 0.5 \\ -0.5 & 0 & 1 \end{pmatrix} \mathbf{x}_{k-1} + \mathbf{w}_k,$$

$$\mathbf{z}_k = \begin{pmatrix} 1 & 0 & 0 \\ 2 & -0.5 & -1 \\ 1 & -1 & 2 \end{pmatrix} \mathbf{x}_k + \mathbf{v}_k.$$

Table 3.1 shows the intervals for noise distributions. In the SE algorithms the initial state ellipsoid has been chosen to be $P_0 = diag(1, 1, 1)$, where $diag(x, y, z)$ is a diagonal matrix

TABLE 3.1: The intervals for noise distributions in the linear system I.

Variable	Interval
w_1	$(-0.003840, 0.003840)$
w_2	$(-0.001272, 0.001272)$
w_3	$(-0.002365, 0.002365)$
v_1	$(-0.003840, 0.003840)$
v_2	$(-0.006427, 0.006427)$
v_3	$(-0.006427, 0.006427)$

having x, y, z as diagonal elements. The initial scaling factor is set to $\sigma_0^2 = 1$, and the initial state is selected as $\mathbf{x}_0 = [2, 0.5, 0.8]^T$, which is the same as that used in the simulation.

3.3.1.1 Steady state case

In this case, all the states, as well as the measurements go to zero as the initial transients subside. The states estimated by each algorithm for the first 100 times steps are shown in figure 3.1. Table 3.2 provides the time-averaged MSE variation. It is evident from the results shown in table 3.2 that there is a trade-off between performing the complete correction step calculation at every time step and the selective correction step calculation, as the time-averaged MSE is higher in the SMU algorithms than the SM and the KF algorithms. Recall that both SM 3 and SM 4 only perform data-selective updates. It was observed that SM 3 performed the full correction step only 22.9% of the time and SM 4 only 23.4% of the time. Therefore, we can observe that the use of the simplified approximation in (2.20), does not result in any adverse effect on the complete correction step calculations. Furthermore, the estimation accuracies of SM 3 and SM 4 are nearly the same.

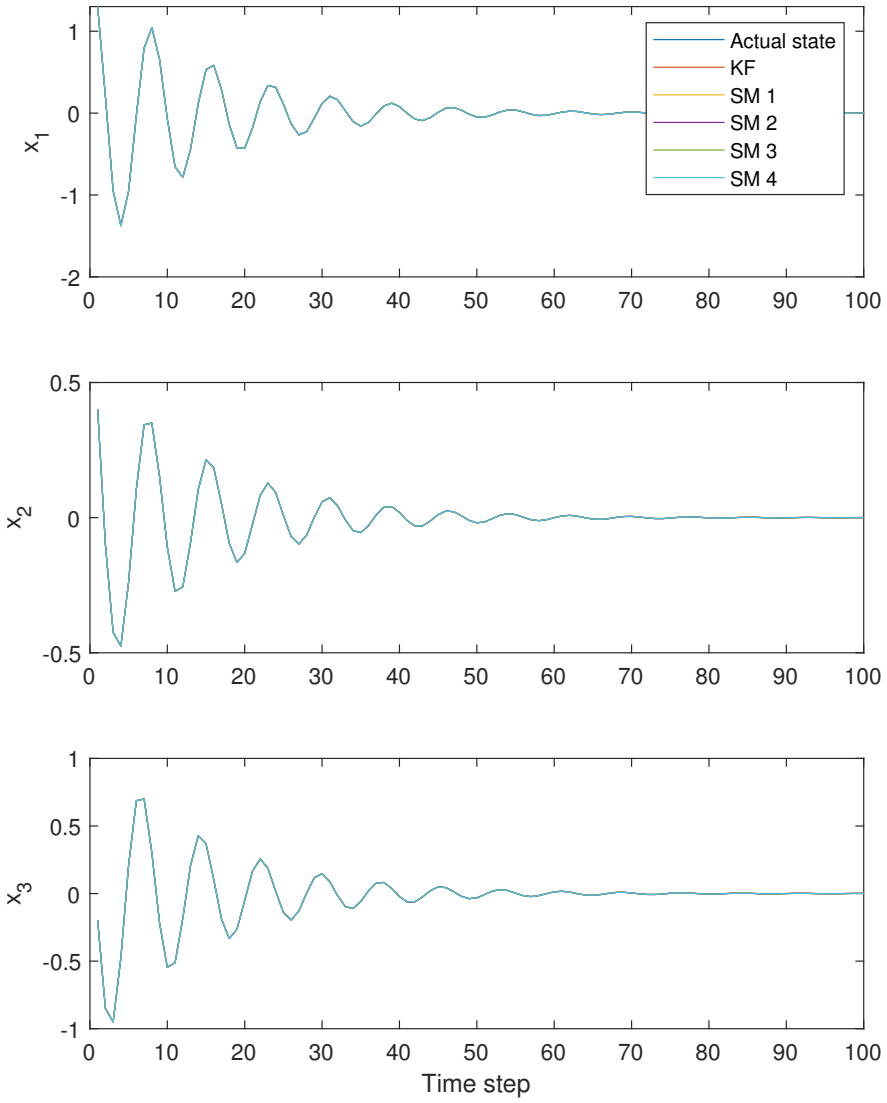

FIGURE 3.1: Steady state case - the estimation results comparison of the linear system I.

The comparisons of the volume of the updated state ellipsoid, given by (2.6) is shown in figure 3.2. The updated state sets obtained by the algorithms SM 3 and SM 4 have

TABLE 3.2: Steady state case - the time-averaged MSE in each state variable in the linear system I.

Algorithm	$e_{x_1}(\times 10^{-5})$	$e_{x_2}(\times 10^{-5})$	$e_{x_3}(\times 10^{-5})$
KF	0.1549	0.0845	0.1627
SM 1	0.1666	0.0930	0.1907
SM 2	0.1701	0.0976	0.2029
SM 3	1.4646	0.2186	0.8357
SM 4	1.2980	0.2003	0.7569

larger volumes compared with those obtained by the algorithms SM 1 and SM 2. Also, SM 3 and SM 4 algorithms take a longer time to reach a steady volume. This is another trade-off due to selective correction step calculations.

3.3.1.2 External disturbance case

A large external disturbance has been introduced to the system by adding an impulse $[0.7714, 0.5498, 0.7332]^T$, to the process noise vector at the 50000^{th} time step after the system achieved its steady state.

Figure 3.3 shows the estimates of the states a few time steps before and after the external disturbance is applied. Note that there are larger deviations in the state estimates produced by SM 1 and SM 2 algorithms compared to the KF algorithm. However, SM 3 and SM 4 algorithms appear to track the states better than SM 1 and SM 2 algorithms. This may be due to the fact that SM 1 and SM 2 use the determinant and the trace criteria respectively to obtain the updated state ellipsoid (2.6).

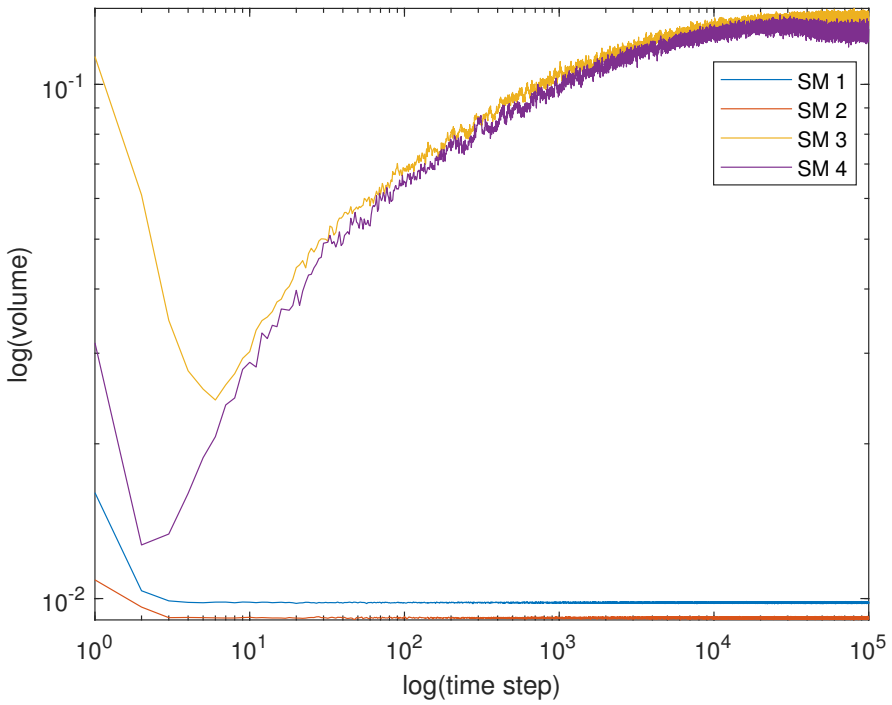

FIGURE 3.2: Steady state case - the comparison of volumes of the updated state ellipsoid in SM algorithms for the linear system I.

The time-averaged MSE comparison is shown in table 3.3. Both the SM 1 and SM 2, and the KF show relatively poor time-averaged MSEs for this case compared to the steady state case. On the other hand, the performance of the SMU algorithms, in this case, is comparable to the steady state case. As in the external disturbance case, the SMU algorithms performed corrective updates only for about 24% of the time which is about 1% higher than that of steady state case.

The comparisons of the volume of the updated state ellipsoid, given by (2.6) is shown in figure 3.4. The updated state sets obtained by the algorithms SM 3 and SM 4 have larger volumes compared with the volumes of the updated state sets obtained by the algorithms SM 1 and SM 2, as in the steady state case. Further, the abrupt volume changes

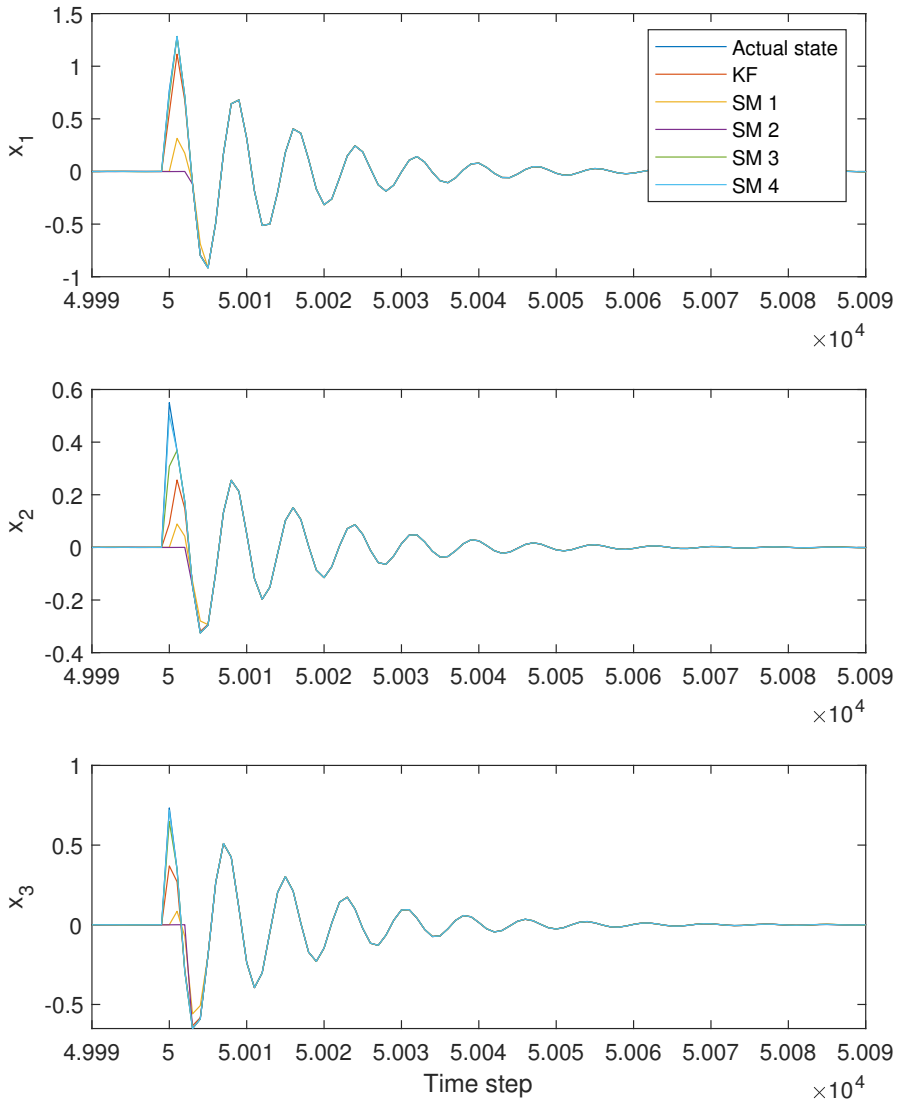

FIGURE 3.3: External disturbance case - the estimation results comparison of the linear system I.

in figure 3.4 are due to re-initializations. The re-initialization is a necessity in SM algorithms when there is a large disturbance. In this case, the predicted measurement will deviate largely

TABLE 3.3: External disturbance case - the time-averaged MSE in each state variable in the linear system I.

Algorithm	$e_{x_1}(\times 10^{-5})$	$e_{x_2}(\times 10^{-5})$	$e_{x_3}(\times 10^{-5})$
KF	0.2302	0.3093	0.3014
SM 1	2.0052	0.4922	0.8620
SM 2	2.9195	0.5643	0.9473
SM 3	1.4162	0.2718	0.8221
SM 4	1.2970	0.2021	0.7550

from the actual measurement, which will give an observation ellipsoid (2.5) outside of the predicted state ellipsoid (2.4). Then, the SM algorithms should be re-initialized to meet the initial assumptions before estimating the states again.

3.3.2 Linear system II

In this experiment, we use the linear discrete-time system considered in [27]. This system has three states and two measurements and is given by,

$$\mathbf{x}_k = \begin{pmatrix} 0 & 1 & 0 \\ 0 & 0 & 1 \\ 0.2 & -0.9 & 1.3 \end{pmatrix} \mathbf{x}_{k-1} + \mathbf{w}_k,$$

$$\mathbf{z}_k = \begin{pmatrix} 1.2 & 1.5 & -0.9 \\ -1.0 & 0.8 & 1.1 \end{pmatrix} \mathbf{x}_k + \mathbf{v}_k.$$

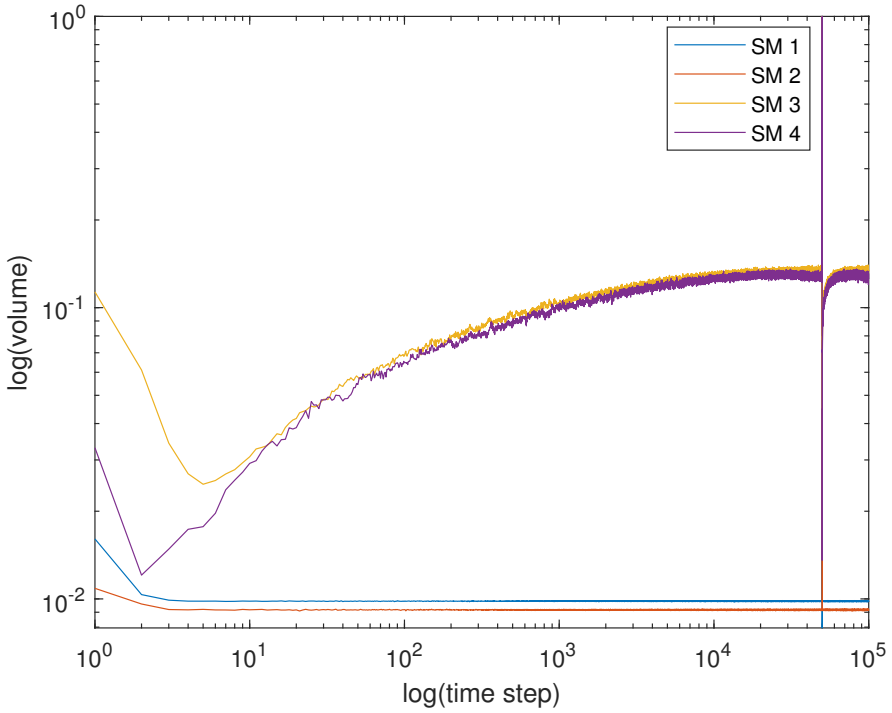

FIGURE 3.4: External disturbance case - the comparison of volumes of the updated state ellipsoid in SM algorithms for the linear system I.

The process and measurement noise are considered to be uniformly distributed in the intervals given in table 3.4 for each of the three states and the two measurements. In the SE algorithms, the initial state ellipsoid has been chosen to be $P_0 = diag(10, 10, 10)$. The initial scaling factor is set to $\sigma_0^2 = 1$, and the initial state is selected as $\mathbf{x}_0 = [4, 0.8, 1]^T$, which is the same as that used in the simulation.

The performance of the SE algorithms has been evaluated using the same criterion as in the previous example. Also, as before two scenarios were considered, the steady state case and the external disturbance case.

TABLE 3.4: The intervals for noise distributions in the linear system II.

Variable	Interval
w_1	$(-0.002036, 0.002036)$
w_2	$(-0.001773, 0.001773)$
w_3	$(-0.001431, 0.001431)$
v_1	$(-0.004259, 0.004259)$
v_2	$(-0.002601, 0.002601)$

3.3.2.1 Steady state case

In this system, all the states and the measurements go to zero after the initial transients are subsided. The state estimated by each algorithm for the first 100 times steps, which show both the transient and steady state behaviors are shown in figure 3.5. Table 3.5 shows the time-averaged MSE of the algorithms. Here also, it is evident that there is a trade-off between performing complete correction step at every time step, and at only some time steps. The time-averaged MSEs of the SMU algorithms are higher than those of the KF and the standard SM algorithms. Most importantly, the SM 3 and SM 4 algorithms performed the correction step only 18% and 19% of total time steps respectively. The accuracy of the SM 3 algorithm is still comparable to that of the SM 4 algorithm.

The volume comparison of the updated state ellipsoid given by (2.6) is presented in figure 3.6. Here also, the updated state ellipsoid obtained by the algorithms SM 3 and SM 4 have larger volumes compared with those obtained by the algorithms SM 1 and SM 2. Also, SM 3 and SM 4 algorithms take more time to reach a steady volume.

The updated state ellipsoids (2.6) calculated by the SMU algorithms have larger volumes than those calculated by the standard SM algorithms, due to selective correction

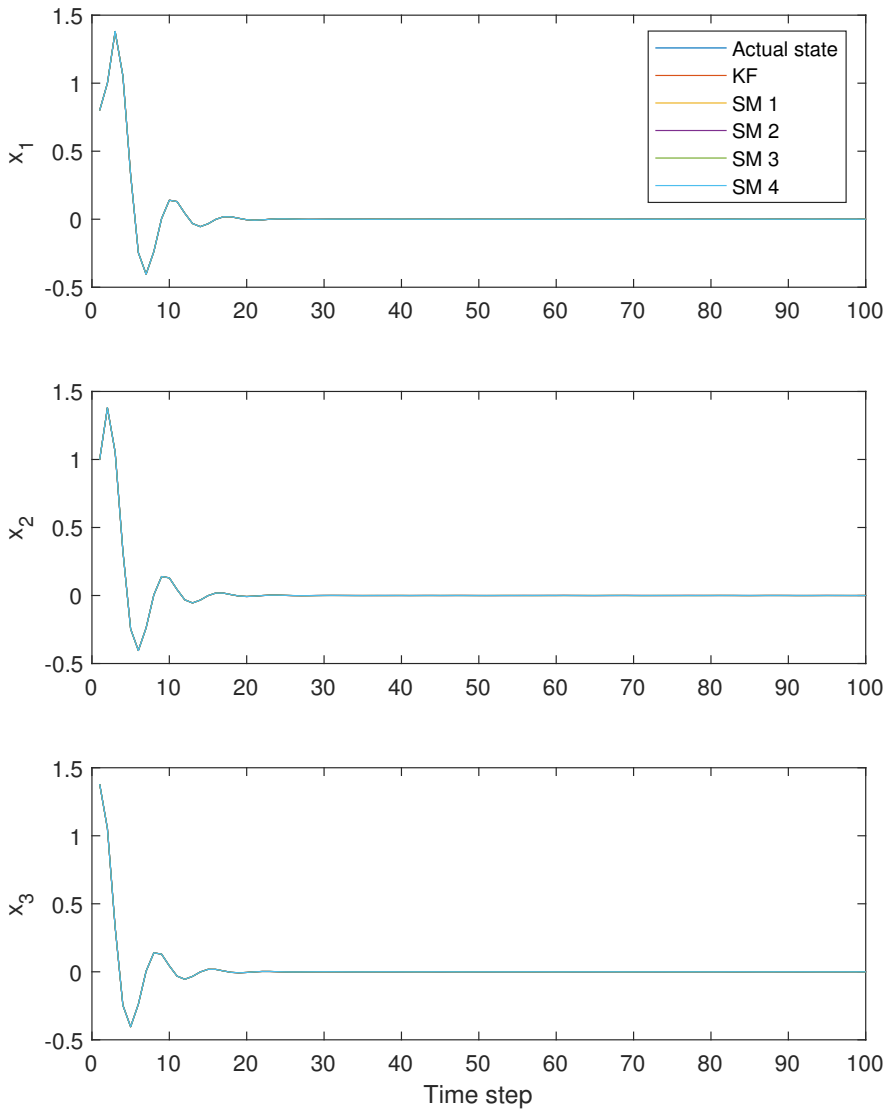

FIGURE 3.5: Steady state case - the estimation results comparison of the linear system II.

step updates. As mentioned earlier, the complete correction step will be done only if the observation data contains new information. If this is not the case, then the predicted values

TABLE 3.5: Steady state case - the time-averaged MSE in each state variable in the linear system II.

Algorithm	$e_{x_1}(\times 10^{-5})$	$e_{x_2}(\times 10^{-5})$	$e_{x_3}(\times 10^{-5})$
KF	0.1148	0.0807	0.1142
SM 1	0.1301	0.0976	0.1329
SM 2	0.1253	0.0901	0.1267
SM 3	0.5230	0.4536	0.3828
SM 4	0.4785	0.4180	0.3606

will be taken as the estimate, and the parameter σ_k^2 will not change until there is a complete correction step calculation. But the volume of the ellipsoid obtained in the prediction step will increase in each time step, as it is the sum of the previous state ellipsoid and the process noise ellipsoid. Also, there is no factor other than σ_k^2 to limit the volume of the predicted and the updated state ellipsoids, and therefore, the volume keeps growing until it reaches a steady volume.

3.3.2.2 External disturbance case

A large disturbance is applied to the system after it achieved its steady state. An impulse of $[1.5427, 1.0995, 1.4664]^T$ is added to the process noise vector at the 50000^{th} time step to simulate the external disturbance.

Figure 3.7 depicts the effect of the external disturbance on the estimated states, which shows a few time steps before and after the external disturbance is applied. It can be seen that SMU algorithms can track the state better than the SM algorithms as well as the KF algorithm. The time-averaged MSE comparison is shown in table 3.6. Here, the SMU

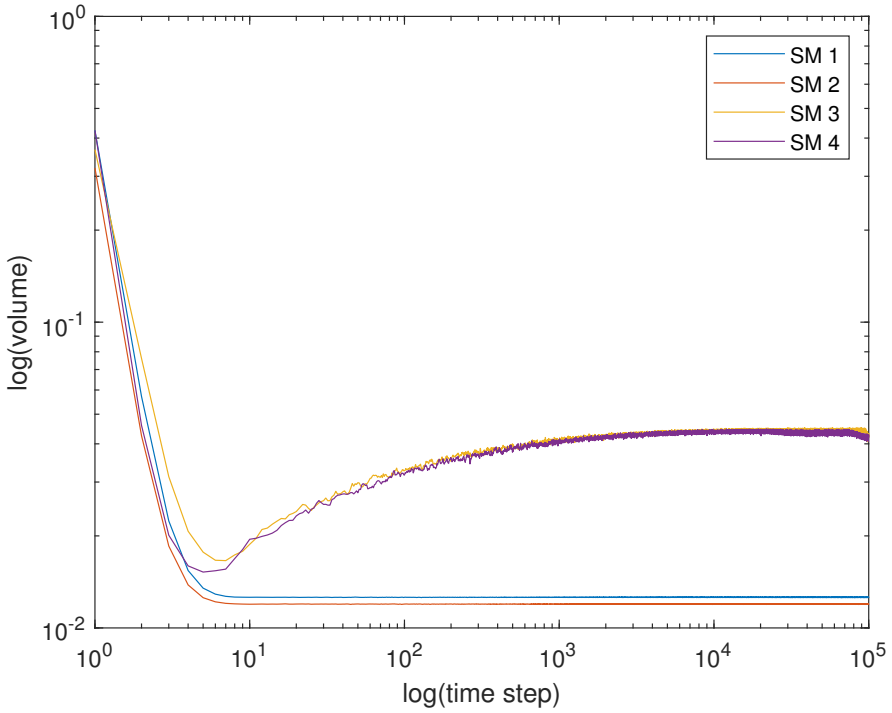

FIGURE 3.6: Steady state case - the comparison of volumes of the updated state ellipsoid in SM algorithms for the linear system II.

algorithms have a lower time-averaged MSE than the SM and KF algorithms. Both SM 3 and SM 4 algorithms performed the correction step only $18 - 20\%$ of the time.

The volume comparison of updated state sets in each SM algorithms is presented in figure 3.8. Here also, the updated state set volumes are larger in both the SMU algorithms when compared with the SM 1 and 2.

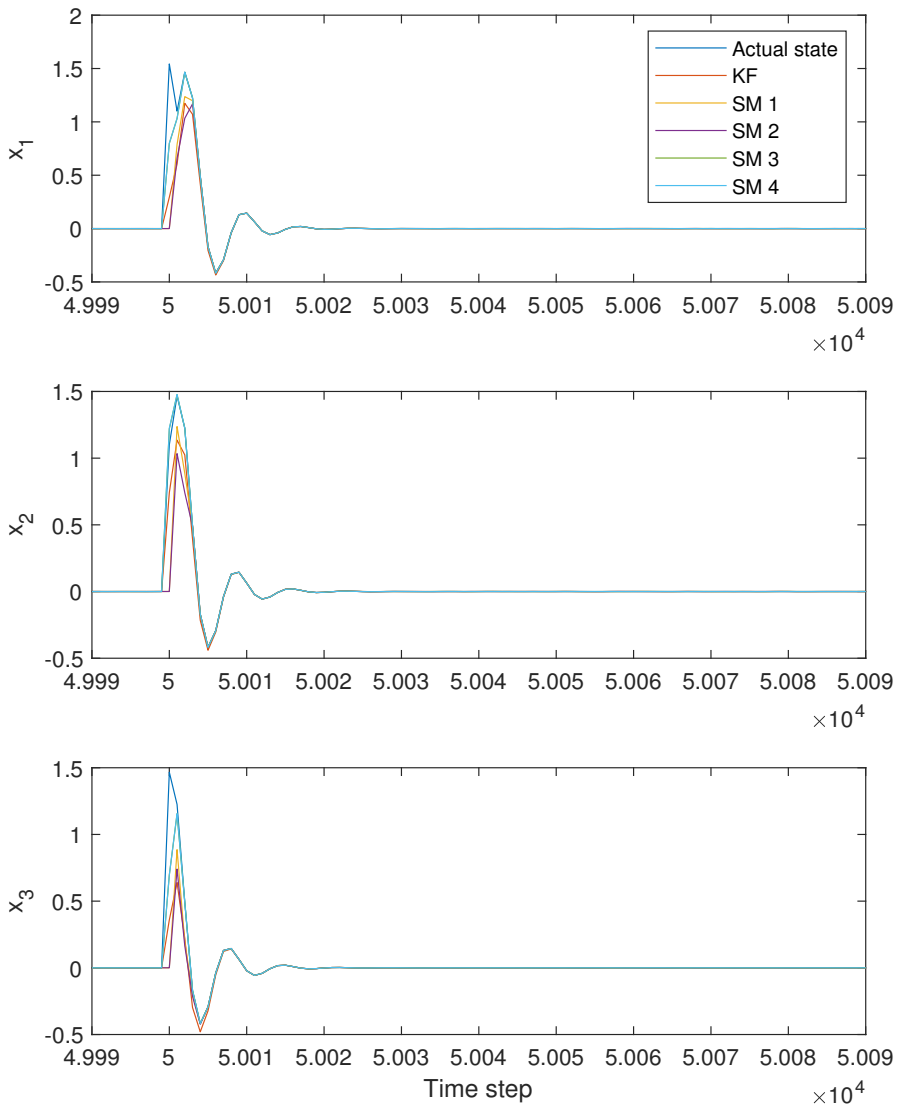

FIGURE 3.7: External disturbance case - the estimation results comparison of the linear system II.

TABLE 3.6: External disturbance case - the time-averaged MSE in each state variable in the linear system II.

Algorithm	$e_{x_1}(\times 10^{-4})$	$e_{x_2}(\times 10^{-4})$	$e_{x_3}(\times 10^{-4})$
KF	0.2039	0.0372	0.1781
SM 1	0.2662	0.1475	0.2487
SM 2	0.2890	0.1721	0.2622
SM 3	0.1079	0.0466	0.0982
SM 4	0.1042	0.0440	0.0962

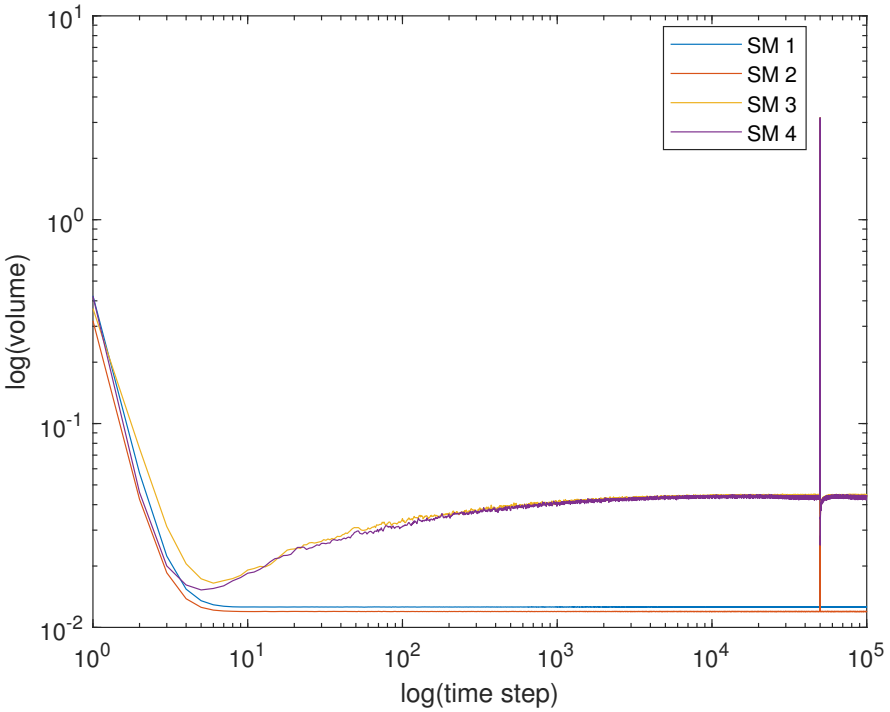

FIGURE 3.8: External disturbance case - the comparison of volumes of the updated state ellipsoid in SM algorithms for the linear system II.

3.3.3 Non-linear system

In order to assess the performance of the SMU algorithm in non-linear systems, a spring-mass-damper system given in [40] has been considered. The system is shown in figure 3.9 and described by the second-order non-linear differential equation (*Duffing's equation*),

$$\frac{d^2y}{dt^2} + k_0 y(1 + k_d y^2) + c\frac{dy}{dt} = 0, \tag{3.3}$$

where y is the displacement, $\frac{dy}{dt}$ is the velocity, $c = 1.2$ is the damping constant, and the two constants $k_0 = 1.5$ and $k_d = 3$. Converting (3.3) to a discrete time state-space representation yields

$$\mathbf{x}_k = \begin{pmatrix} x_{1,k-1} + \Delta t\, x_{2,k-1} \\ x_{2,k-1} + \Delta t\, (-k_0 x_{1,k-1}(1 + k_d x_{1,k-1}^2) - c x_{2,k-1}) \end{pmatrix} + \mathbf{w}_k,$$

$$\mathbf{z}_k = \begin{pmatrix} 1 & 0 \end{pmatrix} \mathbf{x}_k + \mathbf{v}_k,$$

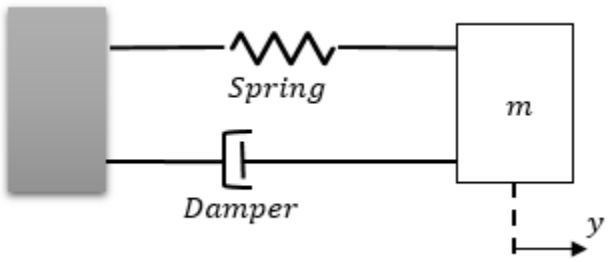

FIGURE 3.9: spring-mass-damper system

TABLE 3.7: The intervals for noise distributions in the non-linear system.

Variable	Interval
w_1	$(-0.01010, 0.01010)$
w_2	$(-0.01550, 0.01550)$
v_1	$(-0.01010, 0.00384)$

where

$$\begin{pmatrix} x_1 \\ \\ x_2 \end{pmatrix} = \begin{pmatrix} y \\ \\ \dfrac{dy}{dt} \end{pmatrix}.$$

For each of the two states and measurement, process and measurement noise are considered to be distributed uniformly in the intervals given in table 3.7. The initial state ellipsoid has been chosen to be $P_0 = diag(1, 1)$, $\sigma_0^2 = 1$ and the initial state is $\mathbf{x}_0 = [0.8, -0.2]^T$. The simulation has also been initialized with the same initial state.

3.3.3.1 Steady state case

In this system, after the initialization of the simulation, all the states as well as the measurements will reach a steady state value of zero.

Figure 3.10 shows the state calculated by each algorithm for the first 2000 times steps. Both the transient and steady state behaviors are shown here. Table 3.8 shows the time-averaged MSE of each algorithm. Here also, it is evident that there is a trade-off in performing selective correction steps, the time-averaged MSEs are relatively higher in SMU algorithms than in the KF and the standard SM algorithms. It was observed that SM 3

and SM 4 respectively performed the correction step only 20.1% and 22.6% of the time. Therefore, we note that the use of the simplifying approximation in (2.20) slightly decrease the number of complete correction step calculation. Further, the estimation accuracies of SM 3 and SM 4 are nearly the same.

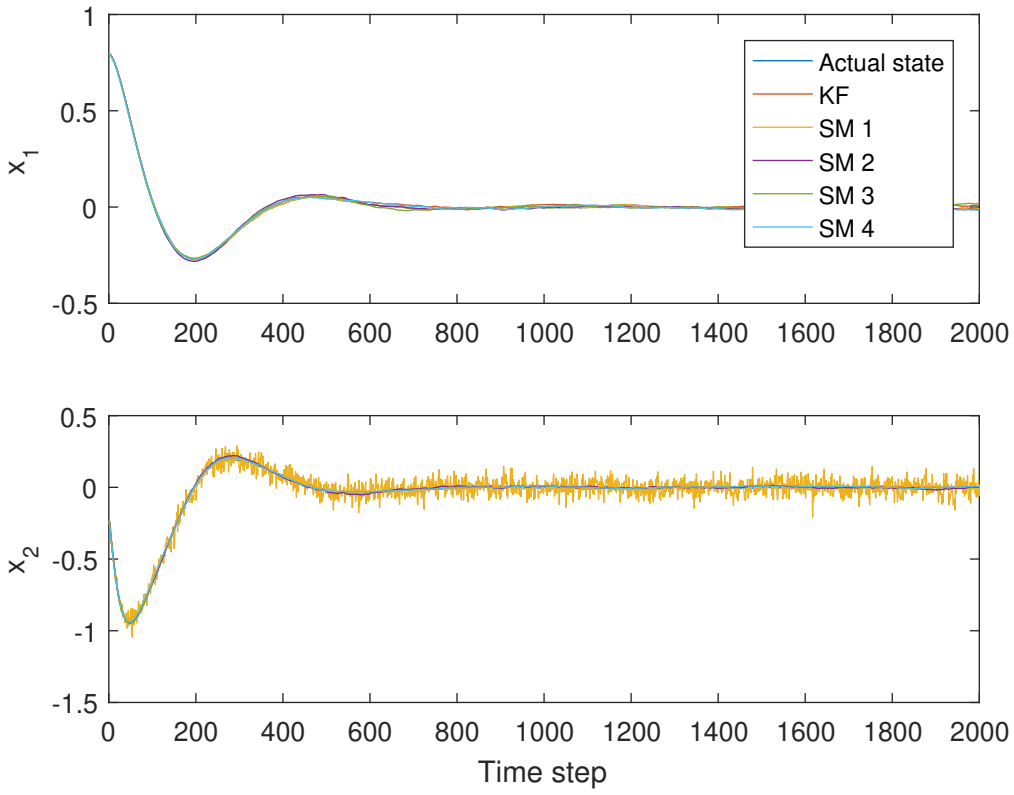

FIGURE 3.10: Steady state case - the estimation results comparison of the non-linear system.

Figure 3.11 shows the volume comparison of the estimated state set in each time step. The volume of the updated state sets obtained by the SM 1 algorithm is larger in this case. Also, the volumes of the updated state sets obtained by SM 3 and SM 4 algorithms are larger than those obtained by SM 2 as well. Furthermore, SM 3 and SM 4 algorithms

TABLE 3.8: Steady state case - the time-averaged MSE in each state variable in the non-linear system.

Algorithm	$e_{x_1}(\times 10^{-4})$	$e_{x_2}(\times 10^{-3})$
KF	0.2109	2.5852
SM 1	0.3397	211.3
SM 2	0.2161	3.1570
SM 3	1.1115	2.7242
SM 4	1.0905	2.7135

take a longer time to reach a steady volume. The time-averaged MSE performance is poor for state x_2 when estimated using the SM 1 algorithm. This is due to the disadvantages of the determinant criterion used in this algorithm to obtain updated state ellipsoid, which is discussed in [26].

3.3.3.2 External disturbance case

After the system reached its steady state, a large external disturbance was applied to the system. An impulse of $[0.7419, -0.8527]^T$ is added to the process noise vector at 50000^{th} time step to create this external disturbance.

Figure 3.12 shows the state estimates a few time steps before and after the external disturbance. Here, the estimate for x_2 produced by SM 1 shows a larger deviation after the disturbance. The time-averaged MSE comparison is shown in table 3.9. All the algorithms show almost the same time-averaged MSE for this case compared to the steady state case. In this case the SMU algorithms performed corrective updates only for about 19.3% of the time for SM 3 and 22.1 % for SM 4.

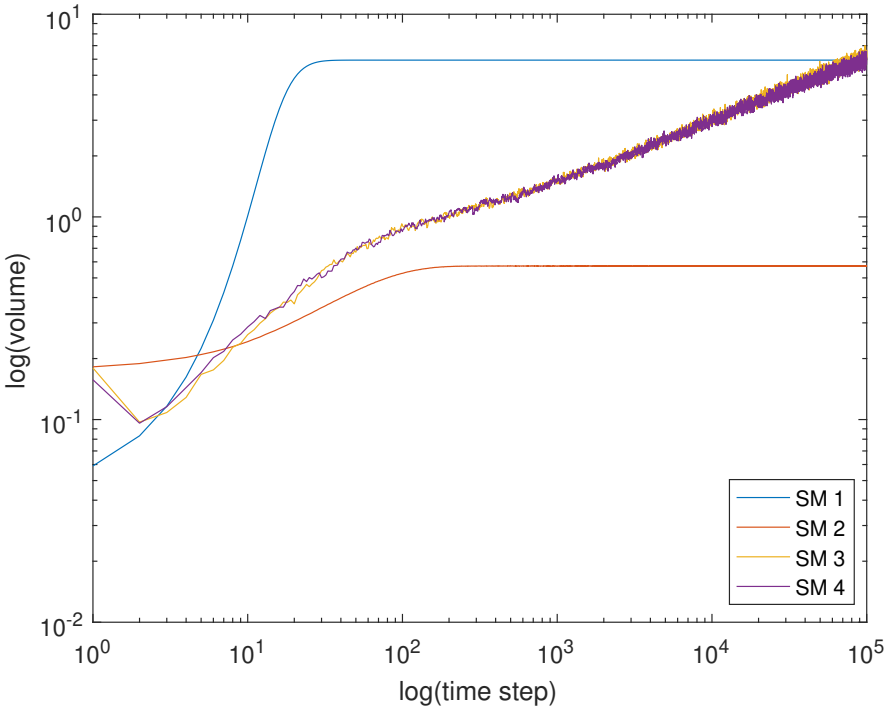

FIGURE 3.11: Steady state case - the comparison of volumes of the updated state ellipsoid in SM algorithms for the non-linear system.

TABLE 3.9: External disturbance case - the time-averaged MSE in each state variable in the non-linear system.

Algorithm	$e_{x_1}(\times 10^{-4})$	$e_{x_2}(\times 10^{-3})$
KF	0.2203	3.1219
SM 1	0.3400	228.5
SM 2	0.2979	3.3853
SM 3	1.2717	3.0459
SM 4	1.2147	3.0109

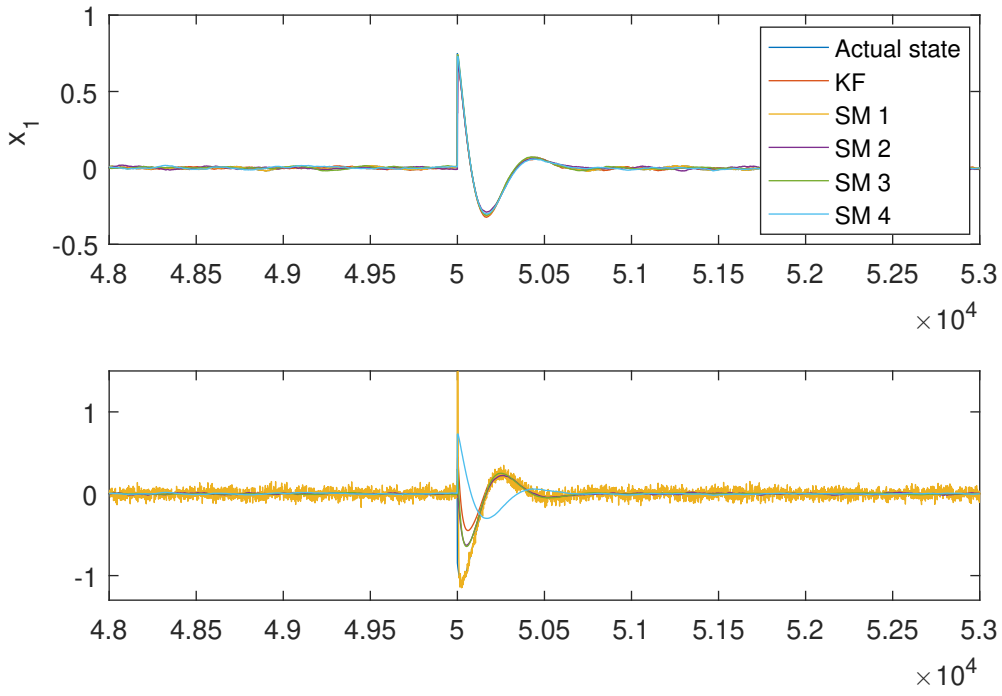

FIGURE 3.12: External disturbance case - the estimation results comparison of the non-linear system.

A comparison of the volume of the updated ellipsoid given by (2.6) is presented in figure 3.13. As in the steady state case, the volumes of updated state sets obtained by the algorithms SM 3 and SM 4 are larger than the volume of updated state sets obtained by the SM 2 algorithm. Further, the abrupt volume change is due to re-initialization as explained in section 3.3.1.2.

3.3.4 The effect of $\sigma_k^2(\lambda_k)$ and $\bar{\sigma}_k^2(\lambda_k)$ minimization

There is always a difference between the time-averaged MSEs, the volume of the updated state sets and the number of correction step percentages of the SM 3 and SM 4. This is

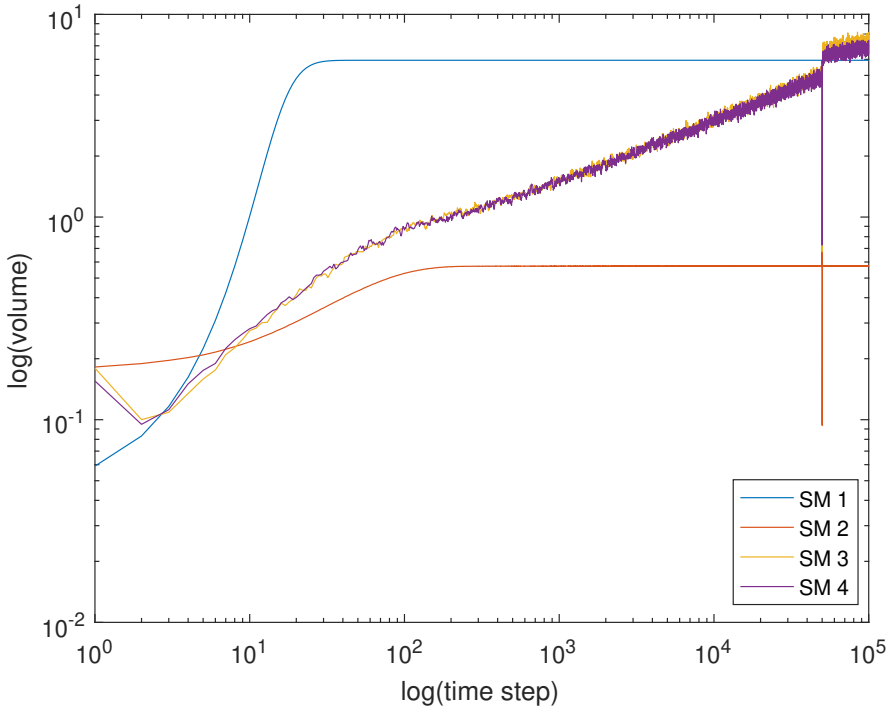

FIGURE 3.13: External disturbance case - the comparison of volumes of the updated state ellipsoid in SM algorithms for the non-linear system.

because the SM 3 uses the $\bar{\sigma}_k^2(\lambda_k)$ minimization criterion, and the SM 4 uses the $\sigma_k^2(\lambda_k)$ minimization criterion, to obtain the updated state set. To illustrate the difference between the criteria and to show that $\bar{\sigma}_k^2(\lambda_k) \geqslant \sigma_k^2(\lambda_k)$, linear system I has been used.

Figures 3.14, 3.15 and 3.16 show the $\sigma_k^2(\lambda_k)$ curve in (2.18) and $\bar{\sigma}_k^2(\lambda_k)$ (*App* $\sigma_k^2(\lambda_k)$, where *app* stands for approximate) curve in (2.20) for arbitrary three separate time steps. The point σ_k^2 shows the actual value used in the SM 3 algorithm, *True min* denote the true minimum of the curve $\sigma_k^2(\lambda_k)$ and *True app min* represent the true minimum of the curve $\bar{\sigma}_k^2(\lambda_k)$ at a particular time step.

Figure 3.14 shows a case where the approximated minimum is very close to the true

minimum of $\sigma_k^2(\lambda_k)$. Figure 3.15 shows the $\sigma_k^2(\lambda_k)$ and $\bar{\sigma}_k^2(\lambda_k)$ curves when the decision is made to skip the complete correction step calculation. Figure 3.16 show a situation where the approximated minimum is deviating considerably from the true minimum of $\sigma_k^2(\lambda_k)$. The difference between the time-averaged MSEs, the updated state set volumes, and the number of correction step percentages of the SM 3 and the SM 4 are mainly caused by the deviations between the approximated and true minimums. Further, a large deviation between the approximated and true minimums at a given time step will affect the next time step and therefore the deviation will accumulate in time, due to the differences in σ_k^2 values calculated. Further, it was observed in this case $\sigma_k^2(\lambda_k) \leqslant \bar{\sigma}_k^2(\lambda_k)$.

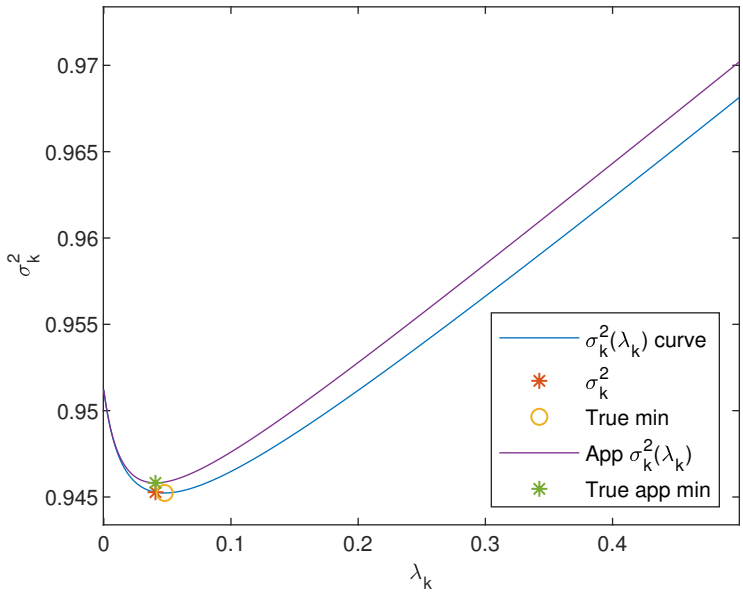

FIGURE 3.14: Case 1 - $\sigma_k^2(\lambda_k)$ and $\bar{\sigma}_k^2(\lambda_k)$ curves.

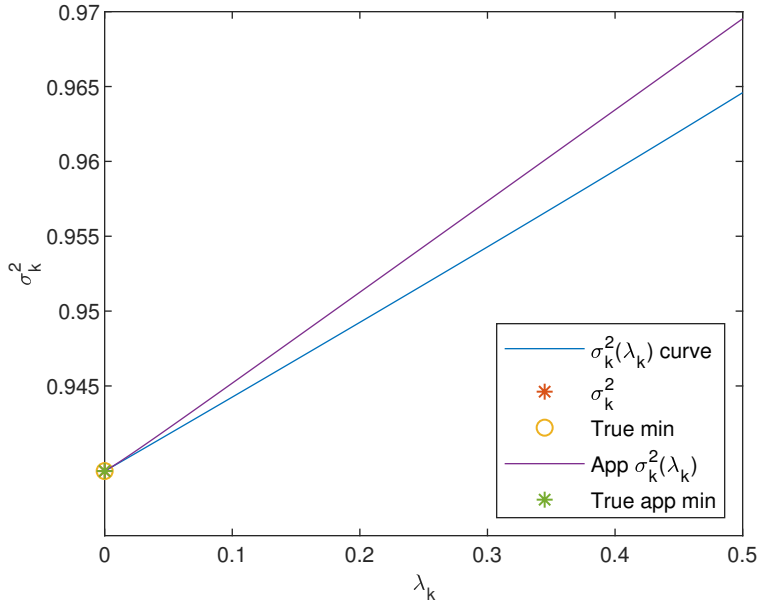

FIGURE 3.15: Case 2 - $\sigma_k^2(\lambda_k)$ and $\bar{\sigma}_k^2(\lambda_k)$ curves.

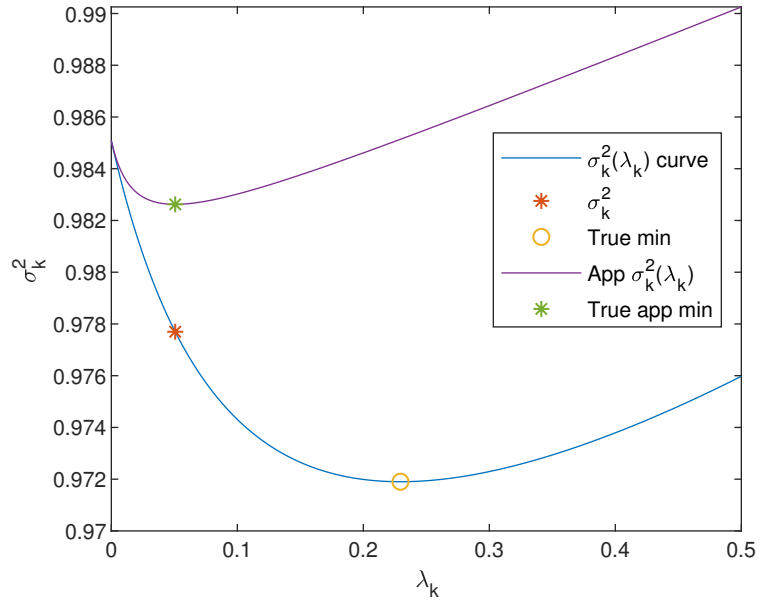

FIGURE 3.16: Case 3 - $\sigma_k^2(\lambda_k)$ and $\bar{\sigma}_k^2(\lambda_k)$ curves.

3.4 Discussion

The center of the updated state set can be used as the point estimate when considering the SM algorithms. Even with selective correction steps, the SMU algorithm achieves estimation results comparable with those of the standard SM and the KF algorithms. These estimation results also indicate that not all the measurements contain important information about the state of a system.

The ellipsoid $E(\mathbf{a}, \sigma^2\mathbf{P})$ is defined by a shape matrix ($\sigma^2\mathbf{P}$) which is symmetric positive definite, and the center $\mathbf{a}$ in (2.15). Therefore, in all SM algorithms, the shape matrices describing the predicted as well estimated ellipsoids at each time step should meet the symmetric positive definite criterion. Consider a time instant, where the error between predicted and true measurements are large enough, and that there will be no intersection between observation set S_k in (2.5) and $E(\hat{\mathbf{x}}_{k|k-1}, \sigma_k^2\mathbf{P}_{k|k-1})$ in (2.4). This will result in an empty set, which will be indicated by a negative σ_k^2 even when $\lambda_k \in (0, 1)$. In this case, the estimated ellipsoid is undefined. In this thesis, when a negative σ_k^2 is detected, the algorithm is re-initialized with an ellipsoid having the shape matrix $\mathbf{P}_0$, $\sigma_0^2 = 1$ and $\hat{\mathbf{x}}_k$ calculated at that time instant as the center. The calculated $\hat{\mathbf{x}}_k$ is used, since it was observed that it is likely to be a better initialization than a random vector. As explained earlier the abrupt volume differences shown in figures 3.2, 3.6 and 3.11 were due to this type of re-initialization.

It has been noted that, the initial state ellipsoid $\sigma_0^2\mathbf{P}_0$, the process noise ellipsoid $\mathbf{W}_k$, and the measurement noise ellipsoid $\mathbf{V}_k$ will affect the performance of the SMU algorithm. The process noise ellipsoid will affect the predicted state ellipsoid at every time step, and the measurement noise ellipsoid will affect the estimated state ellipsoid at selective time steps.

Chapter 4

A Power System Case Study

4.1 Introduction

An electric power system will convert the naturally available energy to the electric form and transport it to consumers over a transmission network. Since the electricity cannot be stored conveniently in sufficient quantities, the power system must maintain an appropriate balance over the generation and transmission due to continually changing demand. In order to analyze the security of a power system and design appropriate control strategies, the power systems operating conditions are categorized into five states, namely, normal, alert, emergency, in extremis, and restorative. If the system can remain in a normal state after the development of a contingency from a list of critical contingencies, then a normal state is defined secure. Typically, contingencies will vary from transmission line outages to generator outages due to unexpected failures of equipment or natural causes like storms. However, if the system has been disturbed and has entered an insecure state, power system control will help bring it to a normal state. [48, 67].

The stability of a power system will aid in maintaining a normal operating condition, after it has been disturbed. As a wide range of devices with different response rates and characteristics affect the dynamic performance of a power system, the stability problem has been viewed as one of maintaining synchronous operation. This is mainly influenced by synchronous machines that generate electrical power. Therefore, tracking the state of synchronous machines will be useful in deciding the control actions.

In this chapter, the SM algorithm with selective correction step update strategy (SMU) is tested on a simple power system example. This example deals with the estimation of the states of a synchronous generator in a single machine infinite bus (SMIB) system. We first describe the procedure used to model a synchronous generator with six states. The numerical results obtained by a simulation study is presented next.

4.2 Synchronous generator model with six states

Here, the synchronous generator is represented by a model with one d-axis and two q-axis amortisseur windings in the *d-q* frame. The first order differential equations used to represent

the generator are given by [67, (13.22-13.31)],

$$
\begin{aligned}
\dot{\delta} &= \omega_0 \Delta\omega, \\
\dot{\Delta\omega} &= \frac{1}{2H}\Big(T_m + T_e - D\Delta\omega\Big), \\
\dot{\psi_{fd}} &= \omega_0\Bigg[e_{fd} - \frac{R_{fd}\psi_{fd}}{X_{fd}} + \frac{R_{fd}X_{ad}^{''}}{X_{fd}}\Big(- i_d + \frac{\psi_{fd}}{X_{fd}} + \frac{\psi_{1d}}{X_{1d}}\Big)\Bigg], \\
\dot{\psi_{1q}} &= \omega_0\Bigg[- \frac{R_{1d}\psi_{1d}}{X_{1d}} + \frac{R_{1d}X_{ad}^{''}}{X_{1d}}\Big(- i_d + \frac{\psi_{fd}}{X_{fd}} + \frac{\psi_{1d}}{X_{1d}}\Big)\Bigg], \\
\dot{\psi_{1q}} &= \omega_0\Bigg[- \frac{R_{1q}\psi_{1q}}{X_{1q}} + \frac{R_{1q}X_{aq}^{''}}{X_{1q}}\Big(- i_q + \frac{\psi_{1q}}{X_{1q}} + \frac{\psi_{2q}}{X_{2q}}\Big)\Bigg], \\
\dot{\psi_{2q}} &= \omega_0\Bigg[- \frac{R_{2q}\psi_{2q}}{X_{2q}} + \frac{R_{2q}X_{aq}^{''}}{X_{2q}}\Big(- i_q + \frac{\psi_{1q}}{X_{1q}} + \frac{\psi_{2q}}{X_{2q}}\Big)\Bigg],
\end{aligned}
\tag{4.1}
$$

where $\dot{a}$ denotes the time derivative of a, the time is in seconds, the rotor angle is in electrical radians, all the other quantities are represented in reciprocal per unit system,

$$
\begin{aligned}
T_e &= e_d i_d + e_q i_q, \\
e_d &= E_R \sin(\delta) - E_I \cos(\delta), \\
e_q &= E_I \sin(\delta) + E_R \cos(\delta), \\
i_d &= \frac{X_{ad}^{''}}{X_d^{''}}\Big(\frac{\psi_{fd}}{X_{fd}} + \frac{\psi_{1d}}{X_{1d}}\Big) - \frac{e_q}{X_d^{''}}, \\
i_q &= \frac{X_{aq}^{''}}{X_q^{''}}\Big(\frac{\psi_{1q}}{X_{1q}} + \frac{\psi_{2q}}{X_{2q}}\Big) + \frac{e_d}{X_q^{''}}, \\
e_{fd} &= \frac{E_{fd}R_{fd}}{X_{ad}},
\end{aligned}
$$

and variable definitions are provided in tables 4.1 and 4.2. E_I, E_R are calculated using terminal voltage and voltage phase angle with respect to the common reference frame. Note that the stator resistance, R_a has been neglected in deriving the equation for T_e, i_d and i_q, and therefore T_e is assumed to be equal to the instantaneous power output of the machine.

TABLE 4.1: Variable definitions of the generator.

Symbol	Quantity	Value
δ	rotor angle (with respect to common reference frame)	
$\Delta\omega$	rotor speed variation	
ψ_{fd}	flux linkage in field winding	
ψ_{1d}	flux linkage in d-axis 1^{st} amortisseur winding	
ψ_{1q}	flux linkage in q-axis 1^{st} amortisseur winding	
ψ_{2q}	flux linkage in q-axis 2^{nd} amortisseur winding	
T_e	air-gap torque	
E_{fd}	supplied field voltage	
T_m	mechanical torque input	
H	inertia constant	3.5 MWs/MVA
D	damping factor	5 p.u.
f_0	base angular frequency	60 Hz

The common R-I reference frame and the machine *d-q* reference frame are shown in figure 4.1 where $\tilde{E}_t$ is the terminal voltage [67, figure 13.10].

By converting the continuous-time differential equations (4.1) to discrete-time equations (4.2) we can obtain a set of equations as in (2.22). The measurement equation (2.23) can be written as (4.3). The state vector is $\boldsymbol{x}_k = [\delta_k \ \Delta\omega_k \ \psi_{fd_k} \ \psi_{1d_k} \ \psi_{1q_k} \ \psi_{2q_k}]^T$, the measurement vector is $\boldsymbol{z}_k = [T_{ek} \ \omega_k]^T$, and E_{fd}, T_m, terminal voltage and voltage phase angle (E_I and E_R) have been taken as inputs to the estimation algorithm.

$$
\begin{aligned}
\delta_k &= \delta_{k-1} + \Delta t \cdot \omega_0 \Delta\omega_{k-1} + w_{1_k}, \\
\Delta\omega_k &= \Delta\omega_{k-1} + \frac{\Delta t}{2H}\left(T_m + T_{ek-1} - D\Delta\omega_{k-1}\right) + w_{2_k}, \\
\psi_{fd_k} &= \psi_{fd_{k-1}} + \Delta t \cdot \omega_0 \left[\frac{E_{fd}R_{fd}}{X_{ad}} - \frac{R_{fd}\psi_{fd_{k-1}}}{X_{fd}} + \frac{R_{fd}X''_{ad}}{X_{fd}}\left(-i_{dk-1} + \frac{\psi_{fd_{k-1}}}{X_{fd}} + \frac{\psi_{1d_{k-1}}}{X_{1d}}\right)\right] + w_{3_k}, \\
\psi_{1d_k} &= \psi_{1d_{k-1}} + \Delta t \cdot \omega_0 \left[-\frac{R_{1d}\psi_{1d_{k-1}}}{X_{1d}} + \frac{R_{1d}X''_{ad}}{X_{1d}}\left(-i_{dk-1} + \frac{\psi_{fd_{k-1}}}{X_{fd}} + \frac{\psi_{1d_{k-1}}}{X_{1d}}\right)\right] + w_{4_k}, \\
\psi_{1q_k} &= \psi_{1q_{k-1}} + \Delta t \cdot \omega_0 \left[-\frac{R_{1q}\psi_{1q_{k-1}}}{X_{1q}} + \frac{R_{1q}X''_{aq}}{X_{1q}}\left(-i_{q_{k-1}} + \frac{\psi_{1q_{k-1}}}{X_{1q}} + \frac{\psi_{2q_{k-1}}}{X_{2q}}\right)\right] + w_{5_k}, \\
\psi_{2q_k} &= \psi_{2q_{k-1}} + \Delta t \cdot \omega_0 \left[-\frac{R_{2q}\psi_{2q_{k-1}}}{X_{2q}} + \frac{R_{2q}L''_{aq}}{X_{2q}}\left(-i_{q_{k-1}} + \frac{\psi_{1q_{k-1}}}{X_{1q}} + \frac{\psi_{2q_{k-1}}}{X_{2q}}\right)\right] + w_{6_k},
\end{aligned}
\tag{4.2}
$$

$$
\boldsymbol{z}_k = \begin{pmatrix} \hat{T}_{ek} \\ \\ \hat{\Delta\omega}_k + 1 \end{pmatrix} + \mathbf{v}_k \tag{4.3}
$$

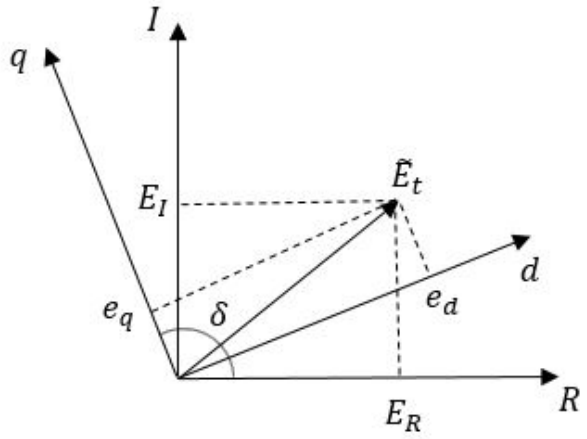

FIGURE 4.1: The common R-I reference frame and the machine *d-q* reference frame.

4.3 Simulation results

4.3.1 Test setup

The experimental set-up is shown in Figure 4.2 [67, figure 5.2]. The SMIB system has been

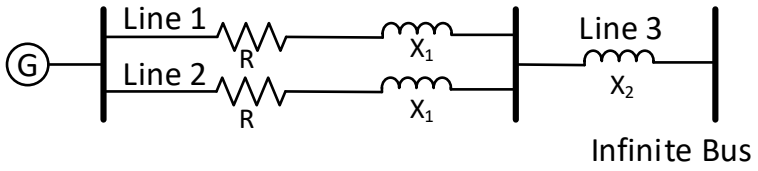

FIGURE 4.2: The experimental setup - SMIB system

modeled in MATLAB with a transmission system having two lines connected to an infinite

bus. The second-order Runge-Kutta method has been used to model the generator in the SMIB system. The line and generator data used here are provided in tables 4.1 and 4.2. Following are the intervals for noise distributions,

$$w_{i_k} \sim U[-10^{-5}, 10^{-5}],$$
$$v_{1_k} \sim U[-0.005, 0.005],$$
$$v_{2_k} \sim U[-0.05, 0.05],$$

where $i = 1, 2, ..., 6$, represent each of the six states of the synchronous generator. If the process noise intervals are large, this SMIB system can become unstable. Therefore suitable values for the process noise intervals were found by trial and error. The measurement noise intervals were based on 10 dB signal to noise ratio. The SMU and the EKF algorithms have been implemented in MATLAB. The ellipsoids containing the process and the measurement noise for the SMU algorithm have been derived using the bounded interval method as described in [21]. Process and measurement noise covariance matrices for the EKF have been derived assuming that a noise interval corresponds to four standard deviations.

The simulation of the system has been conducted with a time step of 1 ms and the measurements have been collected at 10 ms intervals. As it was assumed that the terminal voltage, voltage phase angle, and instantaneous power output of the machine are available at every 0.01 s, which accounts for a PMU sampling rate of 100. The statistical expectations have been estimated with Monte-Carlo trials over 100 different realizations of noise vectors in obtaining the experimental results presented below.

TABLE 4.2: The generator and the line data.

Symbol	Quantity	Value in per unit
R_a	stator resistance	0.0030
X_l	stator leakage reactance	0.1500
X_d	d-axis unsaturated synchronous reactance	1.8098
X_q	q-axis unsaturated synchronous reactance	1.7599
$X_d^{''}$	d-axis unsaturated sub-transient reactance	0.2296
$X_q^{''}$	q-axis unsaturated sub-transient reactance	0.2500
X_{fd}	field leakage reactance	0.1634
X_{1d}	d-axis 1^{st} damper leakage reactance	0.1713
X_{1q}	q-axis 1^{st} damper leakage reactance	0.7252
X_{2q}	q-axis 2^{nd} damper leakage reactance	0.1250
R_{fd}	field resistance	5.9938×10^{-4}
R_{1d}	d-axis 1^{st} damper resistance	0.0284
R_{1q}	q-axis 1^{st} damper resistance	0.0062
R_{2q}	q-axis 2^{nd} damper resistance	0.0237
R	line 1, 2 resistance	0.1250
X_1	line 1, 2 reactance	0.6250
X_2	line 3 reactance	0.1250

4.3.2 Case 1

The SMIB system has been initiated to the steady-state. A balanced fault is then created in the middle of the line 2 at 5 s, and cleared after 1.5 s by removing that line. The estimation results are shown in figure 4.3. The time-averaged MSE given by (3.2) was calculated for each of the states, and is shown in table 4.3. The time-averaged MSE performance of the state δ_k is better in the EKF estimation than that of the SMU estimation. But the time-averaged MSE performance of the other state estimates is better in the SMU estimation than that of

the EKF estimation.

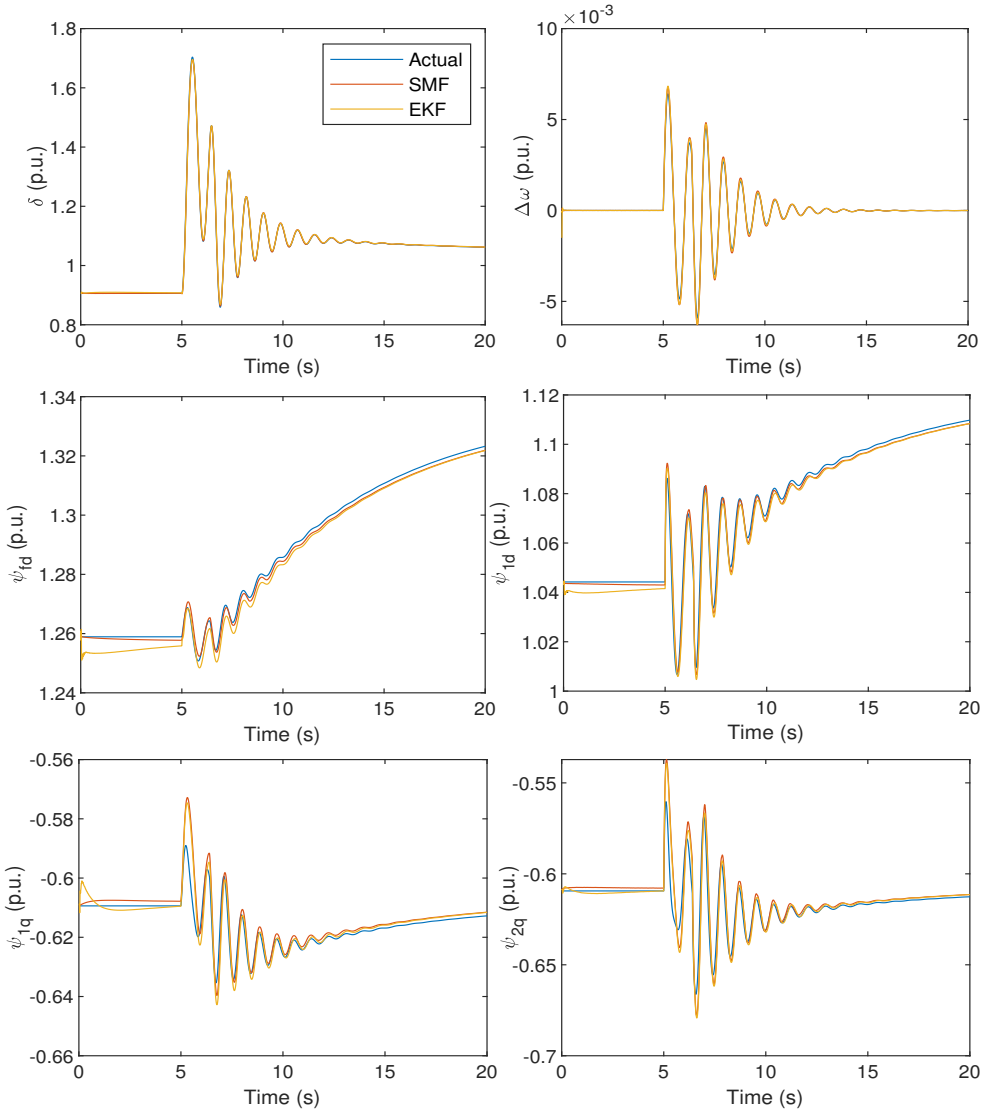

FIGURE 4.3: Case 1 - the estimation results comparison of the generator states.

It was observed that the SMU algorithm commuted the complete correction step to only 33.5 % of the time. This indicates that 66.5 % of the time the predicted state needs

TABLE 4.3: Case 1 - the time-averaged MSEs of the generator states.

Algorithm MSE($\times 10^{-4}$)	KF	SMF
e_{δ_k}	0.1097	0.6152
$e_{\Delta\omega_k}$	0.0007	0.0001
$e_{\psi_{fd_k}}$	0.7893	0.0180
$e_{\psi_{1d_k}}$	0.4909	0.0671
$e_{\psi_{1q_k}}$	0.5097	0.1384
$e_{\psi_{2q_k}}$	0.6974	0.3808

no update. Still, the estimation result obtained from the SMU algorithm is comparable to that of EKF, which indicates that not all the measurements contain innovative information.

4.3.3 Case 2

The SMIB system has been disturbed twice (two fault case). First, a fault is created at the infinite bus and it was cleared and then a second fault is created as before, that is a fault in the middle of line 2 which is subsequently cleared by removing the line. The first fault was applied at 25 s and the second fault was applied at 45 s. The estimation results for this case is shown for the duration of $15 - 60$ s in figure 4.4. The time-averaged MSE in (3.2) was calculated for each of the states during each fault and shown in tables 4.4 and 4.5. As in case 1, the estimation results of the SMU algorithm is comparable to those of the EKF.

A complete correction step is calculated if the parameter $\lambda_k \neq 0$ (2.21). Therefore, by recording the time steps at which $\lambda_k \neq 0$, we can track the occurrence of complete correction steps in each trial. Then, by taking the average over the trials we can obtain the

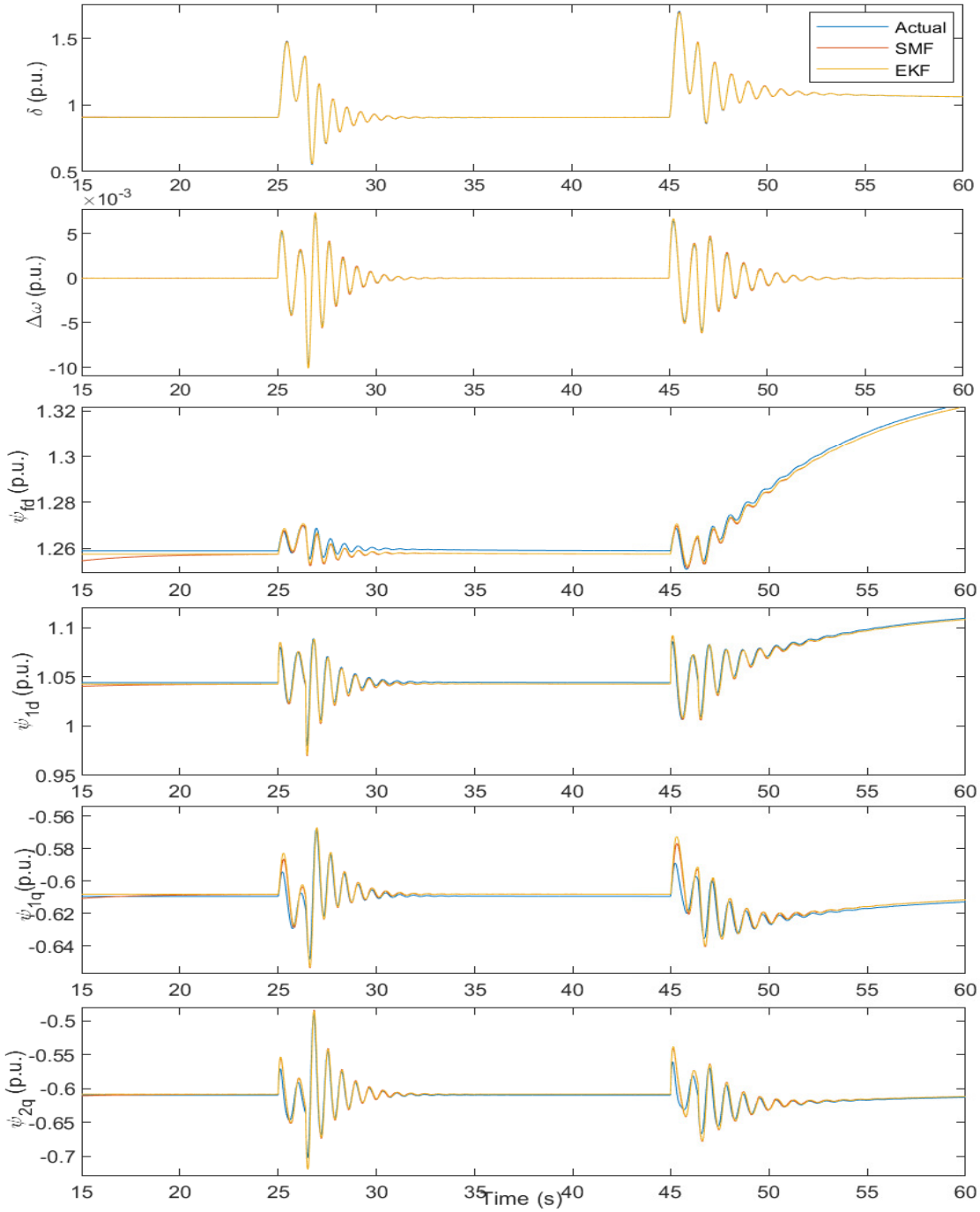

FIGURE 4.4: Case 2 - the estimation results comparison of the generator states.

TABLE 4.4: Case 2 - the time-averaged MSEs of the generator states for the first fault.

Algorithm MSE($\times 10^{-4}$)	KF	SMF
e_{δ_k}	0.1885	0.1613
$e_{\Delta\omega_k}$	0.0001	0.0002
$e_{\psi_{fd_k}}$	0.0311	0.0374
$e_{\psi_{1d_k}}$	0.1236	0.1260
$e_{\psi_{1q_k}}$	0.1718	0.1236
$e_{\psi_{2q_k}}$	0.5714	0.5286

TABLE 4.5: Case 2 - the time-averaged MSEs of the generator states for the second fault.

Algorithm MSE($\times 10^{-4}$)	KF	SMF
e_{δ_k}	0.2430	0.1804
$e_{\Delta\omega_k}$	0.0001	0.0002
$e_{\psi_{fd_k}}$	0.0251	0.0263
$e_{\psi_{1d_k}}$	0.1204	0.1140
$e_{\psi_{1q_k}}$	0.2694	0.1874
$e_{\psi_{2q_k}}$	0.7326	0.6501

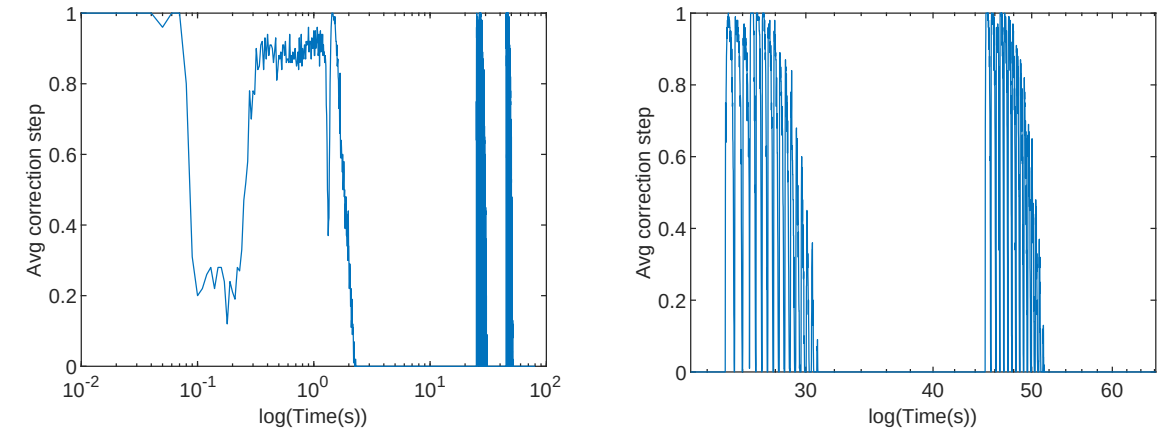

(A) (B)

FIGURE 4.5: The average correction step variation - case 2

average complete correction step variation. This variation is shown in figure 4.5. Figure 4.5 (A) shows the variation of average complete correction step over the whole period $0 - 80$ s, and figure 4.5 (B) shows the variation of average complete correction step over the period $20 - 65$ s.

It can be observed that after initialization, the SMU algorithm performs the complete correction step until the steady-state is reached, after which no correction steps are required until a disturbance occurs. This is an important observation that indicates the possibility of using the SMU algorithm for event-triggered SE.

4.3.3.1 Effects of improper initialization of the SMU algorithm

It has been observed that improper initialization of the algorithm can affect the performance of the SMU algorithm. This will create an adverse effect on the data selective and event-triggered capability of the algorithm.

The SMIB system with two fault case is tested with a different process noise ellipsoid $E(0, \hat{\mathbf{W}}_k)$ which corresponds to noise intervals of $w_{i_k} \sim U[-10^{-3}, 10^{-3}]$. These noise intervals are larger than the ones used earlier which were $w_{i_k} \sim U[-10^{-5}, 10^{-5}]$. The correction step variation over the time period $0 - 80$ s for a single trial is shown in figure 4.6. Unlike before,

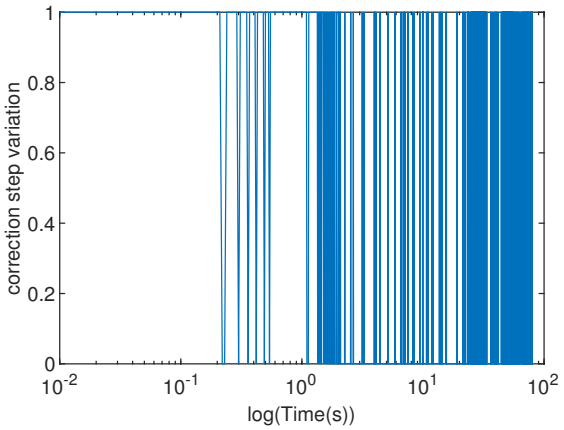

FIGURE 4.6: Correction step variation over the time period of 80 s for a single trial - case 2.

it is very hard to distinguish between a steady state condition and a fault condition as the correction steps occur too frequently.

4.4 Discussion

In power systems, PMUs typically generate measurements at rates much higher than the rates at which the system states change. Therefore, the measurements will not always contain useful information about the power system state, hence, it is not always necessary to communicate the measurements. In this type of situation, if there is a systematic way

to identify whether the measurement contains useful information, it can aid in reducing the communication overhead created by large data flows from the PMUs.

The SMU algorithm presented in this thesis will be useful in identifying whether or not the measurements are informative, by simply checking a condition based on the predicted and the actual measurement. When the MASE is deployed, the SMU algorithm can be implemented at the local estimators. In the event of a state change, the SMU algorithm can identify it based on its data selective capability. This can be used as a criterion to send the information to the centralized estimator for further processing. Consequently, this will significantly reduce the communication overhead in power systems with PMUs.

But an important issue to address here would be the initialization of the SMU algorithm. The experimental results presented in this thesis have shown that improper initialization of the SM algorithm can degrade the data selective capability of the SMU algorithm. In particular, robust methods for proper initialization of noise ellipsoids must be further investigated.

Chapter 5

Conclusion and Future work

This thesis investigated an ellipsoidal SM algorithm that can disregard the uninformative measurements in DSE and its applicability for PS-DSE. The necessity of updating the predicted state set is checked by a condition based on the error between the actual and predicted value of the measurement. This will eliminate the complete correction step calculation if the measurements are uninformative. However, numerical results show that the accuracy of the estimates provided by this algorithm is still comparable with that of the conventional KF algorithm.

5.1 Contributions and conclusions

1. A comprehensive overview of previous work on ellipsoidal SM algorithms for state estimation in both linear and non-linear dynamical systems has been presented.

2. In order to show that the selective correction step update strategy does not create any adverse effect on the estimated state, a detailed comparison with the KF algorithm and two standard SM algorithms has been carried out. In the numerical examples, it was found that the complete correction step calculation was required only during a small fraction of time. The selective correction step update strategy saves considerable computational cost when compared with the standard SM algorithms.

3. The potential applicability of the data selective SM algorithm to event-triggered SE in MASE has been demonstrated through a simulation study of a SMIB system. This study has revealed several important issues that must be addressed in future research, as outlined below.

5.2 Future work

1. The experimental results in Chapter 4 highlight the importance of using robust initialization methods in the SMU algorithm. Towards addressing this issue, systematic methods for selecting the noise ellipsoids must be further investigated. Of particular interest would be adaptive methods for updating these ellipsoids and the investigation of the convergence properties of such methods. A good starting point would be interval analysis-based approach studied in [39, 46].

2. A preliminary investigation of real-time SE using the RTDS simulation software RSCAD [68] has been undertaken during this research. However, this investigation has not been completed due to technical difficulties and lack of time. A complete implementation of a SM state estimator, as considered in this thesis, in the RSCAD environment will be a very useful step towards investigating the MASE concept for smart power grids.

Appendix A

Vector sum of two ellipsoids

A.1 Support functions of sets

A support function $s(\boldsymbol{\eta})$ of a closed convex set $\Omega \in \mathbb{R}^n$ is defined by,

$$\begin{aligned} s(\boldsymbol{\eta}) &= \underset{\mathbf{x}\in\Omega}{max}\, \mathbf{x}^T\boldsymbol{\eta}, \\ \boldsymbol{\eta}^T\boldsymbol{\eta} &= 1, \end{aligned} \tag{A.1}$$

where $\boldsymbol{\eta}$ is any non-zero vector in $\mathbb{R}^n$ satisfying (A.1). The plane with normal $\boldsymbol{\eta}$ and the distance $(\boldsymbol{\eta}^T\boldsymbol{\eta})^{1/2}$ to $s(\boldsymbol{\eta})$ from the origin is a support hyperplane of Ω. In other words, $\boldsymbol{\eta}$ touches the boundary of Ω. [22]. Using the support function, the convex set Ω can be represented as,

$$\Omega = \{\mathbf{x} : \mathbf{x}^T\boldsymbol{\eta} \leq s(\boldsymbol{\eta}),\ \forall\, \boldsymbol{\eta}\}.$$

Theorem A.1. *The support function $s(\boldsymbol{\eta})$ of an ellipsoidal set $E(\boldsymbol{a}, \boldsymbol{P})$ is given by,*

$$s(\boldsymbol{\eta}) = \max_{\boldsymbol{x} \in E(\boldsymbol{a}, \boldsymbol{P})} \boldsymbol{x}^T \boldsymbol{\eta},$$
$$s(\boldsymbol{\eta}) = \boldsymbol{\eta}^T \boldsymbol{a} + (\boldsymbol{\eta}^T \boldsymbol{P} \boldsymbol{\eta})^{1/2}.$$

Proof. For a closed convex set defined by an ellipsoid $E(\mathbf{a}, \mathbf{P})$, solving the constrained problem

$$s(\boldsymbol{\eta}) = \max_{\mathbf{x} \in E(\mathbf{a}, \mathbf{P})} \mathbf{x}^T \boldsymbol{\eta},$$
$$E(\mathbf{a}, \mathbf{P}) = \{\mathbf{x} \in \mathbb{R}^n : (\mathbf{x} - \mathbf{a})^T \mathbf{P}^{-1} (\mathbf{x} - \mathbf{a}) \leq 1\}.$$

Define Lagrange multiplier as τ,

$$L(\mathbf{x}, \tau) = \mathbf{x}^T \boldsymbol{\eta} + \tau[(\mathbf{x} - \mathbf{a})^T \mathbf{P}^{-1} (\mathbf{x} - \mathbf{a}) - 1]. \tag{A.2}$$

Differentiating equation (A.2) with respect to $\mathbf{x}$ and equating it to 0 will give a solution to $\mathbf{x}$.

$$\frac{\partial L}{\partial \mathbf{x}} = \boldsymbol{\eta} + 2\tau \ \mathbf{P}^{-1} (\mathbf{x} - \mathbf{a}),$$
$$\hat{\mathbf{x}} = \mathbf{a} - \frac{\mathbf{P}\boldsymbol{\eta}}{2\tau}.$$

Substituting this $\hat{\mathbf{x}}$ in the boundary of the ellipsoid $(\mathbf{x} - \mathbf{a})^T \mathbf{P}^{-1} (\mathbf{x} - \mathbf{a}) = 1$, where $\mathbf{x}$ attains its maximum values, τ will be

$$\boldsymbol{\eta}^T \mathbf{P} \boldsymbol{\eta} = 4\tau^2,$$
$$\tau = \frac{1}{2} \sqrt{\boldsymbol{\eta}^T \mathbf{P} \boldsymbol{\eta}}.$$

Hence,

$$\mathbf{x}_{max} = \mathbf{a} - \frac{\mathbf{P}\boldsymbol{\eta}}{\sqrt{\boldsymbol{\eta}^T\mathbf{P}\boldsymbol{\eta}}}. \tag{A.3}$$

Multiplying both sides of equation (A.3) by $\boldsymbol{\eta}^T$

$$\boldsymbol{\eta}^T\mathbf{x}_{max} = \boldsymbol{\eta}^T\mathbf{a} - \frac{\boldsymbol{\eta}^T\mathbf{P}\boldsymbol{\eta}}{\sqrt{\boldsymbol{\eta}^T\mathbf{P}\boldsymbol{\eta}}}.$$

Therefore,

$$s(\boldsymbol{\eta}) = \boldsymbol{\eta}^T\mathbf{a} + (\boldsymbol{\eta}^T\mathbf{P}\boldsymbol{\eta})^{1/2}. \tag{A.4}$$

□

Remark A.2. A support function of the sum of convex sets is the sum of the support function of each set [26]. Let Ω_1 and Ω_2 be two closed convex sets with support functions $s_1(\boldsymbol{\eta})$ and $s_2(\boldsymbol{\eta})$. Let Ω_{1+2} be the vector sum of Ω_1 and Ω_2. Then Ω_{1+2} is convex and its support function $s_{1+2}(\boldsymbol{\eta})$ is given by,

$$s_{1+2}(\boldsymbol{\eta}) = s_1(\boldsymbol{\eta}) + s_2(\boldsymbol{\eta}).$$

Further, Ω_1 contains Ω_2, only if [22, 26],

$$s_1(\boldsymbol{\eta}) > s_2(\boldsymbol{\eta}),\ \forall\, \boldsymbol{\eta}. \tag{A.5}$$

A.2 Vector sum of ellipsoids

The existence and uniqueness of the trace criterion and the determinant criterion based optimal ellipsoids containing a given compact set have been presented in [26]. Set of ellipsoids containing the vector sum of ellipsoids is derived using support function theory and Cauchy–Schwarz inequality. An explicit solution for the ellipsoid containing vector sum is presented based on the trace criterion. Following are the important theorems from [26].

Theorem A.3. *Consider a set of K ellipsoids in $\mathbb{R}^n$, $E_k(\boldsymbol{c}_k, \boldsymbol{P}_k)$ for $k = 1, 2, \ldots, K$ and their sum*

$$\Omega_k = \sum_{k=1}^{K} E_k(\boldsymbol{c}_k, \boldsymbol{P}_k).$$

The center of the optimal ellipsoid $E^*(\boldsymbol{c}^*, \boldsymbol{P}^*)$, containing the vector sum of ellipsoids based on both the trace and determinant criteria is,

$$\begin{aligned} \boldsymbol{c}^* &= \sum_{k=1}^{K} \boldsymbol{c}_k, \\ \Omega_k &\subset E^*(\boldsymbol{c}^*, \boldsymbol{P}^*). \end{aligned} \tag{A.6}$$

Remark A.4. The center of the ellipsoids containing the vector sum depends only on the centers of K ellipsoids.

Theorem A.5. *Shape matrix of an ellipsoid $E(c^*, \boldsymbol{P})$ containing the vector sum of ellipsoids in theorem A.3, using the determinant and trace criteria is given by,*

$$\boldsymbol{P} = \sum_{k=1}^{K} \alpha_k^{-1} \boldsymbol{P}_k, \tag{A.7}$$

where vector $\boldsymbol{\alpha} = [\alpha_1\ \alpha_2\ \ldots\ \alpha_K]^T \in \mathbb{R}^K$ *belongs to convex set of all vectors with* $\alpha_k \geq 0$ *and* $\sum_{k=1}^{K} \alpha_k = 1$.

Theorem A.6. *In the family of ellipsoids defined by different selections of* $\boldsymbol{\alpha}$ *in theorem A.5, the minimal trace ellipsoid containing the vector sum of ellipsoids* $E_k(c_k, \boldsymbol{P}_k)$ *for* $k = 1, 2, \ldots, K$ *is given by,*

$$\boldsymbol{P}^* = \left(\sum_{k=1}^{K} \sqrt{tr\ \boldsymbol{P}_k} \right) \left(\sum_{k=1}^{K} \frac{\boldsymbol{P}_k}{\sqrt{tr\ \boldsymbol{P}_k}} \right), \tag{A.8}$$

where

$$\alpha_k^* = \left(\sum_{k=1}^{K} \sqrt{tr\ \boldsymbol{P}_k} \right)^{-1} \sqrt{tr\ \boldsymbol{P}_k}.$$

A.3 Approximating an optimal ellipsoid containing the vector sum of ellipsoids in the prediction step

The optimum ellipsoid $E(\hat{\mathbf{x}}_{k|k-1}, \tilde{\mathbf{P}}_{k|k-1})$, containing vector sum of $\mathbf{F}_{k-1}E(\hat{\mathbf{x}}_{k-1}, \tilde{\mathbf{P}}_{k-1})$ and $E(0, \mathbf{W}_k)$ is obtained by utilizing theorems A.1, A.3, A.5, and A.6, when $K = 2$,

$$E(\hat{\mathbf{x}}_{k|k-1}, \tilde{\mathbf{P}}_{k|k-1}) \supset \mathbf{F}_{k-1}E(\hat{\mathbf{x}}_{k-1}, \tilde{\mathbf{P}}_{k-1}) \oplus E(0, \mathbf{W}_{k-1}).$$

According to (A.5),

$$\begin{aligned} s_{E(\hat{\mathbf{x}}_{k|k-1}, \tilde{\mathbf{P}}_{k|k-1})}(\boldsymbol{\eta}) &\geq s_{F_{k-1}E(\hat{\mathbf{x}}_{k-1}, \tilde{\mathbf{P}}_{k-1})}(\boldsymbol{\eta}) + s_{E(0, \mathbf{W}_{k-1})}(\boldsymbol{\eta}), \\ \boldsymbol{\eta}^T \hat{\mathbf{x}}_{k|k-1} + (\boldsymbol{\eta}^T \tilde{\mathbf{P}}_{k|k-1} \boldsymbol{\eta})^{1/2} &\geq \boldsymbol{\eta}^T F_{k-1} \hat{\mathbf{x}}_{k-1} + (\boldsymbol{\eta}^T F_{k-1} \tilde{\mathbf{P}}_{k-1} F_{k-1}^T \boldsymbol{\eta})^{1/2} + (\boldsymbol{\eta}^T \mathbf{W}_k \boldsymbol{\eta})^{1/2}. \end{aligned} \tag{A.9}$$

From theorem A.3 the center of the predicted state ellipsoid $E(\hat{\mathbf{x}}_{k|k-1}, \tilde{\mathbf{P}}_{k|k-1})$ will be

$$\mathbf{x}_{k|k-1} = \mathbf{F}_{k-1}\hat{\mathbf{x}}_{k-1}.$$

Therefore, (A.9) reduces to

$$(\boldsymbol{\eta}^T\tilde{\mathbf{P}}_{k|k-1}\boldsymbol{\eta})^{1/2} \geq (\boldsymbol{\eta}^T F_{k-1}\tilde{\mathbf{P}}_k F_{k-1}^T\boldsymbol{\eta})^{1/2} + (\boldsymbol{\eta}^T\mathbf{W}_k\boldsymbol{\eta})^{1/2}. \tag{A.10}$$

From theorem A.5 a family of shape matrices can be obtained for predicted state ellipsoid

$$\tilde{\mathbf{P}}_{k|k-1} = \frac{\mathbf{F}_{k-1}\tilde{\mathbf{P}}_k\mathbf{F}_{k-1}^T}{1-p_k} + \frac{\mathbf{W}_k}{p_k}.$$

Then, from theorem A.6 p_k can be derived as,

$$p_k = \frac{\sqrt{trace(\mathbf{W}_k)}}{\sqrt{trace(\mathbf{F}_{k-1}\tilde{\mathbf{P}}_k\mathbf{F}_{k-1}^T)} + \sqrt{trace(\mathbf{W}_k)}} \tag{A.11}$$

Appendix B

Intersection of two ellipsoids

Consider two arbitrary ellipsoids,

$$E_1(\mathbf{x}_1, \mathbf{P}_1) = \{\mathbf{x} \in \mathbb{R} : (\mathbf{x} - \mathbf{x}_1)^T \mathbf{P}_1^{-1} (\mathbf{x} - \mathbf{x}_1) \leqslant 1\},$$
$$E_2(\mathbf{x}_2, \mathbf{P}_2) = \{\mathbf{x} \in \mathbb{R} : (\mathbf{x} - \mathbf{x}_2)^T \mathbf{P}_2^{-1} (\mathbf{x} - \mathbf{x}_2) \leqslant 1\}.$$

The intersection of these two ellipsoids can be contained in another ellipsoid $E_3(\mathbf{x}_3, \mathbf{P}_3)$, where [20]

$$\begin{aligned} E_3(\mathbf{x}_3, \mathbf{P}_3) &= \{\mathbf{x} \in \mathbb{R} : (\mathbf{x} - \mathbf{x}_3)^T \mathbf{P}_3^{-1} (\mathbf{x} - \mathbf{x}_3) \leqslant 1\}, \\ &= \{\mathbf{x} \in \mathbb{R} : (1 - \lambda)(\mathbf{x} - \mathbf{x}_1)^T \mathbf{P}_1^{-1} (\mathbf{x} - \mathbf{x}_1) \\ &\qquad + \lambda (\mathbf{x} - \mathbf{x}_2)^T \mathbf{P}_2^{-1} (\mathbf{x} - \mathbf{x}_2) \leqslant 1\}. \end{aligned} \tag{B.1}$$

Consider the LHS of the inequality in (B.1),

$$
\begin{aligned}
&= (1-\lambda)(\mathbf{x}-\mathbf{x}_1)^T\mathbf{P}_1^{-1}(\mathbf{x}-\mathbf{x}_1) + \lambda(\mathbf{x}-\mathbf{x}_2)^T\mathbf{P}_2^{-1}(\mathbf{x}-\mathbf{x}_2),\\
&= (1-\lambda)(\mathbf{x}-\mathbf{x}_1)^T\mathbf{P}_1^{-1}(\mathbf{x}-\mathbf{x}_1) + \lambda(\mathbf{x}-\mathbf{x}_1+\mathbf{x}_1-\mathbf{x}_2)^T\mathbf{P}_2^{-1}(\mathbf{x}-\mathbf{x}_1+\mathbf{x}_1-\mathbf{x}_2),\\
&= (\mathbf{x}-\mathbf{x}_1)^T\Big((1-\lambda)\mathbf{P}_1^{-1}+\lambda\mathbf{P}_2^{-1}\Big)(\mathbf{x}-\mathbf{x}_1) + 2\lambda(\mathbf{x}-\mathbf{x}_1)^T\mathbf{P}_2^{-1}(\mathbf{x}_1-\mathbf{x}_2)\\
&\qquad + \lambda(\mathbf{x}_1-\mathbf{x}_2)^T\mathbf{P}_2^{-1}(\mathbf{x}_1-\mathbf{x}_2).
\end{aligned}
$$

Adding and subtracting a term $\lambda^2(\mathbf{x}_1-\mathbf{x}_2)^T\mathbf{P}_2^{-1}\Big((1-\lambda)\mathbf{P}_1^{-1}+\rho\mathbf{P}_2^{-1}\Big)^{-1}\mathbf{P}_2^{-1}(\mathbf{x}_1-\mathbf{x}_2)$ will yield

$$
\begin{aligned}
&= (\mathbf{x}-\mathbf{x}_1+\lambda((1-\lambda)\mathbf{P}_1^{-1}+\lambda\mathbf{P}_2^{-1})^{-1}\mathbf{P}_2^{-1}(\mathbf{x}_1-\mathbf{x}_2))^T\Big((1-\lambda)\mathbf{P}_1^{-1}+\lambda\mathbf{P}_2^{-1}\Big)\\
&(\mathbf{x}-\mathbf{x}_1+\lambda((1-\lambda)\mathbf{P}_1^{-1}+\lambda\mathbf{P}_2^{-1})^{-1}\mathbf{P}_2^{-1}(\mathbf{x}_1-\mathbf{x}_2)) + \lambda(\mathbf{x}_1-\mathbf{x}_2)^T\mathbf{P}_2^{-1}(\mathbf{x}_1-\mathbf{x}_2)\\
&- \lambda^2(\mathbf{x}_1-\mathbf{x}_2)^T\mathbf{P}_2^{-1}\Big((1-\lambda)\mathbf{P}_1^{-1}+\lambda\mathbf{P}_2^{-1}\Big)^{-1}\mathbf{P}_2^{-1}(\mathbf{x}_1-\mathbf{x}_2). \qquad \text{(B.2)}
\end{aligned}
$$

Taking the last two terms in (B.2) to the RHS of the inequality given in (B.1), the RHS of the inequality will yield

$$
\begin{aligned}
&= 1-\lambda(\mathbf{x}_1-\mathbf{x}_2)^T\mathbf{P}_2^{-1}(\mathbf{x}_1-\mathbf{x}_2)\\
&+ \lambda^2(\mathbf{x}_1-\mathbf{x}_2)^T\mathbf{P}_2^{-1}\Big((1-\lambda)\mathbf{P}_1^{-1}+\lambda\mathbf{P}_2^{-1}\Big)^{-1}\mathbf{P}_2^{-1}(\mathbf{x}_1-\mathbf{x}_2),\\
&= 1-(\mathbf{x}_1-\mathbf{x}_2)^T\Big(\lambda\mathbf{P}_2^{-1}-\lambda^2\mathbf{P}_2^{-1}\Big((1-\lambda)\mathbf{P}_1^{-1}+\lambda\mathbf{P}_2^{-1}\Big)^{-1}\mathbf{P}_2^{-1}\Big)(\mathbf{x}_1-\mathbf{x}_2),\\
&= 1-(\mathbf{x}_1-\mathbf{x}_2)^T\left(\frac{\mathbf{P}_1}{(1-\lambda)}+\frac{\mathbf{P}_2}{\lambda}\right)^{-1}(\mathbf{x}_1-\mathbf{x}_2).
\end{aligned}
$$

Finally, the center and the shape matrix of the ellipsoid $E_3(\mathbf{x}_3, \mathbf{P}_3)$ in (B.1) is obtained

$$\begin{aligned}
\mathbf{x}_3 &= \mathbf{x}_1 - \lambda((1-\lambda)\mathbf{P}_1^{-1} + \lambda\mathbf{P}_2^{-1})^{-1}\mathbf{P}_2^{-1}(\mathbf{x}_1 - \mathbf{x}_2), \\
\mathbf{P}_3 &= \gamma\left((1-\lambda)\mathbf{P}_1^{-1} + \lambda\mathbf{P}_2^{-1}\right)^{-1}, \\
\gamma &= 1 - (\mathbf{x}_1 - \mathbf{x}_2)^T\left(\frac{\mathbf{P}_1}{(1-\lambda)} + \frac{\mathbf{P}_2}{\lambda}\right)^{-1}(\mathbf{x}_1 - \mathbf{x}_2).
\end{aligned}$$

B.1 The intersection of the predicted state set and the observation set in the SM algorithm with selective correction step update strategy

An ellipsoid $E(\hat{\mathbf{x}}_k, \sigma_k^2\mathbf{P}_k)$ containing the intersection of the predicted state set $E(\hat{\mathbf{x}}_{k|k-1}, \sigma_{k|k-1}^2\mathbf{P}_{k|k-1})$, and the observation set S_k can be derived. Recall

$$\begin{aligned}
E(\hat{\mathbf{x}}_k, \sigma_k^2\mathbf{P}_k) &= \{\mathbf{x}_k \in \mathbb{R}^n : (\mathbf{x}_k - \hat{\mathbf{x}}_k)^T\mathbf{P}_k^{-1}(\mathbf{x}_k - \hat{\mathbf{x}}_k) \leq \sigma_k^2\}, \\
E(\hat{\mathbf{x}}_{k|k-1}, \sigma_{k|k-1}^2\mathbf{P}_{k|k-1}) &= \{\mathbf{x}_k \in \mathbb{R}^n : (\mathbf{x}_k - \hat{\mathbf{x}}_{k|k-1})^T\mathbf{P}_{k|k-1}^{-1}(\mathbf{x}_k - \hat{\mathbf{x}}_{k|k-1}) \leq \sigma_{k|k-1}^2\}, \\
S_k &= \{\mathbf{x}_k \in \mathbb{R}^n : (\mathbf{z}_k - \mathbf{H}_k\mathbf{x}_k)^T\mathbf{V}_k^{-1}(\mathbf{z}_k - \mathbf{H}_k\mathbf{x}_k) \leq 1\}.
\end{aligned}$$

Then, $E(\hat{\mathbf{x}}_k, \sigma_k^2\mathbf{P}_k)$ can be written as a combination of the two sets $E(\hat{\mathbf{x}}_{k|k-1}, \sigma_{k|k-1}^2\mathbf{P}_{k|k-1})$ and S_k as in (B.1)

$$\begin{aligned}
E(\hat{\mathbf{x}}_k, \sigma_k^2\mathbf{P}_k) = \{\mathbf{x}_k \in \mathbb{R}^n : &(1-\lambda_k)(\mathbf{x}_k - \hat{\mathbf{x}}_{k|k-1})^T\mathbf{P}_{k|k-1}^{-1}(\mathbf{x}_k - \hat{\mathbf{x}}_{k|k-1}) \\
&+ \lambda_k(\mathbf{z}_k - \mathbf{H}_k\mathbf{x}_k)^T\mathbf{V}_k^{-1}(\mathbf{z}_k - \mathbf{H}_k\mathbf{x}_k) \leq (1-\lambda_k)\sigma_{k|k-1}^2 + \lambda_k\}.
\end{aligned} \tag{B.3}$$

The inequality in (B.3) can be simplified as follows,

$$\begin{aligned}(1-\lambda_k)(\mathbf{x}_k-\hat{\mathbf{x}}_{k|k-1})^T\mathbf{P}_{k|k-1}^{-1}(\mathbf{x}_k-\hat{\mathbf{x}}_{k|k-1})+\lambda_k(\mathbf{z}_k-\mathbf{H}_k\mathbf{x}_k)^T\mathbf{V}_k^{-1}(\mathbf{z}_k-\mathbf{H}_k\mathbf{x}_k)&\\ \leq (1-\lambda_k)\sigma_{k|k-1}^2+\lambda_k,&\\ (1-\lambda_k)(\mathbf{x}_k-\hat{\mathbf{x}}_{k|k-1})^T\mathbf{P}_{k|k-1}^{-1}(\mathbf{x}_k-\hat{\mathbf{x}}_{k|k-1})+\lambda_k\big((\mathbf{z}_k-\mathbf{H}_k\hat{\mathbf{x}}_{k|k-1})-\mathbf{H}_k(\mathbf{x}_k-\hat{\mathbf{x}}_{k|k-1})\big)^T&\\ \mathbf{V}_k^{-1}\big((\mathbf{z}_k-\mathbf{H}_k\hat{\mathbf{x}}_{k|k-1})-\mathbf{H}_k(\mathbf{x}_k-\hat{\mathbf{x}}_{k|k-1})\big)\leq(1-\lambda_k)\sigma_{k|k-1}^2+\lambda_k.&\end{aligned}$$

Letting $\boldsymbol{\delta}_k=\mathbf{z}_k-H\hat{\mathbf{x}}_{k|k-1}$,

$$\begin{aligned}&(\mathbf{x}_k-\hat{\mathbf{x}}_{k|k-1})^T\big[(1-\lambda_k)\mathbf{P}_{k|k-1}^{-1}+\lambda_k\mathbf{H}_k^T\mathbf{V}_k^{-1}\mathbf{H}_k\big](\mathbf{x}_k-\hat{\mathbf{x}}_{k|k-1})+\lambda_k\boldsymbol{\delta}_k^T\mathbf{V}_k^{-1}\boldsymbol{\delta}_k\\ &-2\lambda_k(\mathbf{x}_k-\hat{\mathbf{x}}_{k|k-1})^T\mathbf{H}_k^T\mathbf{V}_k^{-1}\boldsymbol{\delta}_k \quad\leq\quad (1-\lambda_k)\sigma_{k|k-1}^2+\lambda_k,\\ &(\mathbf{x}_k-\hat{\mathbf{x}}_{k|k-1})^T\big[(1-\lambda_k)\mathbf{P}_{k|k-1}^{-1}+\lambda_k\mathbf{H}_k^T\mathbf{V}_k^{-1}\mathbf{H}_k\big](\mathbf{x}_k-\hat{\mathbf{x}}_{k|k-1})\\ &-2\lambda_k(\mathbf{x}_k-\hat{\mathbf{x}}_{k|k-1})^T\mathbf{H}_k^T\mathbf{V}_k^{-1}\boldsymbol{\delta}_k \quad\leq\quad (1-\lambda_k)\sigma_{k|k-1}^2+\lambda_k-\lambda_k\boldsymbol{\delta}_k^T\mathbf{V}_k^{-1}\boldsymbol{\delta}_k.\end{aligned}$$

Let $\mathbf{P}_k^{-1}=(1-\lambda_k)\mathbf{P}_{k|k-1}^{-1}+\lambda_k\mathbf{H}_k^T\mathbf{V}_k^{-1}\mathbf{H}_k$ and adding a term $\lambda_k^2(\mathbf{H}_k^T\mathbf{V}_k^{-1}\boldsymbol{\delta}_k)^T\mathbf{P}_k(\mathbf{H}_k^T\mathbf{V}_k^{-1}\boldsymbol{\delta}_k)$ to both sides will yield

$$\begin{aligned}&(\mathbf{x}_k-\hat{\mathbf{x}}_{k|k-1})^T\mathbf{P}_k^{-1}(\mathbf{x}_k-\hat{\mathbf{x}}_{k|k-1})-2\lambda_k(\mathbf{x}_k-\hat{\mathbf{x}}_{k|k-1})^T\mathbf{H}_k^T\mathbf{V}_k^{-1}\boldsymbol{\delta}_k\\ &\quad+\lambda_k^2(\mathbf{H}_k^T\mathbf{V}_k^{-1}\boldsymbol{\delta}_k)^T\mathbf{P}_k(\mathbf{H}_k^T\mathbf{V}_k^{-1}\boldsymbol{\delta}_k) \quad\leq\quad (1-\lambda_k)\sigma_{k|k-1}^2+\lambda_k-\lambda_k\boldsymbol{\delta}_k^T\mathbf{V}_k^{-1}\boldsymbol{\delta}_k\\ &\qquad\qquad+\lambda_k^2(\mathbf{H}_k^T\mathbf{V}_k^{-1}\boldsymbol{\delta}_k)^T\mathbf{P}_k(\mathbf{H}_k^T\mathbf{V}_k^{-1}\boldsymbol{\delta}_k).\end{aligned}$$

Letting $\hat{\mathbf{x}}_k=\hat{\mathbf{x}}_{k|k-1}+\lambda_k\mathbf{P}_k(\mathbf{H}_k^T\mathbf{V}_k^{-1}\boldsymbol{\delta}_k)$,

$$\begin{aligned}(\mathbf{x}_k-\hat{\mathbf{x}}_k)^T\mathbf{P}_k^{-1}(\mathbf{x}_k-\hat{\mathbf{x}}_k)\leq(1-\lambda_k)\sigma_{k|k-1}^2+\lambda_k-\lambda_k\boldsymbol{\delta}_k^T\mathbf{V}_k^{-1}\boldsymbol{\delta}_k&\\ +\lambda_k^2(\mathbf{H}_k^T\mathbf{V}_k^{-1}\boldsymbol{\delta}_k)^T\mathbf{P}_k(\mathbf{H}_k^T\mathbf{V}_k^{-1}\boldsymbol{\delta}_k).&\end{aligned}$$

RHS of this inequality can be further simplified using Woodbury matrix identity.

$$\begin{aligned}(1-\lambda_k)\sigma^2_{k|k-1}+\lambda_k-\boldsymbol{\delta}_k^T\big(\lambda_k\mathbf{V}_k^{-1}-\lambda_k^2\mathbf{V}_k^{-1}\mathbf{H}_k\mathbf{P}_k\mathbf{H}_k^T\mathbf{V}_k^{-1}\big)\boldsymbol{\delta}_k \\ =(1-\lambda_k)\sigma^2_{k|k-1}+\lambda_k-\boldsymbol{\delta}_k^T\Bigg[\left(\frac{\mathbf{V}_k}{\lambda_k}\right)^{-1}-\left(\frac{\mathbf{V}_k}{\lambda_k}\right)^{-1}\mathbf{H}_k\Bigg[\left(\frac{\mathbf{P}_{k|k-1}}{1-\lambda_k}\right)^{-1} \\ +\mathbf{H}_k^T\left(\frac{\mathbf{V}_k}{\lambda_k}\right)^{-1}\mathbf{H}_k\Bigg]^{-1}\mathbf{H}_k^T\left(\frac{\mathbf{V}_k}{\lambda_k}\right)^{-1}\Bigg]\boldsymbol{\delta}_k. \quad \text{(B.4)}\end{aligned}$$

Define a matrix,

$$\mathbf{Q}_k=\left(\frac{\mathbf{V}_k}{\lambda_k}\right)+\mathbf{H}_k\left(\frac{\mathbf{P}_{k|k-1}}{1-\lambda_k}\right)\mathbf{H}^T.$$

Using Woodbury matrix identity $\mathbf{Q}_k^{-1}$ is given by,

$$\mathbf{Q}_k^{-1}=\left(\frac{\mathbf{V}_k}{\lambda_k}\right)^{-1}-\left(\frac{\mathbf{V}_k}{\lambda_k}\right)^{-1}\mathbf{H}_k\Bigg[\left(\frac{\mathbf{P}_{k|k-1}}{1-\lambda_k}\right)^{-1}+\mathbf{H}_k^T\left(\frac{\mathbf{V}_k}{\lambda_k}\right)^{-1}\mathbf{H}_k\Bigg]^{-1}\mathbf{H}_k^T\left(\frac{\mathbf{V}_k}{\lambda_k}\right)^{-1}.$$

Therefore, (B.4)

$$\begin{aligned}(1-\lambda_k)\sigma^2_{k|k-1}+\lambda_k-\boldsymbol{\delta}_k^T\big(\lambda_k\mathbf{V}_k^{-1}-\lambda_k^2\mathbf{V}_k^{-1}\mathbf{H}_k\mathbf{P}_k\mathbf{H}_k^T\mathbf{V}_k^{-1}\big)\boldsymbol{\delta}_k \\ =(1-\lambda_k)\sigma^2_{k|k-1}+\lambda_k-\boldsymbol{\delta}_k^T\mathbf{Q}_k^{-1}\boldsymbol{\delta}_k.\end{aligned}$$

Further, $\mathbf{P}_k^{-1}=(1-\lambda_k)\mathbf{P}_{k|k-1}^{-1}+\lambda_k\mathbf{H}_k^T\mathbf{V}_k^{-1}\mathbf{H}_k$, the shape matrix $\mathbf{P}_k$ of the ellipsoid $E(\hat{\mathbf{x}}_k,\sigma_k^2\mathbf{P}_k)$ using Woodbury matrix identity is given by,

$$\begin{aligned}\mathbf{P}_k&=\big[(1-\lambda_k)\mathbf{P}_{k|k-1}^{-1}+\lambda_k\mathbf{H}_k^T\mathbf{V}_k^{-1}\mathbf{H}_k\big]^{-1},\\&=\left(\frac{\mathbf{P}_{k|k-1}}{1-\lambda_k}\right)-\left(\frac{\mathbf{P}_{k|k-1}}{1-\lambda_k}\right)\mathbf{H}_k^T\Bigg[\left(\frac{\mathbf{V}_k}{\lambda_k}\right)+\mathbf{H}_k\left(\frac{\mathbf{P}_{k|k-1}}{1-\lambda_k}\right)\mathbf{H}_k^T\Bigg]^{-1}\mathbf{H}_k\left(\frac{\mathbf{P}_{k|k-1}}{1-\lambda_k}\right).\end{aligned}$$

Define

$$\mathbf{K}_k = \frac{1}{1-\lambda_k}\mathbf{P}_{k|k-1}\mathbf{H}_k^T\mathbf{Q}_k^{-1}.$$

Then, $\mathbf{P}_k$ can be rewrite

$$\mathbf{P}_k = \frac{1}{1-\lambda_k}[\mathbf{I}-\mathbf{K}_k\mathbf{H}_k]\mathbf{P}_{k|k-1}.$$

Remark B.1. Woodbury matrix identity: Consider different set of matrices $\mathbf{A}, \mathbf{C}, \mathbf{U}$ and $\mathbf{V}$. The inverse of $[A+UCV]$ is given by,

$$[\mathbf{A}+\mathbf{UCV}]^{-1} = \mathbf{A}^{-1} - \mathbf{A}^{-1}\mathbf{U}(\mathbf{C}^{-1}-\mathbf{VA}^{-1}\mathbf{U})^{-1}\mathbf{VA}^{-1}. \tag{B.5}$$

Consider the matrix $\mathbf{K}_k$,

$$\begin{aligned}
\mathbf{K}_k &= \frac{1}{1-\lambda_k}\mathbf{P}_{k|k-1}\mathbf{H}_k^T\mathbf{Q}_k^{-1},\\
&= \frac{1}{1-\lambda_k}\mathbf{P}_k\mathbf{P}_k^{-1}\mathbf{P}_{k|k-1}\mathbf{H}_k^T\mathbf{Q}_k^{-1},\\
&= \frac{1}{1-\lambda_k}\mathbf{P}_k[(1-\lambda_k)\mathbf{P}_{k|k-1}^{-1}+\lambda_k\mathbf{H}_k^T\mathbf{V}_k^{-1}\mathbf{H}_k]\mathbf{P}_{k|k-1}\mathbf{H}_k^T\mathbf{Q}_k^{-1},\\
&= \lambda_k\mathbf{P}_k\left[\frac{\mathbf{P}_{k|k-1}^{-1}}{\lambda_k}+\mathbf{H}_k^T\frac{\mathbf{V}_k^{-1}}{(1-\lambda_k)}\mathbf{H}_k\right]\mathbf{P}_{k|k-1}\mathbf{H}_k^T\mathbf{Q}_k^{-1},\\
&= \lambda_k\mathbf{P}_k\left[\frac{\mathbf{H}_k^T}{\lambda_k}+\mathbf{H}_k^T\frac{\mathbf{V}_k^{-1}}{(1-\lambda_k)}\mathbf{H}_k\mathbf{P}_{k|k-1}\mathbf{H}_k^T\right]\mathbf{Q}_k^{-1},\\
&= \lambda_k\mathbf{P}_k\mathbf{H}_k^T\mathbf{V}_k^{-1}\left[\frac{\mathbf{V}_k}{\lambda_k}+\mathbf{H}_k\frac{\mathbf{P}_{k|k-1}}{(1-\lambda_k)}\mathbf{H}_k\right]\mathbf{Q}_k^{-1},\\
&= \lambda_k\mathbf{P}_k\mathbf{H}_k^T\mathbf{V}_k^{-1}.
\end{aligned}$$

Thus, $\hat{\mathbf{x}}_k = \hat{\mathbf{x}}_{k|k-1} + \lambda_k \mathbf{P}_k \mathbf{H}_k^T \mathbf{V}_k^{-1} \boldsymbol{\delta}_k$ can be rewrite as,

$$\hat{\mathbf{x}}_k = \hat{\mathbf{x}}_{k|k-1} + \mathbf{K}_k \boldsymbol{\delta}_k.$$

Finally, $E(\hat{\mathbf{x}}_k, \sigma_k^2 \mathbf{P}_k) = \{\mathbf{x}_k \in \mathbb{R}^n : (\mathbf{x}_k - \hat{\mathbf{x}}_k)^T \mathbf{P}_k^{-1} (\mathbf{x}_k - \hat{\mathbf{x}}_k) \leq \sigma_k^2\}$ is where

$$\begin{aligned}
\hat{\mathbf{x}}_k &= \hat{\mathbf{x}}_{k|k-1} + \mathbf{K}_k \boldsymbol{\delta}_k, \\
\mathbf{P}_k &= \frac{1}{1-\lambda_k} [\mathbf{I} - \mathbf{K}_k \mathbf{H}_k] \mathbf{P}_{k|k-1}, \\
\sigma_k^2 &= (1-\lambda_k)\sigma_{k|k-1}^2 + \lambda_k - \boldsymbol{\delta}_k^T \mathbf{Q}_k^{-1} \boldsymbol{\delta}_k, \\
\mathbf{K}_k &= \frac{1}{1-\lambda_k} \mathbf{P}_{k|k-1} \mathbf{H}_k^T \mathbf{Q}_k^{-1}, \\
\mathbf{Q}_k &= \left(\frac{\mathbf{V}_k}{\lambda_k} \right) + \mathbf{H}_k \left(\frac{\mathbf{P}_{k|k-1}}{1-\lambda_k} \right) \mathbf{H}^T, \\
\boldsymbol{\delta}_k &= \mathbf{z}_k - H \hat{\mathbf{x}}_{k|k-1}.
\end{aligned}$$

Appendix C

Selection of an bounding ellipsoid for a set

The performance of the SM algorithm lies in the relative size of the approximation of the state set. These approximations are optimum in the sense of their volume. But there can be other optimal approximation criteria as well [25]. When a state set is bounded by an ellipsoid, the choice of the bounding ellipsoid is not unique, and need to find an optimal ellipsoid based on some criteria [22]. If an ellipsoid $E(\mathbf{a}, \mathbf{P})$ defined as in (2.1) is characterized by a scalar optimality criterion or a cost function J, which is defined as $L(\mathbf{P})$ a function of shape matrix of the ellipsoid

$$J[E(\mathbf{a}, \mathbf{P})] = L(\mathbf{P}).$$

For all $\mathbf{P}$, which are symmetric and non-negative definite, $L(\mathbf{P})$ is smooth and monotone for following generalized optimality criteria. Monotone means, for arbitarary shape matrices $\mathbf{P}_1$ and $\mathbf{P}_2$, $L(\mathbf{P}_1) \geq L(\mathbf{P}_2)$ if the difference $(\mathbf{P}_1 - \mathbf{P}_2)$ is a nonnegative definite matrix (if $E(\mathbf{a}, \mathbf{P}_1) \supset E(\mathbf{a}, \mathbf{P}_2)$ holds, then $L(\mathbf{P}_1) \geq L(\mathbf{P}_2)$). [21, 25].

1. Volume of an ellipsoid $E(\mathbf{a}, \mathbf{P})$ is given by,

$$Vol(E(\mathbf{a}, \mathbf{P})) = \frac{\pi^{n/2}(det\, \mathbf{P})^{1/2}}{\Gamma(\frac{n}{2}+1)}, \tag{C.1}$$

where Γ is the Eular gamma function. Hence, volume of an ellipsoid is proportional to the square of the product of the lengths of its axes. The cost function, which is also called the determinant criterion is defined as,

$$L(\mathbf{P}) = (det\mathbf{P})^{1/2}.$$

Minimization of this cost function might result in a very narrow ellipsoid, which will impose extremely large uncertainties in some directions even though the volume tends to zero. Further, calculating the determinant of matrices is cumbersome and inefficient [26].

2. In some cases, the volume of a set in an n-dimensional subspace is not of interest, such as when some state coordinates are insignificant and need no estimate. In such a situation, project the ellipsoid $E(\mathbf{a}, \mathbf{P})$ onto the direction of a vector $\mathbf{v}$, where $\mathbf{v}$ is a given nonzero vector with appropriate dimensions. The projection of $E(\mathbf{a}, \mathbf{P})$ onto the direction of the vector $\mathbf{v}$ is given by [69],

$$\Pi_v(E(\mathbf{a}, \mathbf{P})) = \frac{2\langle \mathbf{Pv}, \mathbf{v}\rangle^{1/2}}{\|\mathbf{v}\|},$$

where $\langle\ .\ ,\ .\ \rangle$ represent the inner product and $\|.\|$ represent the norm. Cost function would be of the following form,

$$L(P) = \langle \mathbf{Pv}, \mathbf{v}\rangle. \tag{C.2}$$

3. Sum of the squared semi-axis of an ellipsoid $E(\mathbf{a}, \mathbf{P})$, the trace criterion.

$$L(\mathbf{P}) = Tr\,(\mathbf{P}). \tag{C.3}$$

4. If $\mathbf{C}$ is a symmetric positive definite matrix with same dimensions as $\mathbf{P}$ in $E(\mathbf{a}, \mathbf{P})$ (projection of the ellipsoid to a subspace when appropriate $\mathbf{C}$ is chosen),

$$L(\mathbf{P}) = Tr\,(\mathbf{CP}). \tag{C.4}$$

   This is a generalization of trace criterion and called a linear optimality criterion [21].

5. Sum of semi-axes of an ellipsoid $E(\mathbf{a}, \mathbf{P})$ in the forth power.

$$L(\mathbf{P}) = Tr\,(\mathbf{P}^2). \tag{C.5}$$

First criterion is used extensively in literature casting aside its disadvantages. It is well established in literature that for first and third criteria there exists "a unique smallest ellipsoid containing a compact set with non-empty interior". [26].

Appendix D

A bound on the scalar variable σ_k^2

Consider the scalar variable σ_k^2 defined in (2.18)

$$\begin{aligned}\sigma_k^2 &= (1-\lambda_k)\sigma_{k|k-1}^2 + \lambda_k - \boldsymbol{\delta}_k^T \mathbf{Q}_k^{-1} \boldsymbol{\delta}_k, \\ &= (1-\lambda_k)\sigma_{k|k-1}^2 + \lambda_k - \boldsymbol{\delta}_k^T \left(\frac{1}{1-\lambda_k} \mathbf{H}_k \mathbf{P}_{k|k-1} \mathbf{H}_k^T + \frac{1}{\lambda_k} \mathbf{V}_k \right)^{-1} \boldsymbol{\delta}_k.\end{aligned}$$

Substitute $\bar{\mathbf{V}}_k^T \bar{\mathbf{V}}_k$ to $\mathbf{V}_k^{-1}$, where $\bar{\mathbf{V}}_k^T$ is the upper triangular matrix obtained by the Cholesky factorization of $\mathbf{V}_k^{-1}$. Then,

$$\begin{aligned}\sigma_k^2 &= (1-\lambda_k)\sigma_{k|k-1}^2 + \lambda_k - \boldsymbol{\delta}_k^T \left(\frac{1}{1-\lambda_k} \mathbf{H}_k \mathbf{P}_{k|k-1} \mathbf{H}_k^T + \frac{1}{\lambda_k} (\bar{\mathbf{V}}_k^T \bar{\mathbf{V}}_k)^{-1} \right)^{-1} \boldsymbol{\delta}_k, \\ &= (1-\lambda_k)\sigma_{k|k-1}^2 + \lambda_k - \lambda_k (1-\lambda_k) \bar{\boldsymbol{\delta}}_k^T (\lambda_k \mathbf{G}_k + (1-\lambda_k)\mathbf{I})^{-1} \bar{\boldsymbol{\delta}}_k.\end{aligned}$$

where

$$\mathbf{G}_k = \bar{\mathbf{V}}_k \mathbf{H}_k \mathbf{P}_{k|k-1} \mathbf{H}_k^T \bar{\mathbf{V}}_k^T,$$
$$\bar{\boldsymbol{\delta}}_k = \bar{\mathbf{V}}_k \boldsymbol{\delta}_k.$$

A simplified but approximate bound on σ_k^2 can be obtained by assigning a scalar value to the matrix $(\lambda_k \mathbf{G}_k + (1-\lambda_k)\mathbf{I})$. This will eliminate the complex mathematics to some extent, when minimizing σ_k^2. Taking $\bar{g}_k$ as the norm or the maximum eigenvalue of $\mathbf{G}_k$,

$$\|\lambda_k \mathbf{G}_k + (1-\lambda_k)\mathbf{I}\|_2 \leqslant \lambda_k \bar{g}_k + 1 - \lambda_k.$$

Then, the bound $\bar{\sigma_k^2}(\lambda_k)$ is given by,

$$\bar{\sigma_k^2}(\lambda_k) = (1-\lambda_k)\sigma_{k|k-1}^2 + \lambda_k - \lambda_k(1-\lambda_k)\frac{\bar{\boldsymbol{\delta}}_k^T \bar{\boldsymbol{\delta}}_k}{(1-\lambda_k) + \lambda_k \bar{g}_k}.$$

This will define an upper bound to σ_k^2 due to the consideration of the maximum eigenvalue or the norm of the matrix $\mathbf{G}_k$. By minimizing $\bar{\sigma_k^2}(\lambda_k)$ with respect to λ_k we can obtain an optimum solution to λ_k that minimizes σ_k^2.

Since $\bar{\sigma_k^2}(\lambda_k)$ is a function of λ_k, the function $\bar{\sigma_k^2}(\lambda_k)$ should be convex in the domain $0 \leqslant \lambda_k \leqslant 1$ to have a local minimum. The second order conditions [70] state that, a function is convex if and only if the domain of the function is convex and the hessian or the second derivative of the function is positive semidefinite. The domain of $\bar{\sigma}_k^2(\lambda_k)$ is convex and

therefore, differentiate $\bar{\sigma}_k^2(\lambda_k)$ twice with respect to λ_k. Taking the first derivative will yield

$$\begin{aligned}\frac{d\bar{\sigma}_k^2(\lambda_k)}{d\lambda_k} &= -\sigma_{k|k-1}^2 + 1 - \bar{\boldsymbol{\delta}}_k^T\bar{\boldsymbol{\delta}}\left(\frac{(1-2\lambda_k)(1-\lambda_k+\lambda_k\bar{g}_k)-\lambda_k(1-\lambda_k)(\bar{g}_k-1)}{(1-\lambda_k+\lambda_k\bar{g}_k)^2}\right),\\ &= -\sigma_{k|k-1}^2 + 1 - \bar{\boldsymbol{\delta}}_k^T\bar{\boldsymbol{\delta}}\left(\frac{1-2\lambda_k+\lambda_k^2-\lambda_k^2\bar{g}_k}{(1-\lambda_k+\lambda_k\bar{g}_k)^2}\right),\\ &= 1 - \sigma_{k|k-1}^2 - \bar{\boldsymbol{\delta}}_k^T\bar{\boldsymbol{\delta}}\left(\frac{(1-\lambda_k)^2-\lambda_k^2\bar{g}_k}{(1-\lambda_k+\lambda_k\bar{g}_k)^2}\right).\end{aligned}$$

Taking the second derivative of $\bar{\sigma}_k^2(\lambda_k)$ with respect to λ_k will yield

$$\frac{d^2\bar{\sigma}_k^2(\lambda_k)}{d\lambda_k^2} = \frac{2\|\bar{\boldsymbol{\delta}}\|_2^2\bar{g}_k}{(1-\lambda_k+\lambda_k\bar{g}_k)^3}.$$

$\mathbf{G}_k$ is positive definite from matrix properties, $\bar{g}_k > 0$ as it is the norm or the maximum eigenvalue of $\mathbf{G}_k$ and $\|\bar{\boldsymbol{\delta}}\|_2^2 \geqslant 0$. Therefore, within $0 \leqslant \lambda_k \leqslant 1$, $\dfrac{d^2\bar{\sigma}_k^2(\lambda_k)}{d\lambda_k^2} \geqslant 0$ and $\bar{\sigma}_k^2(\lambda_k)$ is convex.

Remark D.1. Consider the matrix, $\mathbf{G}_k = \bar{\mathbf{V}}_k\mathbf{H}_k\mathbf{P}_{k|k-1}\mathbf{H}_k^T\bar{\mathbf{V}}_k^T$. The matrices $\mathbf{V}_k$ and $\mathbf{P}_{k|k-1}$ are positive definite matrices and $\mathbf{H}_k \in \mathbb{R}^{m\times n}$ has rank m. Since $\mathbf{V}_k$ is a positive definite matrix, $\bar{\mathbf{V}}_k$ is also a positive definite matrix. Therefore, $\mathbf{G}_k$ is a positive definite matrix.

By equating the first derivative of $\bar{\sigma}_k^2(\lambda_k)$ to zero we can obtain the local minimum within $0 \leqslant \lambda_k \leqslant 1$,

$$\begin{aligned}\frac{d\bar{\sigma}_k^2}{d\lambda_k} &= 0,\\ 0 &= 1 - \sigma_{k|k-1}^2 - \bar{\boldsymbol{\delta}}_k^T\bar{\boldsymbol{\delta}}\left(\frac{(1-\lambda_k)^2-\lambda_k^2\bar{g}_k}{(1-\lambda_k+\lambda_k\bar{g}_k)^2}\right).\end{aligned}$$

Define $\beta_k = \dfrac{1-\sigma^2_{k|k-1}}{\bar{\boldsymbol{\delta}}_k^T \bar{\boldsymbol{\delta}}_k}$. Then, can rewrite the above equation

$$\begin{aligned}
0 &= \beta_k - \left(\frac{(1-\lambda_k)^2 - \lambda_k^2 \bar{g}_k}{1-\lambda_k+\lambda_k\bar{g}_k}\right), \\
&= \beta_k(1-\lambda_k+\lambda_k\bar{g}_k)^2 - (1-\lambda_k)^2 + \lambda_k^2\bar{g}_k, \\
&= \beta_k(1-\lambda_k+\lambda_k\bar{g}_k)^2 - (1-\lambda_k)^2 + \lambda_k^2\bar{g}_k, \\
&= \beta_k(1-2\lambda_k(1-\bar{g}_k)+\lambda_k^2(1-\bar{g}_k)^2) - 1 + 2\lambda_k - \lambda_k^2(1-\bar{g}_k), \\
&= \beta_k(1-2\lambda_k(1-\bar{g}_k)+\lambda_k^2(1-\bar{g}_k)^2) - 1 + 2\lambda_k - \lambda_k^2(1-\bar{g}_k), \\
&= (\beta_k - 1) - 2\lambda_k(\beta_k(1-\bar{g}_k)-1) + \lambda_k^2(1-\bar{g}_k)(\beta_k(1-\bar{g}_k)-1).
\end{aligned}$$

If $\bar{g}_k = 1$, the optimum value of λ_k is

$$\lambda_k^* = \frac{1-\beta_k}{2}. \tag{D.1}$$

If $\bar{g}_k \neq 1$

$$\begin{aligned}
\lambda_k &= \frac{\beta_k(1-\bar{g}_k)-1) \pm \sqrt{(\beta_k(1-\bar{g}_k)-1)^2 - (\beta_k-1)(1-\bar{g}_k)(\beta_k(1-\bar{g}_k)-1)}}{(1-\bar{g}_k)(\beta_k(1-\bar{g}_k)-1)}, \\
&= \frac{1}{(1-\bar{g}_k)}\left(1 \pm \sqrt{\frac{-\bar{g}_k}{(\beta_k(1-\bar{g}_k)-1)}}\right), \\
&= \frac{1}{(1-\bar{g}_k)}\left(1 \pm \sqrt{\frac{\bar{g}_k}{(1+\beta_k(\bar{g}_k-1))}}\right).
\end{aligned}$$

Since $\lambda_k \in (0,1)$, the optimum value of λ_k is

$$\lambda_k^* = \frac{1}{(1-\bar{g}_k)}\left(1 - \sqrt{\frac{\bar{g}_k}{(1+\beta_k(\bar{g}_k-1))}}\right).$$

But if the function $\bar{\sigma_k^2}(\lambda_k)$ is increasing function for $\lambda_k \in (0,1)$ or has critical point at $\lambda_k = 0$,

finding the minimum is not necessary. If the first derivative of $\bar{\sigma_k^2}(\lambda_k)$ evaluated at $\lambda_k = 0$ is greater than or equal to zero, then, the function $\bar{\sigma_k^2}(\lambda_k)$ is an increasing function or has critical point at $\lambda_k = 0$. Since,

$$\left.\frac{d\bar{\sigma_k^2}(\lambda_k)}{d\lambda_k}\right|_{\lambda_k=0} = 1 - \sigma_{k|k-1}^2 - \bar{\boldsymbol{\delta}}_k^T\bar{\boldsymbol{\delta}},$$

$\lambda_k^* = 0$ when $1 - \sigma_{k|k-1}^2 - \bar{\boldsymbol{\delta}}_k^T\bar{\boldsymbol{\delta}} \geqslant 0$. This means, if $\sigma_{k|k-1}^2 + \bar{\boldsymbol{\delta}}_k^T\bar{\boldsymbol{\delta}} \leqslant 1$ then $\lambda_k^* = 0$. There for the optimum λ_k is given by,

$$\lambda_k^* = \begin{cases} 0 & \sigma_{k|k-1}^2 + \bar{\boldsymbol{\delta}}_k^T\bar{\boldsymbol{\delta}}_k \leq 1, \\ \dfrac{1-\beta_k}{2} & \bar{g}_k = 1, \\ \dfrac{1}{1-\bar{g}_k}\left[1 - \sqrt{\dfrac{\bar{g}_k}{1+\beta_k(\bar{g}_k - 1)}}\right] & \bar{g}_k \neq 1. \end{cases}$$

The complete correction step calculations will be done only if $\sigma_k^2 < \sigma_{k-1}^2$ when the measurements are available.

Appendix E

Overview of the Kalman filter

In 1960 R. E. Kalman introduced an effective filtering algorithm that is optimal for the Gaussian noise process. This algorithm solves the conventional Wiener problem combining two main ideas, the state space representation of dynamical systems and linear filtering regarded as orthogonal projection in Hilbert space [11]. Also in 1959 R. S. Bucy found explicit relationships between the optimal weighting functions and the error variances for an extended version of the Wiener problem. He also provided a rigorous derivation of the variance equations and those of the optimal filter for a wide class of non-stationary signal and noise statistics. [12]. Combining the individual approaches in [12] Kalman and Bucy obtained a major improvement and generalization of the conventional Wiener problem using time-domain methods, the best linear state estimate and error covariance based on past data. The two main assumptions were, the process model is sufficiently accurate and given by a linear time-varying dynamical system excited by white noise, and the system is discrete or the observed signals contain an additive noise component. [12, 40, 71].

Kalman-Bucy filter techniques incorporate the uncertainty characteristics into the

calculations using white noise components. As mentioned earlier, this is a two-step procedure, which outputs an estimate of the highest probability state and error covariance. If the signal and noise are jointly Gaussian, then the KF is an optimal minimum mean square error estimator and if not it the optimal least minimum mean square error estimator. [71]. In the prediction step, the posterior distribution of the states will be calculated based on past information. Then in the Correction step, an estimate which minimizes the expectation of the measurement error under the a posteriori distribution will be calculated. [23].

The KF has been defined for linear systems and for nonlinear systems the KF is used after using linearization approaches. This modified KF technique is called the EKF.

E.1 The Kalman filter for state estimation in a linear system

Consider the linear system described in equation (2.2).

$$\mathbf{x}_k = \mathbf{F}_{k-1}\mathbf{x}_{k-1} + \mathbf{w}_k,$$
$$\mathbf{z}_k = \mathbf{H}_k\mathbf{x}_k + \mathbf{v}_k.$$

In order to formulate the KF following assumptions are made.

1. Initial state $\mathbf{x}_0$ is a random variable with known mean μ_0 and covariance of initial estimation error is $\mathbf{P}_0$.

2. $\mathbf{F}_{k-1}$ and $\mathbf{H}_k$ are known at each time step.

3. $\mathbf{w}_k$ is a random vector which captures the uncertainties in the model (considered as process noise).

4. $\mathbf{v}_k$ is a random vector which denotes the measurement noise.

5. Both $\mathbf{v}_k$ and $\mathbf{w}_k$ are white noise processes, zero mean random sequences with known covariances.

6. Both $\mathbf{v}_k$ and $\mathbf{w}_k$ are uncorrelated with $\mathbf{x}_0$.

$$E[\mathbf{w}_k] = 0 \ \ , E[\mathbf{w}_k \mathbf{w}_k^T] = \mathbf{Q}_k \ , \ E[\mathbf{w}_k \mathbf{w}_j^T] = 0 \ \ \forall \ k \neq j,$$
$$E[\mathbf{v}_k] = 0 \ \ , E[\mathbf{v}_k \mathbf{v}_k^T] = \mathbf{R}_k \ , \ E[\mathbf{v}_k \mathbf{v}_j^T] = 0 \ \ \forall \ k \neq j,$$
$$E[\mathbf{w}_k \mathbf{v}_j^T] = 0 \ \ \forall \ k \& j \ , \ E[\mathbf{w}_k \mathbf{x}_0] = 0 \ \ \forall \ k \ , \ E[\mathbf{v}_k \mathbf{x}_0] = 0 \ \ \forall \ k.$$

The KF algorithm can be initialized by considering the initial state information. At initial time step,

$$\hat{\mathbf{x}}_0 = E[\mathbf{x}_0] = \mu_0$$
$$\mathbf{P}_0 = E[(\mathbf{x}_0 - \hat{\mathbf{x}}_0)(\mathbf{x}_0 - \hat{\mathbf{x}}_0)^T]$$

Therefore, at time step $(k-1)$ we have $\hat{\mathbf{x}}_{k-1}$ and P_{k-1}. The predicted state at time step k can be calculated as, $\hat{\mathbf{x}}_{k|k-1} = \mathbf{F}_{k-1}\hat{\mathbf{x}}_{k-1}$ the best prediction given the past measurements,

and the predicted covariance matrix is

$$\begin{aligned}
\mathbf{P}_{k|k-1} &= E[(\mathbf{x}_{k|k-1} - \hat{\mathbf{x}}_{k|k-1})(\mathbf{x}_{k|k-1} - \hat{\mathbf{x}}_{k|k-1})^T], \\
&= E[(\mathbf{F}_{k-1}\mathbf{x}_{k-1} + \mathbf{w}_k - \mathbf{F}_{k-1}\hat{\mathbf{x}}_{k-1})(\mathbf{F}_{k-1}\mathbf{x}_{k-1} + \mathbf{w}_k - \mathbf{F}_{k-1}\hat{\mathbf{x}}_{k-1})^T], \\
&= E[(\mathbf{F}_{k-1}(\mathbf{x}_{k-1} - \hat{\mathbf{x}}_{k-1}) + \mathbf{w}_k)(\mathbf{F}_{k-1}(\mathbf{x}_{k-1} - \hat{\mathbf{x}}_{k-1}) + \mathbf{w}_k)^T], \\
&= \mathbf{F}_{k-1}E[(\mathbf{x}_{k-1} - \hat{\mathbf{x}}_{k-1})(\mathbf{x}_{k-1} - \hat{\mathbf{x}}_{k-1})^T]\mathbf{F}_{k-1}^T + E[\mathbf{w}_k\mathbf{w}_k^T], \\
&= \mathbf{F}_{k-1}\mathbf{P}_{k-1}\mathbf{F}_{k-1}^T + \mathbf{Q}_{k-1}.
\end{aligned}$$

The prediction step can be summarized as,

$$\begin{aligned}
\hat{\mathbf{x}}_{k|k-1} &= \mathbf{F}_{k-1}\hat{\mathbf{x}}_{k-1}, \\
\mathbf{P}_{k|k-1} &= \mathbf{F}_{k-1}\mathbf{P}_{k-1}\mathbf{F}_{k-1}^T + \mathbf{Q}_{k-1}.
\end{aligned}$$

As and when the measurements are available in the time step k the predicted state can be corrected. Assume that $\hat{\mathbf{x}}_k = \hat{\mathbf{x}}_{k|k-1} + \mathbf{K}_k\boldsymbol{\delta}_k$, where $\boldsymbol{\delta}_k = \mathbf{z}_k - \mathbf{H}_k\hat{\mathbf{x}}_{k|k-1}$. To obtain the covariance of the estimated state, minimize the sum of variances in $\mathbf{P}_k$ with respect to $\mathbf{K}_k$.

$$\begin{aligned}
\mathbf{P}_k &= E[(\mathbf{x}_k - \hat{\mathbf{x}}_k)(\mathbf{x}_k - \hat{\mathbf{x}}_k)^T], \\
&= E[(\mathbf{x}_k - (\hat{\mathbf{x}}_{k|k-1} + \mathbf{K}_k\boldsymbol{\delta}_k))(\mathbf{x}_k - (\hat{\mathbf{x}}_{k|k-1} + \mathbf{K}_k\boldsymbol{\delta}_k))^T], \\
&= E[(\mathbf{x}_k - (\hat{\mathbf{x}}_{k|k-1} + \mathbf{K}_k(\mathbf{z}_k - \mathbf{H}_k\hat{\mathbf{x}}_{k|k-1})))(\mathbf{x}_k - (\hat{\mathbf{x}}_{k|k-1} + \mathbf{K}_k(\mathbf{z}_k - \mathbf{H}_k\hat{\mathbf{x}}_{k|k-1})))^T].
\end{aligned}$$

But $\mathbf{z}_k = \mathbf{H}_k\mathbf{x}_k + \mathbf{v}_k$ and

$$\begin{aligned}
\mathbf{P}_k &= E[((I - \mathbf{K}_k\mathbf{H}_k)(\mathbf{x}_k - \hat{\mathbf{x}}_{k|k-1}) + \mathbf{K}_k\mathbf{v}_k)((I - \mathbf{K}_k\mathbf{H}_k)(\mathbf{x}_k - \hat{\mathbf{x}}_{k|k-1}) + \mathbf{K}_k\mathbf{v}_k)^T], \\
&= (I - \mathbf{K}_k\mathbf{H}_k)E[(\mathbf{x}_k - \hat{\mathbf{x}}_{k|k-1})(\mathbf{x}_k - \hat{\mathbf{x}}_{k|k-1})^T](I - \mathbf{K}_k\mathbf{H}_k)^T + \mathbf{K}_k E[\mathbf{v}_k\mathbf{v}_k^T]\mathbf{K}_k^T, \\
&= (I - \mathbf{K}_k\mathbf{H}_k)\mathbf{P}_{k|k-1}(I - \mathbf{K}_k\mathbf{H}_k)^T + \mathbf{K}_k\mathbf{R}_k\mathbf{K}_k^T, \qquad \text{(E.1)} \\
&= \mathbf{P}_{k|k-1} - 2\mathbf{P}_{k|k-1}\mathbf{H}_k^T\mathbf{K}_k^T + \mathbf{K}_k(\mathbf{H}_k\mathbf{P}_{k|k-1}\mathbf{H}_k^T + \mathbf{R}_k)\mathbf{K}_k^T.
\end{aligned}$$

Minimizing $\mathbf{P}_k$ with respect to $\mathbf{K}_k$ will yield

$$\frac{\partial \mathbf{P}_k}{\partial \mathbf{K}_k} = -2\mathbf{P}_{k|k-1}\mathbf{H}_k^T + 2\mathbf{K}_k(\mathbf{H}_k\mathbf{P}_{k|k-1}\mathbf{H}_k^T + \mathbf{R}_k).$$

Therefore,

$$\mathbf{K}_k = \mathbf{P}_{k|k-1}\mathbf{H}_k^T(\mathbf{H}_k\mathbf{P}_{k|k-1}\mathbf{H}_k^T + \mathbf{R}_k)^{-1}.$$

We can summarize the correction step calculations as,

$$\begin{aligned}
\hat{\mathbf{x}}_k &= \hat{\mathbf{x}}_{k|k-1} + \mathbf{K}_k\boldsymbol{\delta}_k, \\
\mathbf{P}_k &= (\mathbf{I} - \mathbf{K}_k\mathbf{H}_k)\mathbf{P}_{k|k-1}, \\
\mathbf{K}_k &= \mathbf{P}_{k|k-1}\mathbf{H}_k^T(\mathbf{H}_k\mathbf{P}_{k|k-1}\mathbf{H}_k^T + \mathbf{R}_k)^{-1}, \\
\boldsymbol{\delta}_k &= \mathbf{z}_k - \mathbf{H}_k\hat{\mathbf{x}}_{k|k-1}.
\end{aligned}$$

These two steps, the prediction step and the correction step will be carried out sequentially for the estimation of states at each time step.

E.2 The Kalman filter for state estimation in a non-linear system

Consider the non-linear system given by equations (2.22-2.23),

$$\mathbf{x}_k = f(\mathbf{x}_{k-1}) + \mathbf{w}_k, \tag{E.2}$$

$$\mathbf{z}_k = h(\mathbf{x}_k) + \mathbf{v}_k, \tag{E.3}$$

where, functions $f(.)$ and $h(.)$ are assumed to be differentiable functions having continuous first derivative. Since, the first order non-linearities in the dynamic and the observation model are continuous, we can expand $f(.)$ and $h(.)$ using Taylor series and neglect the higher order terms in order to linearize the functions at a given point.

Expanding (E.2) using Taylor series about $\hat{\mathbf{x}}_{k-1}$,

$$\begin{aligned}\mathbf{x}_k &= f(\hat{\mathbf{x}}_{k-1}) + \left.\frac{\partial f(\mathbf{x})}{\partial \mathbf{x}}\right|_{\mathbf{x}=\hat{\mathbf{x}}_{k-1}} \mathbf{e}_{k-1} + \epsilon_{process}(\hat{\mathbf{x}}_{k-1}) + \mathbf{w}_k, \\ &= f(\hat{\mathbf{x}}_{k-1}) + \mathbf{F}_{k-1}\mathbf{e}_{k-1} + \mathbf{w}_k, \end{aligned} \tag{E.4}$$

where $\mathbf{F}_{k-1} = \left.\frac{\partial f(\mathbf{x})}{\partial \mathbf{x}}\right|_{\mathbf{x}=\hat{\mathbf{x}}_{k-1}}$, $\mathbf{e}_{k-1} = \mathbf{x}_{k-1} - \hat{\mathbf{x}}_{k-1}$, and $\epsilon_{process}(\hat{\mathbf{x}}_{k-1})$ represent the higher order terms and considered negligible. Taking the expected value of $\mathbf{x}_k$ given all the previous observations $\mathbf{Z}_{k-1}$,

$$E[\mathbf{x}_k|\mathbf{Z}_{k-1}] = E[f(\mathbf{x})|_{\mathbf{x}\ =\hat{\mathbf{x}}_{k-1}}|\mathbf{Z}_{k-1}]. \tag{E.5}$$

Since $E[\mathbf{F}_{k-1}\mathbf{e}_{k-1}|\mathbf{Z}_{k-1}] = 0$ and $E[\mathbf{w}_k|\mathbf{Z}_{k-1}] = 0$, we have

$$\hat{\mathbf{x}}_{k|k-1} = f(\hat{\mathbf{x}}_{k-1}).$$

Substituting this result in predicted state error equation,

$$\begin{aligned}\mathbf{e}_{k|k-1} &= \mathbf{x}_{k|k-1} - \hat{\mathbf{x}}_{k|k-1},\\ &\approx \mathbf{F}_{k-1}\mathbf{e}_k + \mathbf{w}_k.\end{aligned}$$

The predicted error covariance is given by,

$$\begin{aligned}\mathbf{P}_{k|k-1} &= E[\mathbf{e}_{k|k-1}\mathbf{e}_{k|k-1}^T],\\ &= \mathbf{F}_{k-1}\mathbf{P}_{k-1}\mathbf{F}_{k-1}^T + \mathbf{Q}_k.\end{aligned}$$

Thus, we have prediction step equations as in linear system.

Using the same argument as above linearize the measurement equation (E.3) about $\hat{\mathbf{x}}_{k|k-1}$ and neglecting the higher order terms

$$\mathbf{z}_k = h(\mathbf{x})|_{\mathbf{x}=\hat{\mathbf{x}}_{k|k-1}} + \mathbf{H}_k\mathbf{e}_{k|k-1} + \mathbf{v}_k,$$

where $\mathbf{H}_k = \left.\dfrac{\partial h(\mathbf{x})}{\partial \mathbf{x}}\right|_{\mathbf{x}=\hat{\mathbf{x}}_{k|k-1}}$ and $\mathbf{e}_{k|k-1} = \mathbf{x}_{k|k-1} - \hat{\mathbf{x}}_{k|k-1}$. Taking the expected value of $\mathbf{z}_k$ given all the observations $\mathbf{Z}_k$ will yield

$$\hat{\mathbf{z}}_k = h(\hat{\mathbf{x}}_{k|k-1}),$$

as $E[\mathbf{H}_k\mathbf{e}_{k|k-1}|\mathbf{Z}_k] = 0$ and $E[\mathbf{v}_k|\mathbf{Z}_k] = 0$. The estimated state can be represented using the same equation as linear case with this modification,

$$\hat{\mathbf{x}}_k = \hat{\mathbf{x}}_{k|k-1} + \mathbf{K}_k\boldsymbol{\delta}_k,$$
$$\boldsymbol{\delta}_k = \mathbf{z}_k - h(\hat{\mathbf{x}}_{k|k-1}).$$

Substituting this result in the error equation $\mathbf{e}_k$,

$$\begin{aligned}
\mathbf{e}_k &= \mathbf{x}_k - \hat{\mathbf{x}}_k, \\
&= f(\mathbf{x}_{k-1}) + \mathbf{w}_k - \hat{\mathbf{x}}_{k|k-1} - \mathbf{K}_k(\mathbf{z}_k - h(\hat{\mathbf{x}}_{k|k-1})), \\
&= f(\mathbf{x}_{k-1}) + \mathbf{w}_k - f(\hat{\mathbf{x}}_{k-1}) - \mathbf{K}_k(h(\mathbf{x}_k) + \mathbf{v}_k - h(\hat{\mathbf{x}}_{k|k-1})), \\
&= \mathbf{F}_{k-1}\mathbf{e}_{k-1} + \mathbf{w}_k - \mathbf{K}_k(\mathbf{H}_k\mathbf{e}_k + \mathbf{v}_k), \\
&= \mathbf{F}_{k-1}\mathbf{e}_{k-1} + \mathbf{w}_k - \mathbf{K}_k\mathbf{H}_k(\mathbf{F}_{k-1}\mathbf{e}_{k-1} + \mathbf{w}_k) + \mathbf{K}_k\mathbf{v}_k, \\
&= (\mathbf{I} - \mathbf{K}_k\mathbf{H}_k)\mathbf{F}_{k-1}\mathbf{e}_{k-1} + (\mathbf{I} - \mathbf{K}_k\mathbf{H}_k)\mathbf{w}_k + \mathbf{K}_k\mathbf{v}_k.
\end{aligned}$$

Then the estimated error covariance is given by,

$$\begin{aligned}
\mathbf{P}_k &= E[\mathbf{e}_k\mathbf{e}_k^T], \\
&= (\mathbf{I} - \mathbf{K}_k\mathbf{H}_k)\mathbf{F}_{k-1}\mathbf{P}_{k-1}\mathbf{F}_{k-1}^T(\mathbf{I} - \mathbf{K}_k\mathbf{H}_k)^T + (\mathbf{I} - \mathbf{K}_k\mathbf{H}_k)\mathbf{Q}_k(\mathbf{I} - \mathbf{K}_k\mathbf{H}_k)^T + \mathbf{K}_k\mathbf{R}\mathbf{K}_k^T, \\
&= (\mathbf{I} - \mathbf{K}_k\mathbf{H}_k)\mathbf{P}_{k|k-1}(\mathbf{I} - \mathbf{K}_k\mathbf{H}_k)^T + \mathbf{K}_k\mathbf{R}\mathbf{K}_k^T.
\end{aligned}$$

This is same as (E.1) and hence the derivation from here is same as the linear KF. The prediction and correction step can be summarized as follows.

Prediction step :

$$\begin{aligned}
\hat{\mathbf{x}}_{k|k-1} &= f(\hat{\mathbf{x}}_{k-1}), \\
\mathbf{P}_{k|k-1} &= \mathbf{F}_{k-1}\mathbf{P}_{k-1}\mathbf{F}_{k-1}^T + \mathbf{Q}_{k-1}, \\
\mathbf{F}_{k-1} &= \left.\frac{\partial f(\mathbf{x})}{\partial \mathbf{x}}\right|_{\mathbf{x}=\hat{\mathbf{x}}_{k-1}}.
\end{aligned}$$

Correction step:

$$\begin{aligned}
\hat{\mathbf{x}}_k &= \hat{\mathbf{x}}_{k|k-1} + \mathbf{K}_k\boldsymbol{\delta}_k, \\
\mathbf{P}_k &= (\mathbf{I} - \mathbf{K}_k\mathbf{H}_k)\mathbf{P}_{k|k-1}, \\
\mathbf{K}_k &= \mathbf{P}_{k|k-1}\mathbf{H}_k^T(\mathbf{H}_k\mathbf{P}_{k|k-1}\mathbf{H}_k^T + \mathbf{R}_k)^{-1}, \\
\boldsymbol{\delta}_k &= \mathbf{z}_k - h(\hat{\mathbf{x}}_{k|k-1}), \\
\mathbf{H}_k &= \left.\frac{\partial h(\mathbf{x})}{\partial \mathbf{x}}\right|_{\mathbf{x}=\hat{\mathbf{x}}_{k|k-1}}.
\end{aligned}$$

Bibliography

[1] Y.-F. Huang, S. Werner, J. Huang, N. Kashyap, and V. Gupta, "State estimation in electric power grids: meeting new challenges presented by the requirements of the future grid," *IEEE Signal Processing Magazine*, vol. 29, pp. 33–43, Sept. 2012.

[2] I. S. Association *et al.*, "Ieee standard for synchrophasor measurements for power systems," *IEEE Std C*, vol. 37, pp. 1–61, 2011.

[3] A. Monticelli, "Electric power system state estimation," *Proceedings of the IEEE*, vol. 88, pp. 262–282, Feb. 2000.

[4] A. Debs and R. Larson, "A dynamic estimator for tracking the state of a power system," *IEEE Transactions on Power Apparatus and Systems*, vol. PAS-89, pp. 1670–1678, Sept. 1970.

[5] Z. Huang, K. Schneider, and J. Nieplocha, "Feasibility studies of applying kalman filter techniques to power system dynamic state estimation," in *2007 International Power Engineering Conference (IPEC 2007)*, pp. 376–382, IEEE, 2007.

[6] E. Ghahremani and I. Kamwa, "Dynamic state estimation in power system by applying the extended Kalman filter With unknown inputs to phasor measurements," *IEEE Transactions on Power Systems*, vol. 26, pp. 2556–2566, Nov. 2011.

[7] G. Valverde and V. Terzija, "Unscented Kalman filter for power system dynamic state estimation," *IET Generation, Transmission & Distribution*, vol. 5, no. 1, p. 29, 2011.

[8] M. R. Karamta and J. Jamnani, "Implementation of extended Kalman filter based dynamic state estimation on SMIB system incorporating UPFC dynamics," *Energy Procedia*, vol. 100, pp. 315–324, Nov. 2016.

[9] H. P. Hsu, *Schaum's outline of theory and problems of signals and systems*. Schuam's outline series, New York, NY: McGraw-Hill, 1995.

[10] W. Miller and J. Lewis, "Dynamic state estimation in power systems," *IEEE Transactions on Automatic Control*, vol. 16, pp. 841–846, Dec. 1971.

[11] R. E. Kalman, "A new approach to linear filtering and prediction problems," *Journal of basic Engineering*, vol. 82, no. 1, pp. 35–45, 1960.

[12] R. E. Kalman and R. S. Bucy, "New results in linear filtering and prediction theory," *Journal of basic engineering*, vol. 83, no. 1, pp. 95–108, 1961.

[13] S. J. Julier and J. K. Uhlmann, "New extension of the kalman filter to nonlinear systems," in *Signal processing, sensor fusion, and target recognition VI*, vol. 3068, pp. 182–193, International Society for Optics and Photonics, 1997.

[14] S. G. Mohinder and P. A. Angus, *Kalman Filtering: Theory and Practice Using MATLAB.* Wiley, 2015.

[15] C. Tsai and L. Kurz, "An adaptive robustizing approach to kalman filtering," *Automatica*, vol. 19, pp. 279–288, May 1983.

[16] E. Fogel and Y. Huang, "On the value of information in system identification—bounded noise case," *Automatica*, vol. 18, pp. 229–238, Mar. 1982.

[17] S. Dasgupta and Yih-Fang Huang, "Asymptotically convergent modified recursive least-squares with data-dependent updating and forgetting factor for systems with bounded noise," *IEEE Trans. Inf. Theory.*, vol. 33, pp. 383–392, May 1987.

[18] Y. Huang, "A recursive estimation algorithm using selective updating for spectral analysis and adaptive signal processing," *IEEE Trans. Acoust., Speech, Signal Process.*, vol. 34, pp. 1331–1334, Oct. 1986.

[19] P. L. Combettes, "The foundations of set theoretic estimation," *Proceedings of the IEEE*, vol. 81, pp. 182–208, Feb. 1993.

[20] F. Schlaepfer and F. Schweppe, "Continuous-time state estimation under disturbances bounded by convex sets," *IEEE Trans. Autom. Control.*, vol. 17, pp. 197 – 205, Apr. 1972.

[21] F. L. Chernousko, *State Estimation for Dynamic Systems.* CRC Press, Inc.: Boca Raton,FL, 1994.

[22] F. Schweppe, "Recursive state estimation: unknown but bounded errors and system inputs," *IEEE Trans. Autom. Control.*, vol. AC-13, pp. 22–28, Feb. 1968.

[23] H. S. Witsenhausen, "Sets of possible states of linear systems given perturbed observations," *IEEE Trans. Autom. Control.*, vol. 13, pp. 556–558, Oct. 1968.

[24] D. Bertsekas and I. Rhodes, "Recursive state estimation for a set-membership description of uncertainty," *IEEE Trans. Automat. Contr.*, vol. 16, pp. 117–128, Apr. 1971.

[25] I. Elishakoff, *Whys and Hows in Uncertainty Modelling: Probability, Fuzziness and Anti-Optimization.* Springer, 1999.

[26] C. Durieu, . Walter, and B. Polyak, "Multi-input multi-output ellipsoidal state bounding," *Journal of Optimization Theory and Applications*, vol. 111, pp. 273–303, Nov. 2001.

[27] D. G. Maksarov and J. P. Norton, "State bounding with ellipsoidal set description of the uncertainty," *International Journal of Control*, vol. 65, pp. 847–866, Nov. 1996.

[28] D. G. Maksarov and J. P. Norton, "Computationally efficient algorithms for state estimation with ellipsoidal approximations," *Int. J. Adapt. Control Signal Process.*, vol. 16, pp. 411–434, Aug. 2002.

[29] G. Belforte and B. Bona, "An improved parameter identification algorithm for signals with unknown-but-bounded errors," *IFAC Proceedings Volumes*, vol. 18, pp. 1507–1512, July 1985.

[30] V. Broman and M. Shensa, "Polytopes, a novel approach to tracking," in *1986 25th IEEE Conference on Decision and Control*, (Athens, Greece), pp. 1749–1752, IEEE, Dec. 1986.

[31] S. Mo and J. Norton, "Fast and robust algorithm to compute exact polytope parameter bounds," *Mathematics and Computers in Simulation*, vol. 32, pp. 481–493, Dec. 1990.

[32] L. Chisci, A. Garulli, and G. Zappa, "Recursive set membership state estimation via parallelotopes," *IFAC Proceedings Volumes*, vol. 27, pp. 1327–1332, July 1994.

[33] L. Jaulin and E. Walter, "Set inversion via interval analysis for nonlinear bounded-error estimation," *Automatica*, vol. 29, pp. 1053–1064, July 1993.

[34] V. Puig, P. Cuguero, and J. Quevedo, "Worst-case state estimation and simulation of uncertain discrete-time systems using zonotopes," in *2001 European Control Conference (ECC)*, (Porto), pp. 1691–1697, IEEE, Sept. 2001.

[35] K. Tsakalis and Lijuan Song, "Set-membership estimation for weakly nonlinear models: an application to the adaptive control of semiconductor manufacturing processes," in *Proceedings of 1994 33rd IEEE Conference on Decision and Control*, vol. 2, (Lake Buena Vista, FL, USA), pp. 1066–1071, IEEE, 1994.

[36] E. Walter and H. Piet-Lahanier, "Robust nonlinear parameter estimation in the bounded noise case," in *1986 25th IEEE Conference on Decision and Control*, (Athens, Greece), pp. 1037–1042, IEEE, Dec. 1986.

[37] R. E. Moore, *Methods and Application of Interval Analysis*. Philadelphia: SIAM, 1979.

[38] J. Shamma and Kuang-Yang Tu, "Approximate set-valued observers for nonlinear systems," *IEEE Trans. Automat. Contr.*, vol. 42, pp. 648–658, May 1997.

[39] E. Scholte and M. Campbell, "Online nonlinear guaranteed estimation with application to a high performance aircraft," in *Proceedings of the 2002 American Control Conference (IEEE Cat. No.CH37301)*, vol. 1, (Anchorage, AK, USA), pp. 184–190, American Automatic Control Council, May 2002.

[40] E. Scholte and M. E. Campbell, "A nonlinear set-membership filter for on-line applications," *Int. J. Robust Nonlinear Control*, vol. 13, pp. 1337 – 1358, Oct. 2003.

[41] L. Jaulin, I. Braems, M. Kieffer, and r. Walter, "Nonlinear state estimation using forward-backward propagation of intervals in an algorithm," in *Scientific Computing, Validated Numerics, Interval Methods* (W. Krämer and J. W. von Gudenberg, eds.), pp. 191–201, Boston, MA: Springer US, 2001.

[42] J. P. Norton, "Identification and application of bounded- parameter models," *Automatica*, vol. 23, no. 4, pp. 497–507, 1987.

[43] S. Gollamudi, S. Nagaraj, S. Kapoor, and Y. F. Huang, "Set-membership state estimation with optimal bounding ellipsoids," *International Symposium on Information Theory and its Applications*, p. 5, 1996.

[44] S. Kapoor, S. Gollamudi, S. Nagaraj, and Y. Huang, "Tracking of time-varying parameters using optimal bounding ellipsoid algorithms," in *Proceedings of the Annual Allerton Conference on Communication Control and Computing*, vol. 34, pp. 392–401, Citeseer, 1996.

[45] Y. Liu, Y. Zhao, and F. Wu, "Ellipsoidal state-bounding-based set-membership estimation for linear system with unknown-but-bounded disturbances," *IET Control Theory & Applications*, vol. 10, no. 4, pp. 431–442, 2016.

[46] Y. Liu, Y. Zhao, and F. Wu, "Extended ellipsoidal outer-bounding set-membership estimation for nonlinear discrete-time systems with unknown-but-bounded disturbances," *Discrete Dynamics in Nature and Society*, vol. 2016, 2016.

[47] B. Zhou, J. Han, and G. Liu, "A UD factorization-based nonlinear adaptive set-membership filter for ellipsoidal estimation," *Int. J. Robust Nonlinear Control*, vol. 18, pp. 1513–1531, Nov. 2008.

[48] A. Abur and A. G. Exposito, *Power System State Estimation: Theory and Implementation*, vol. 24 of *Power Engineering (Willis)*. CRC Press, Mar. 2004.

[49] F. Schweppe and J. Wildes, "Power system static-state estimation, part I: exact model," *IEEE Transactions on Power Apparatus and Systems*, vol. PAS-89, pp. 120–125, Jan. 1970.

[50] F. Schweppe and D. Rom, "Power system static-state estimation, part II: approximate model," *IEEE Transactions on Power Apparatus and Systems*, vol. PAS-89, pp. 125–130, Jan. 1970.

[51] F. Schweppe, "Power system static-state estimation, part III: Implementation," *IEEE Transactions on Power Apparatus and Systems*, vol. PAS-89, pp. 130–135, Jan. 1970.

[52] F. Schweppe and R. Masiello, "A tracking static state estimator," *IEEE Transactions on Power Apparatus and Systems*, vol. PAS-90, pp. 1025–1033, May 1971.

[53] A. Leite da Silva, M. Do Coutto Filho, and J. de Queiroz, "State forecasting in electric power systems," *IEE Proceedings C Generation, Transmission and Distribution*, vol. 130, no. 5, p. 237, 1983.

[54] M. Brown Do Coutto Filho, J. de Souza, and R. Freund, "Forecasting-aided state estimation—part II: implementation," *IEEE Transactions on Power Systems*, vol. 24, pp. 1678–1685, Nov. 2009.

[55] S. Wang, W. Gao, and A. P. S. Meliopoulos, "An alternative method for power system dynamic state estimation based on unscented transform," *IEEE Transactions on Power Systems*, vol. 27, pp. 942–950, May 2012.

[56] F. Aminifar, M. Shahidehpour, M. Fotuhi-Firuzabad, and S. Kamalinia, "Power system dynamic state estimation with synchronized phasor measurements," *IEEE Transactions on Instrumentation and Measurement*, vol. 63, pp. 352–363, Feb. 2014.

[57] M. Brown Do Coutto Filho and J. de Souza, "Forecasting-aided state estimation—part I: panorama," *IEEE Transactions on Power Systems*, vol. 24, pp. 1667–1677, Nov. 2009.

[58] J. Zhao, M. Netto, and L. Mili, "A robust iterated extended kalman filter for power system dynamic state estimation," *IEEE Transactions on Power Systems*, vol. 32, pp. 3205–3216, July 2016.

[59] J. Mandal, "Incorporating nonlinearities of measurement function in power system dynamic state estimation," *IEE Proceedings - Generation, Transmission and Distribution*, vol. 142, no. 3, p. 289, 1995.

[60] A. Leite da Silva, M. Do Coutto Filho, and J. de Queiroz, "State forecasting in electric power systems," *IEE Proceedings C Generation, Transmission and Distribution*, vol. 130, no. 5, p. 237, 1983.

[61] E. Farantatos, G. K. Stefopoulos, G. J. Cokkinides, and A. P. Meliopoulos, "PMU-based dynamic state estimation for electric power systems," in *2009 IEEE Power & Energy Society General Meeting*, (Calgary, Canada), pp. 1–8, IEEE, July 2009.

[62] Junjian Qi, Guangyu He, Shengwei Mei, and Feng Liu, "Power system set membership state estimation," in *2012 IEEE Power and Energy Society General Meeting*, (San Diego, CA), pp. 1–7, IEEE, July 2012.

[63] J. Zhao, G. Zhang, K. Das, G. N. Korres, N. M. Manousakis, A. K. Sinha, and Z. He, "Power system real-Time monitoring by using PMU-based robust state estimation method," *IEEE Transactions on Smart Grid*, vol. 7, pp. 300–309, Jan. 2016.

[64] A. Sharma, S. Srivastava, and S. Chakrabarti, "Testing and validation of power system dynamic state estimators using real time digital simulator (rtds)," *IEEE Transactions on Power Systems*, vol. 31, no. 3, pp. 2338–2347, 2015.

[65] J. Qi, G. He, S. Mei, and F. Liu, "Power system set membership state estimation," in *2012 IEEE Power and Energy Society General Meeting*, pp. 1–7, IEEE, 2012.

[66] X. Qing, F. Yang, and X. Wang, "Extended set-membership filter for power system dynamic state estimation," *Electric Power Systems Research*, vol. 99, pp. 56–63, 2013.

[67] P. Kundur, N. J. Balu, and M. G. Lauby, *Power system stability and control*, vol. 7. McGraw-hill New York, 1994.

[68] RTDS Technologies Inc., "Real Time Digital Simulator Hardware Manual," tech. rep., RTDS Technologies Inc., 2008.

[69] F. Chernousko, "Ellipsoidal state estimation for dynamical systems," *Nonlinear Analysis: Theory, Methods & Applications*, vol. 63, pp. 872–879, Nov. 2005.

[70] S. Boyd and L. Vandenberghe, *Convex optimization*. Cambridge university press, 2004.

[71] S. M. Kay, *Fundamentals of statistical signal processing*. Prentice Hall PTR, 1993.